DOKUZ EYLÜL UNIVERSITY
GRADUATE SCHOOL OF NATURAL AND APPLIED
SCIENCES

EXPERIMENTAL STUDY OF SEDIMENT TRANSPORT AND NUMERICAL SOLUTION WITH FINITE VOLUME METHOD

by
Amin GHAREHBAGHI

July, 2011
İZMİR

EXPERIMENTAL STUDY OF SEDIMENT TRANSPORT AND NUMERICAL SOLUTION WITH FINITE VOLUME METHOD

A Thesis Submitted to the
Graduate School of Natural and Applied Sciences of Dokuz Eylül University In
Partial Fulfillment of the Requirements for the Degree of Master of Science in
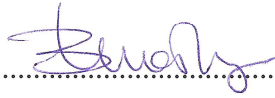**Civil Engineering, Hydraulics Hydrology Water Resources Program**

by
Amin GHAREHBAGHI

July, 2011
İZMİR

M.Sc THESIS EXAMINATION RESULT FORM

We have read the thesis entitled **"EXPERIMENTAL STUDY OF SEDIMENT TRANSPORT AND NUMERICAL SOLUTION WITH FINITE VOLUME METHOD"** completed by **AMIN GHAREHBAGHI** under supervision of **ASSOC. PROF. BİROL KAYA** and we certify that in our opinion it is fully adequate, in scope and in quality, as a thesis for the degree of Master of Science.
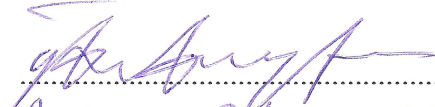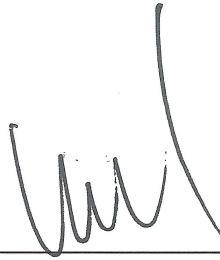
....

Assoc. Prof. Birol KAYA

Supervisor

....
Prof. Dr. M. Şükrü GÜNEY

....
Prof. Dr. Gökmen TAYFUR

(Juri Member)

(Juri Member)

Prof.Dr.Mustafa SABUNCU

Director

Graduate School of Natural and Applied Sciences

ACKNOWLEDGMENTS

EXPERIMENTAL STUDY OF SEDIMENT TRANSPORT AND NUMERICAL SOLUTION WITH FINITE VOLUME METHOD

ABSTRACT

Because of simplicity and reasonable results that can be obtained by one dimensional solution, the use of these predictions are increasing. In this thesis, one dimensional solution for sediment transport equations by finite volume method is proposed. Depending to the sensitive of the solution, sediment transport equations solved by implicit and explicit schemes. In this research, both kinematic wave and the dynamic wave models are investigated. Moreover both the equilibrium and non-equilibrium form of solutions are investigated. Finally the model is verified by the laboratory research. The results are generally simulated well.

Keywords : Sediment transport, 1-D model, Finite volume method, Kinematic wave model, Dynamic wave model, Equilibrium, Non-equilibrium.

KATI MADDE TAŞINIMININ DENEYSEL ARAŞTIRILMASI VE SONLU HACİMLER YÖNTEMİYLE ÇÖZÜMÜ

ÖZ

Bir boyutlu yöntemler basitlik ve yeterli derecede doğru sonuçlar elde edebilmelerinden dolayı çok sayıda araştırmacı tarafından kullanılmaktadırlar. Bu tez kapsamında katı madde taşınımını sonlu hacimler yöntemiyle bir boyutlu olarak çözümü yapılmıştır. Çözümün hassasiyetine bağlı olarak katı madde taşınımının denklemleri explicit ve implicit yaklaşımlarla incelenmiştir. Bu araştırma, kinematik ve dinamik dalga yöntemleri üzerinde yapılmıştır. Artı olarak çözümler dengede ve dengede olmayan durumlar için de incelenmiştir. Son olarak üretilmiş modeler labraturda yapılan deneysel çalışmaların sonuçları ile karşılaştırılmıştır. Modellerin sonuçu ile laburatuar sonuçları genelde büyük derecede uyum sağlamıştır.

Anahtar sözcükler : Katı madde taşınımı, Bir boyutlu, Sonlu hacimler yöntemi, Kinematik dalga yöntemi, Dinamik dalga yöntemi, Dengede, Dengesiz.

CONTENTS

CHAPTER ONE
INTRODUCTION

Human beings are trying to understand and control the rules of rivers, back to ancient time. According to historical research, approximately six thousand years ago, Chinese constructed dams along the Yellow River. Nearly at the same time the structure of flood control and irrigation systems were began in Mesopotamia. Approximately ten centuries later Egyptians started to make same buildings on Nile River.

A sediment particle is a material that formed by physical and chemical influence of nature phenomena like sun, water and etc. The size and shape of these particles are various. From large boulders to colloidal in size and from rounded to angular in shape. They also vary in specific gravity and mineral composition. These particles can be transported by difference ways like wind and water. When transport done by water, it is called fluvial or marine sediment transport.

Motion of particles can be shown in three models. 1. Rolling and/or sliding 2.Saltating or hopping 3.Suspended particle motions. All of them depend to the strength of flow.
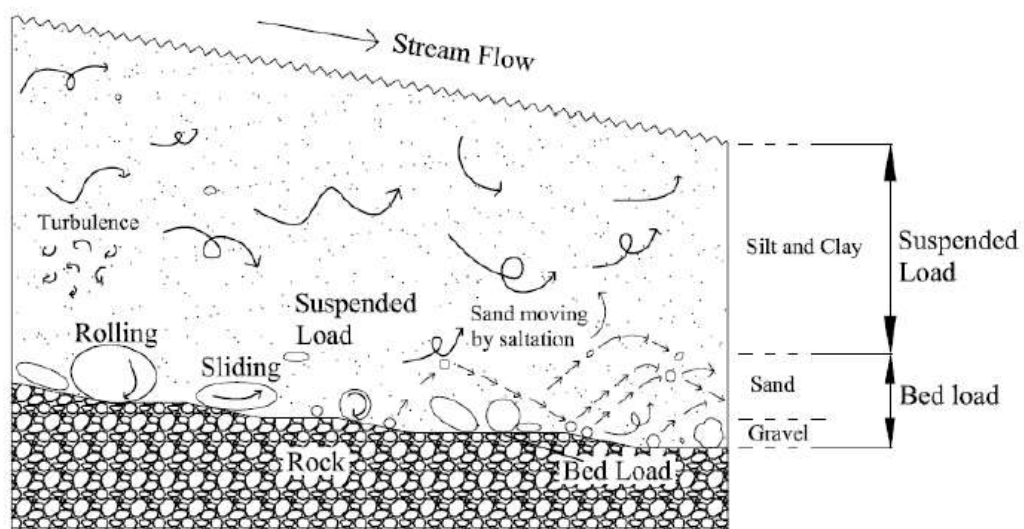
Figure 1.1. Different modes of sediment transport. (Singh,2005)

To achieve the most efficiency in reservoir design, it is very important to predict the sediment deposition, and to adjust the storage level and reservoir operation in accordance with the results of prediction.

Because the influence of acceleration in longitude direction is stronger than latitude and depth of flow directions, for simplification, channel or river in one dimension can be assumed.

Because of some special features of one dimensional numerical methods like efficiency and simplicity, these models have been widely used in design and calculation works.

The aim of this thesis is develop one dimensional numerical method for both of equilibrium and non equilibrium situation by finite volume method in order to predict the sediment transport in channels and rivers.

CHAPTER TWO
LITERATURE REVIEW

One of the hardest and complicated phenomena in the nature is to understand of river flow and motion of sediment particles. In order to overcome this problem, many of scientists investigate it in rivers or laboratory conditions. These are really helpful to understand the concept of subject and useful to present the experimental relations, but need to spend a lot of time and money and use advanced of equipments. Because of these reasons and for finding more suitable predictions, the mathematical methods have been developed. Depending to the conditions; one, two or three dimensional methods can be used.

One-dimensional (1-D) models can be used in short- and long-term simulations of flow and sediment transport processes in rivers, reservoirs, and estuaries. Two-dimensional (2-D) and three-dimensional (3-D) models can be used to predict more complex morphodynamic processes that need more details like complex flow conditions in curved and braided channels and around river training works, piers of bridges, spur-dikes, and water intake structures. Scientists try to develop different kind of numerical methods that can solve the continuity and momentum equations of mass together. These equations are usually solved in three ways: 1. Kinematic wave model 2.Diffusion wave model and 3.Dynamic wave model. Most of researchers tried to solve the governing relations in equilibrium conditions. Moreover most of them apply the finite difference method in order to predict flow conditions and sediment transport phenomenon.

Fuladipanah et al. (2010) developed a new one dimensional fully coupled numerical model for calculating flow and suspended load. Their models are appropriate for sandy rivers in unsteady flow conditions. For discretization of equations the implicit finite difference method is used and the Reynolds Transport Theory is used to convert system analysis to control volume analysis. For calibration and validation of the model, they used measured flow and suspended load data from a reach between Ahwaz and Mollasani stations, Karoon River, Iran.

Fang et al. (2008) used the Preissmann implicit four-point finite difference method for the discretization of the Saint-Venant equations and the discretized equations, solved with using the pentadiagonal matrix algorithm. For the calibration of the model, they used the data that measured from the Yantan Reservoir on the Hongshui River and the Sanmenxia Reservoir on the Yellow River. According to the report, comparison of the calculated water level and river bed deformation with field measurements showed predictions of flow, sediment transport, bed changes, and bed-material sorting in various situations, with reasonable accuracy and reliability.

Bombar (2006) under her PhD thesis studied the experimental and theoretical sediment transport process. She analyzed the inception motion and the bed load transport rate under unsteady flow conditions. Bor (2008) in her Msc. thesis investigated the numerical modeling of unsteady and non-equilibrium sediment transport in rivers.

Tayfur and Singh (2006) developed a mathematical model, based on the kinematic wave theory that predict the evolution and movement of bed profiles in alluvial channels under the equilibrium conditions. In order to discretization the equations, the explicit finite difference method was used. To test the model, flume and field data was used. One year later, they improved the model, for non-equilibrium conditions.

Paquier (1998) solved the Saint Venant equations by the finite difference method. They used the second-order Godunov-type explicit scheme.

de Vries (1965) used the explicit finite difference scheme to simulation water and bed level changes in one dimensional.

Many of investigators tried to simulate the flow and sediment movement with other numerical methods. Some of these researches are given below.

Rahuel et al. (1989), Cui et al. (1996), Kassem and Chaudhry (1998), Cao and

Egiashira (1999), Capart (2000), Cao et al. (2001), Capart and Young (2002), Di Cristo et al. (2002) and Kebapcıoğlu (2009) are the researchers that studied the unsteady flow models in recent years with numerical methods. Most of these researchers used the finite difference method for their simulations. Cunge et al. (1980) introduced the unsteady model equations derived from the Saint-Venant hypotheses to simulate river flood wave propagation.

Recently, the new numerical methods like the Transfer Matrix and Differential Quadrature Methods are applied in solution of St. Venant equations. Daneshfaraz and Kaya (2008) used the Transfer Matrix Method in solution of wave propagation in open channels. Kaya and Arısoy (2010) examined the long wave propagation in open channel flow by using DQM. In other research, in the continue of these studies Kaya et al. (2010) and Kaya et al. (2011) are investigated the flood propagation in rivers.

Seo et al. (2009) studied the one dimensional advection and diffusion equations to analyze the suspended sediment transport and finite element method employed as a solving technique .They applied the Galerkin Method.

Wu and Wang (2008) solved the one-dimensional explicit finite-volume model for sediment transport with transient flows over movable beds.

Van Niekerk et al. (1992), developed a model to simulate erosion and deposition in a relatively straight, non-bifurcating alluvial channel. In this model, the individual size-density fractions of bed material were considered.

Cunge et al. (1980) developed one dimensional model, for prediction of alluvial hydraulics. Chang (1982) presented a model for erodible channels.

Han (1980) provided a method for non-equilibrium transport of non-uniform suspended load. Wang et al. (2008), developed method for the one dimensional non-equilibrium sediment transport equations

Many unsteady models have also been developed and applied for estuaries and other geographical features.

Armanini and di Silvio (1988), and Bell and Sutherland (1983), provided unsteady models for movable bed channels.

Rahuel et al. (1989) developed and tested a new computational methodology for the fully coupled simulation of unsteady water and sediment movement in alluvial rivers. In their methodology, the non-uniform bed load transport was studied, and sorting and armoring effects were considered. In another research, Kaya and Gokmen (2011) examined the bed load transport equations by using Differential Quadrature Method.

Wu et al. (2004) and Wu (2004) used Rahuel's model in order to calculate the non-equilibrium transport of non-uniform total load under unsteady flow conditions in channels with hydraulic structures.

Aydöner (2010) investigated the bed forms during the sediment transport process under M.Sc.Thesis. Bombar et al. (2010) investigated the bed load transport experimentally and numerically.

Many of researchers like Lu (2001) and Leupi and Altinakar (2005) tried to simulate flow and sediment movement in two or three dimensions. Many of them developed software to predict flow and sediment transports under different situations. One dimensional models were generally designed for non-cohesive sediment transport with the capacities to simulate simple processes of cohesive sediment transport. These models include HEC-6 (U.S. Army Corps of Engineers, 1993), GSTARS2.1, and GSTARS3 (Yang and Simoes, 2002) and GSTAR-1D (Yang et al., 2005). EFDC1D (Hamrick 2001) is a 1D sediment transport model that includes settling, deposition and resuspension of multiple size classes of sediments.

CHAPTER THREE
SEDIMENT PARTICLES IN FLOW

3.1 Properties of Water and Sediment Particles

3.1.1 Water Density

Density of water ρ_f can be defined as the ratio of mass of water per unit volume. In the international unit (SI) system it is 1,000 $kg.m^{-3}$ at $4^o C$.

$$\rho_f = \frac{m}{V} \tag{3.1}$$

where, m is mass (M) and V is volume (L^3)

Various relationships between water density and temperature could be found in Table 3.1.

Table 3.1 Relation between density and viscosity of water and temperature (Wu,2007)

Temperature (C)	Density ($kg.m^{-3}$)	Dynamic viscosity ($N.s.m^{-2}$)	Kinematic viscosity ($m^2.s^{-1}$)
0	1000	1.79×10^{-3}	1.79×10^{-6}
5	1000	1.51×10^{-3}	1.51×10^{-6}
10	1000	1.31×10^{-3}	1.31×10^{-6}
15	999	1.14×10^{-3}	1.14×10^{-6}
20	998	1.00×10^{-3}	1.00×10^{-6}
25	997	8.91×10^{-4}	8.94×10^{-7}
30	996	7.79×10^{-4}	8.00×10^{-7}
35	994	7.20×10^{-4}	7.25×10^{-7}
40	992	6.53×10^{-4}	6.58×10^{-7}

3.1.2 Specific Weight of Water

The specific weight of water γ_f defined as the ratio of weight of water per unit volume, often in $N.m^{-3}$.

The relationship between specific weight and water density is

$$\gamma_f = \rho_f.g \tag{3.2}$$

where, g *is* the gravitational acceleration ($L.T^{-2}$) and equals about 9.81 m· s^{-2}, γ_f is specific weight of water ($M.L^{-2}.T^{-2}$), ρ_f is density of water ($M.L^{-3}$)

3.1.3 Water Viscosity

The dynamic viscosity of water, μ is defined as the constant of ratio of the shear stress, τ, to the deformation, *du/dy*, as follows:

$$\tau = \mu.\frac{du}{dy} \tag{3.3}$$

where, μ, is the dynamic viscosity ($M.L^{-1}.T^{-1}$), $\dfrac{du}{dy}$ is the gradient of velocity (T^{-1}), and τ is the shear stress ($M.L^{-1}.T^{-2}$)

The kinematical viscosity ($L^2.T^{-1}$) v, is the ratio of the dynamic viscosity to the density:

$$v = \frac{\mu}{\rho} \tag{3.4}$$

In common temperatures water viscosity depends on molecular interactions. By increasing temperatures, cohesion decreases and on water viscosity decreases (Table 3.1). Also the kinematical viscosity can be calculated by (Wu, 2007)

$$v = (1.785 - 0.0584T + 0.00116T^2 - 0.0000102T^3) \times 10^{-6} (m^2.s^{-1}) \tag{3.5}$$

where T is the temperature in degrees of Celsius.

For a fluid-sediment mixture the kinematical viscosity coefficient can be expressed as

$$\nu_m = \frac{\eta_m}{\rho_m} \tag{3.6}$$

where η_m is the dynamic viscosity coefficient in fluid-sediment mixture($M.L^{-1}.T^{-1}$), ρ_m is the density of fluid-sediment mixture ($\rho_f(1-C)+\rho_s.C$) ($M.L^{-3}$), C is the concentration of sediment ($V_s/(V_s+V_f)$), and V_s and V_f are the volume of sediment and water.

3.1.4 Sediment Density

Sediment density ρ_s is defined as proportion of the mass of sediment per unit volume. ($M.L^{-3}$). The density of a mixture of sediment is near to that of quartz. The density of quartz particles is about 2,650 $kg.m^{-3}$ so it can be assumed this value as a sediment density for natural rivers. Density of sediment depends on the material of sediment but it is not influenced by change of temperature.

3.1.5 Sediment Specific Weight

The specific weight of sediment γ_s is defined by the weight of sediment per unit volume, ($N.m^{-3}$). It is related to the sediment density by:

$$\gamma_s = \rho_s.g \tag{3.7}$$

where, γ_s is specific weight of sediment particles ($M.L^{-2}.T^{-2}$), ρ_s is density of sediment particles ($M.L^{-3}$)

The specific weight of submerged sediment particle can be defined by

Archimedes principle. According to this rule, the specific weight of submerged sediment is equal to difference of the specific weights of sediment and water $\gamma_s - \gamma_f$.

3.1.6 Specific Gravity of Sediment Particles

The proportion of specific weight of sediment to specific weight of water at a standard reference temperature that is generally equal to $4^o C$ is called specific gravity of sediment. The specific gravity of quartz particles is:

$$G = \frac{\gamma_s}{\gamma_f} = \frac{\rho_s}{\rho_f} = 2.65 \tag{3.8}$$

3.1.7 Size of Sediment Particles

Generally the word of sediment is used for Gravel, Sand, Silt or Clay. Different ways are available to measure the size of sediment particles. Measurements with rulers, optical methods, photographic methods or sieving are some of them.

Sediment particle size may be represented by nominal diameter, sieve diameter, and fall diameter. The nominal diameter, d, is given by:

$$d = \sqrt[3]{\frac{6V_s}{\pi}} \tag{3.9}$$

where, d is the nominal diameter (mm), V_s is the volume of the sediment particle.

The sieve diameter defined as the length of opening parts of sieve which just particles with smaller length can pass. For naturally sediment particles that in the range between 0.2 to 20 mm, the sieve diameter can be consider as 0.9 times of the nominal diameter on the average.

The standard fall diameter is the diameter of a sphere that has a specific gravity of 2.65 and has the same terminal settling velocity as the given particle in quiescent, distilled water at a temperature of $24^o C$ (Wu, 2007).

The classification of sediment particles that generally used in river engineering is given in Table 3.2.

Table3.2 Sediment grad scale (Wu,2007)

Class	Size range(mm)	Class	Size range(mm)
Very Large boulders	4.000-2.000	Coarse sand	1-0.5
Large boulders	2.000-1.000	Medium sand	0.5-0.25
Medium boulders	1.000-5.00	Fine sand	0.25-0.125
Small boulders	500-250	Very fine sand	0.125-0.062
Large cobbles	250-130	Coarse sit	0.062-0.031
Small cobbles	130-64	Medium sit	0.031-0.016
Very coarse gravel	64-32	Fine sit	0.016-0.008
Coarse gravel	32-16	Very fine sit	0.008-0.004
Medium gravel	16-8	Coarse clay	0.004-0.002
Fine gravel	8-4	Medium clay	0.002-0.001
Very fine gravel	4-2	Fine clay	0.001-0.0005
Very coarse sand	2-1	Very fine clay	0.0005-0.00024

3.1.8 Shape

Generally Corey shape factor is used for comparing between the shape of sediment particles. This factor can be expressed as:

$$SF = \frac{c}{a.b} \tag{3.10}$$

where, a is the length along longest axis perpendicular to other two axes, b is the length along intermediate axis perpendicular to other two axes, c is the length along short axis perpendicular to other two axes.

This equation can not take into account the distribution of the surface area and the volume of the particle. For example, the shape factor of a sphere that has a same length for diameter with cube length, is equal (SF =1). To overcome this shortcoming another shape factor given as:

$$SF_* = SF \frac{d_s}{d_n} \tag{3.11}$$

where SF_* is the shape factor, d_s is the diameter of a shape having the same surface area as that of the particle, d_n is the diameter of a shape having the same volume as that of the particle.

3.2 Settling of Sediment Particles

3.2.1 General Considerations

Settling or fall velocity is a mean velocity on that refers to fall down velocity of sediment particles in motionless water. It is depends to density, shape and volume of the particle and the viscosity and density of the fluid. A sediment particle can be affected by gravity, buoyant force and drag force throughout settling process. Its submerged weight that could be defined as difference between the gravity and buoyant forces, is expressed as:

$$W_s = (\rho_s - \rho).g.a_1.d^3 \tag{3.12}$$

where d is the size of sediment particle, $a_1 d^3$ is equal to the volume of the sediment particle, a_1 is the value of $\pi/6$ for a spherical particle. Because of considering low concentration (a single particle) it must be attention that ρ is actually given as the pure water density ρ_f.

The drag force is the result of the tangential shear stress exerted by the fluid (skin drag) and the pressure difference (form drag) on the particle, (Wu, 2007).
It can be given in the general form as:

$$F_d = C_d.\rho.a_2.d^2.\frac{\omega_s^2}{2} \tag{3.13}$$

where, C_d is the *Dr*ag coefficient, ω_s is the settling velocity, $a_2 d^2$ is the projected

area of the particle on the plane normal to the direction of settling, a_2 is the value of $\dfrac{\pi}{4}$ for a spherical particle.

In the terminal level of settling drag force should be equal to the submerged weight. So,

$$\omega_s = (\frac{a_1}{a_2} \frac{2}{C_d} \frac{\rho_s - \rho}{\rho} gd)^{\frac{1}{2}} \qquad (3.14)$$

3.2.2 Settling Velocity of Sediment Particles

Settling velocity for sediment particles with irregular shapes and rough surfaces are different in comparison with spherical particles. Many of researchers studied in this field and tried to developed experimental formula whose some are summarized.

3.2.2.1 Rouse Approch (1938)

Reynolds number really influences in drage coefficent of a sphere particles. For particles with Reynolds number greater then 2, the particle fall velocity is determined experimentally. Rouse (1938) suggested that for most natural sands, that shape factor is 0.7 and for $d_s=0.2mm$, the value of 0.024 m/s can be used.

3.2.2.2 Rubey (1933)

Rubey (1933), suggested the following relation for the settling velocity of natural sediment particles:

$$\omega_s = F \sqrt{(\frac{\rho_s}{\rho} - 1).g.d} \qquad (3.15)$$

where $F = 0.79$ for particles larger than 1 mm settling in water with temperatures between 10 and $25^o C$. For smaller grain sizes, F is determined by:

$$F = [\frac{2}{3} + \frac{36v^2}{g.d^3(\frac{\rho_s}{\rho}-1)}]^{\frac{1}{2}} - [\frac{36v^2}{g.d^3(\frac{\rho_s}{\rho}-1)}]^{\frac{1}{2}}$$

(3.16)

3.2.2.3 Zhang (1961)

Zhang (1961), considered sediment particles drag force in the transition region between laminar and turbulent as:

$$F_d = C_1.\rho.v.d.\omega_s + C_2.\rho.d^2\omega_s^2$$

(3.17)

where C_1 and C_2 are coefficients.

By using many laboratory data, Zhang suggested relations for the settling velocity of naturally worn sediment particles:

$$\omega_s = \sqrt{(13.95\frac{v}{d})^2 + 1.09(\frac{\rho_s}{\rho}-1).g.d} - 13.95\frac{v}{d}$$

(3.18)

The Zhang formula can be used in a wide range of sediment sizes from laminar to turbulent settling regions.

3.2.2.4 Van Rijn (1984b)

Van Rijn (1984b) suggested the following set of equations for settling velocity by using Stokes law equation. For sediment particles smaller than 0.1 mm

$$\omega_s = \frac{1}{18}\frac{\rho_s - \rho}{\rho} g \frac{d^2}{v}$$

(3.19)

Using the Zanke (1977) formula for particles from 0.1 to 1 mm:

$$\omega_s = 10\frac{v}{d}\left\{\left[1 + 0.01(\frac{\rho_s}{\rho}-1)\frac{gd^3}{v^2}\right]^{1/2} - 1\right\}$$

(3.20)

and for particles larger that 1 mm:

$$\omega_s = 1.1 \left[(\frac{\rho_s}{\rho} - 1) g d \right]^{1/2} \qquad (3.21)$$

The general form of these equations can be expressed as:

$$C_d = \left[(\frac{M}{R_e})^{\frac{1}{n}} + N^{\frac{1}{n}} \right]^n \qquad (3.22)$$

In Table 3.3 the list of values that are given by different investigators for these coefficients for naturally worn sediment particles, could be found.

Table3.3 Values of M, N and n (Wu, 2007)

Author	M	N	N
Rubey(1933)	24	2.1	1
Zhang(1961)	34	1.2	1
Zanke(1977)	24	1.1	1
Raudkivi(1990)	32	1.2	1
Julien(1995)	24	1.5	1
Cheng(1997)	32	1	1.5

In order to determine the settling velocity of naturally worn sediment particles Cheng (1997) suggested the following relation:

$$\omega_s = \frac{v}{d} (\sqrt{25 + 1.2 D_*^2} - 5)^{1.5} \qquad (3.23)$$

where D_* can be calculated as

$$D_* = d[(\rho_s / \rho - 1) g / v^2]^{1/3} \qquad (3.24)$$

In above equations that are used for determining settling velocity of sediment particles, the Corey shape factor is usually about 0.7. Many of researchers like Krumbein (1942), Corey (1949), had experimentally studied the influence of shape of particles on the settling velocity. According to these studies, the Subcommittee on

Sedimentation of the U.S. Interagency Committee on Water Resources (1957) proposed a series of curves. By this curves, with paying attention to particle size, Corey shape factor, and water temperature, presented the settling velocity of sediment particles can be determined (Figure 3.1).
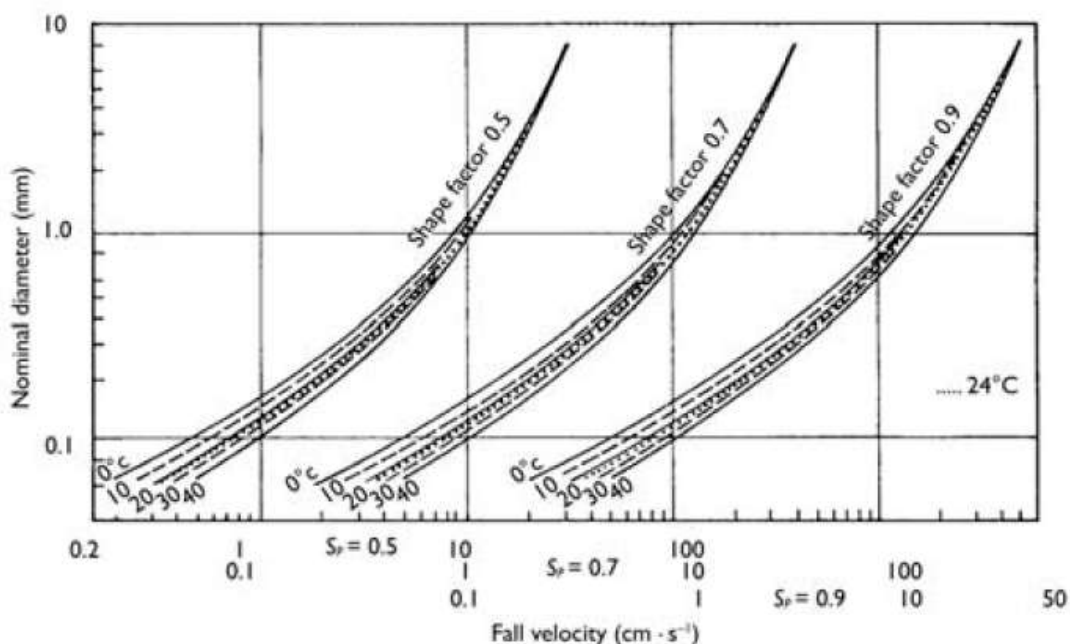

Figure 3.1 Relation of fall velocity with particle size, shape factor, and temperature (U.S. Interagency Committee, 1957).

Because of interpolations that must be used in order to found the solution, this graphical relation is not practical. With considering the influence of size, density, shape factor, and roundness factor of sediment particles, Dietrich (1982) suggested an empirical formula that can determine the settling velocity of sediment from laminar to turbulent settling regions. Because of a need to use the roundness factor that is rarely measured these relations are inconvenient.

Jimenez and Madsen (2003) tried to simplify the use of this relation, but it is still hard to use it. Wu and Wang (2006), with drived field data that measured by Krumbein (1942), Corey (1949), Wilde (1952), Schulz *et al.* (1954), and Romanovskii (1972), calibrated the coefficients '*M*', '*N*', and '*n*in Equation (3.22) as:

$$M = 53.5e^{-0.65S_P} \qquad N = 5.65e^{-2.5S_P} \qquad n = 0.7 + 0.9S_P \qquad (3.25)$$

where *SP* is the Corey shape factor that can be defined by $S_P = \dfrac{c}{\sqrt{ab}}$.

The comparison between measured drag coefficients and those calculated using equation (3.22) with coefficients determined by Equation (3.25) can be found in Figure 3.2. Because in Figure 3.2, the data is in reach of Re > 3, for range of *Re* < 3 they used the data sets of Zegzhda, Arkhangel'skii, and Sarkisyan compiled by Cheng (1997). In three sets of study naturally worn sediment particles were used so their Corey shape factors can be assumed as 0.7. The relationship between $^{,}C_d$ and $^{,}R_e$ can be seen in Figure 3.3.

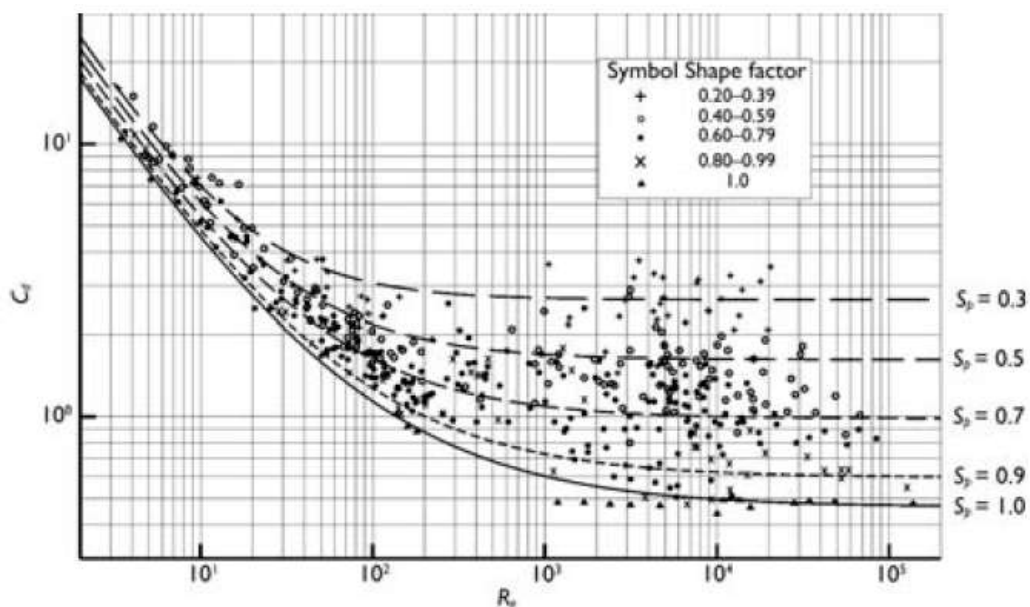Figure 3.2 Drag coefficient as function of Reynolds number and particle shape (Wu and Wang.2006).
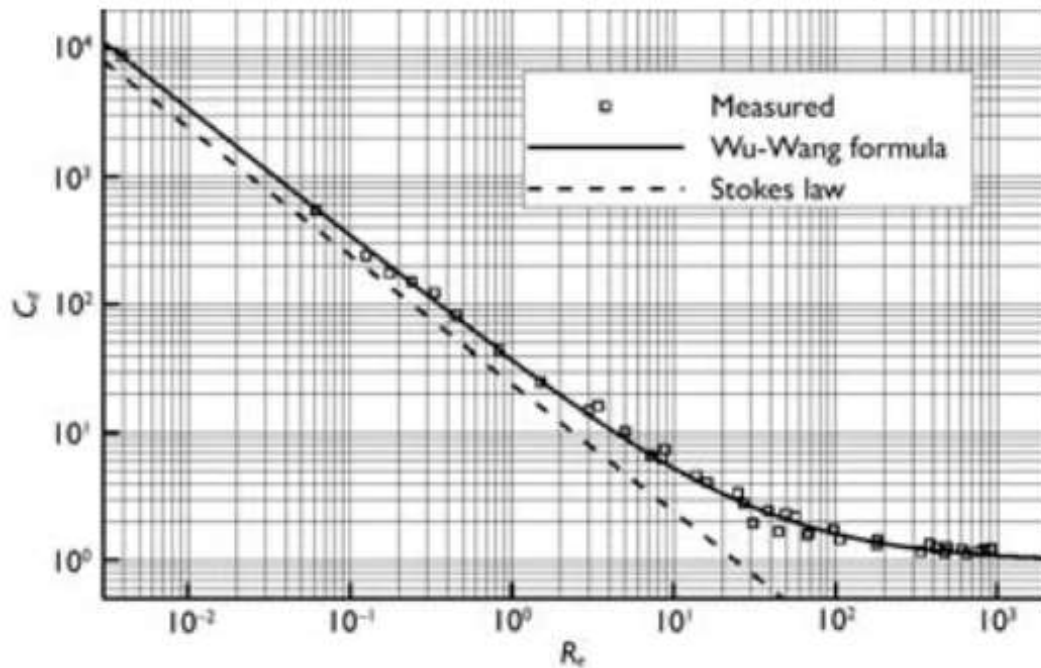
Figure 3.3 Drag coefficient as function of Reynolds number for naturally worn sediment particles ($S_p = 0.7$) (Wu and Wang, 2006).

Substituting Equation (3.22) into Equation (3.14), the general equation for settling velocity can be expressed as: (Wu and Wang, 2006)

$$\omega_s = \frac{M_v}{M_d}[\sqrt{\frac{1}{4}+(\frac{4N}{3M^2}D_*^3)^{\frac{1}{n}}}-\frac{1}{2}]^n \tag{3.26}$$

The size of sediment (d) in Equation (3.26) should be the nominal diameter (m), and value of drag coefficient C_d can be found in Figure 3.2

3.3 Inception Movement

3.3.1 Incipient Motion of Sediment Particles

The effecting forces on the non-cohesive sediment particles are drag forces (F_D), lift forces (F_L) and the submerged weight W_s (Figure 3.4).
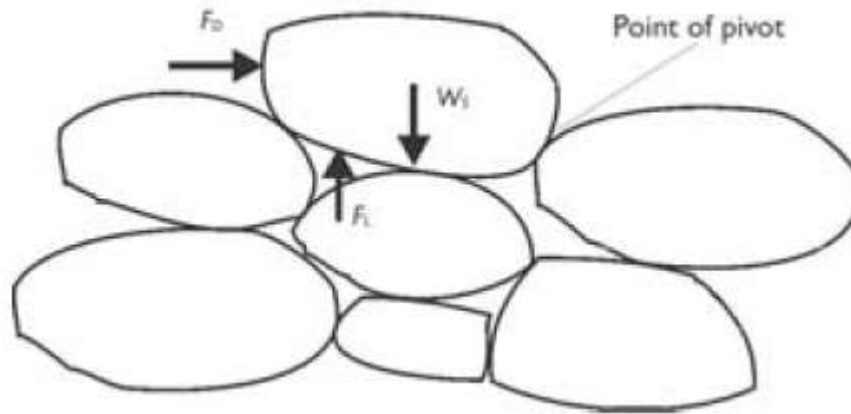
Figure 3.4 Forces on a sediment particle on bed.(Wu, 2007).

With increasing the strength of water, sediment particles on the bed load begin to move. This phenomenon is called as incipient motion. The inception of sediment particles can be classified into three parts: rolling, sliding, and saltating.

The balance of force for a sediment particle in rolling case at incipient motion can be expressed as:

$$-k_1\,dW_s + k_2\,dF_D + k_3 dF_L = 0 \tag{3.27}$$

where $k_1 d$, $k_2 d$, and $k_3 d$ are the distances from the lines of action of forces W_s, F_D, and F_L to the point of pivot.

and the influence of drag and lift forces on the sediment particles can be determined by

$$F_D = C_D a_2 d^2 \rho \frac{u_b^2}{2} \tag{3.28}$$

$$F_L = C_L a_3 d^2 \rho \frac{u_b^2}{2} \tag{3.29}$$

where u_b is the effect of velocity of bottom on the sediment particles. $a_2 d^2$ and $a_3 d^2$

are the projected areas of the particle on the planes normal to the flow direction and the vertical direction, respectively and C_D and C_L are the drag and lift coefficients, related to particle shape, position on the bed.

Substitute the Equations (3.12), (3.28), and (3.29), into Equation (3.27), critical bottom velocity for sediment incipient motion can be written as:

$$u_{bc} = (\frac{2k_1 a_1}{k_2 a_2 C_D + k_3 a_3 C_L} - \frac{\rho_s - \rho}{\rho} gd)^{1/2}$$ (3.30)

3.3.2 Incipient Motion of a Group of Sediment Particles

There are two approaches in order to estimate the incipient motion of group of sediment particles: stochastic and deterministic approaches.

The stochastic approach considers the sediment incipient motion as a random phenomenon due to the stochastic properties of turbulent flow and sediment transport. This approach usually does not adopt a threshold value of sediment transport rate as the criterion at which the sediment particles start moving. The pioneer using the stochastic approach for sediment transport is Einstein (1942, 1950), (Wu, 2007).

The deterministic approach can introduce a certain value for inception motion of sediment particles. In this approach, the assumption that the value of bed-load transport rate is zero, is meaningless. With various studies, investigators found that even when the power of flow is much weaker than the critical condition that proposed by Shields (1936), there are still some moving on sediment particles. Kramer (1935) defined three types for movement of bed load material: 1.weak movement that only a few part of fine materials can move on the bottom. 2. Medium movement that particles with mean diameter start the motion and 3. General movement that all the mixture is in movement. By the way, this classification is only qualitative and difficult to use. For this reason, in order to determine the incipient motion of sediment particles, several low levels of bed load transport rate were defined. For example Waterways Experiment Station, U.S. Army Corps of Engineers,

suggested $q_{b*} = 14 cm^3 m^{-1} \min^{-1}$, and $q_{b*}/(\rho_s d w_s) = 0.000317$ by Han and He (1984).

Yalin (1972), also suggested a quantitative criterion related to the number of particles moving on the bed.

Because of interactions among different size of classes in a mixture of non-uniform sediment particles the threshold criterion for incipient motion is more complex.

Parker et al. (1982), proposed the following relations in order to determine the incipient motion of non-uniform sediment particles on gravel beds:

$$W_k^* = \frac{q_{b*k}(\frac{\rho_s}{\rho}-1)}{\rho_{bk}(ghS_f)^{0.5}hS_f} = 0.002 \tag{3.31}$$

where W_k^* is a dimensionless bed-load transport rate, q_{b*k} is the volumetric transport rate per unit width for the kth size class of bed load, ρ_{bk} is the fraction by weight of the k th size class in bed material, h is the flow depth, and S_f is the energy slope.

3.3.3 Incipient Movement for Uniform Sediment Particles

Power-law distribution of velocity is

$$u = \frac{m+1}{m}(\frac{z}{h})^{1/m}U \tag{3.32}$$

Using Equation (3.32) and Equation (3.30), the critical average velocity for sediment motion can be written as:

$$U_c = k(\frac{\rho_s - \rho}{\rho}gd)^{1/2}(\frac{h}{d})^{1/m} \tag{3.33}$$

where U_c is the averaged of critical velocity over the cross-section ($m.s^{-1}$), and K is the experimental coefficient . For example, Shamov (1959), used $m = 6$ and $K = 1.14$,

while Zhang (1961), used $m = 7$ and $K = 1.34$. Paying attention to similarity of Equations (3.14), and (3.33) the following formula for the critical mean velocity can be obtained.

$$\frac{U_c}{\omega_s} = \begin{cases} 0.66 + 2.5/[\log(U_* d / v) - 0.06] & 1.2 < U_* d / v < 70 \\ 2.05 & U_* d / v \geq 70 \end{cases} \tag{3.34}$$

where U_* is the bed shear velocity.

In order to write critical shear stress, logarithmic distribution of velocity can be used

$$u = 5.75 U_* \log(30.2 \frac{zx_s}{k_s}) \tag{3.35}$$

The critical shear stress is

$$\frac{\tau_c}{(\gamma_s - \gamma)d} = \frac{2k_1 a_1}{k_2 a_2 C_D + k_3 a_3 C_L} \frac{1}{[5.75\log(30.2 z_d x_s / k_s]^2} \tag{3.36}$$

where τ_c is the critical shear stress for incipient movement of sediment particles, z_d is the height at which the bottom velocity acts on the particle, k_s is the height of bed roughness, and x_s is a correction factor that depends to the Reynolds number roughness $k_s U_* / v$ in general situations and a value of 1 can be used.

Parameters of C_D, C_L, and x_s in Equation (3.36), are functions of flow conditions. So Equation (3.36) can be rewritten as

$$\frac{\tau_c}{(\gamma_s - \gamma)d} = f(U_* d / v) \tag{3.37}$$

This equation is suggested by Shields (1936). $\dfrac{\tau_c}{(\gamma_s - \gamma)d}$ is a dimensionless parameter that is called as the critical Shields number and the symbol of this parameter is Θ_c. Many of investigators tried to modify Shields curve using wide

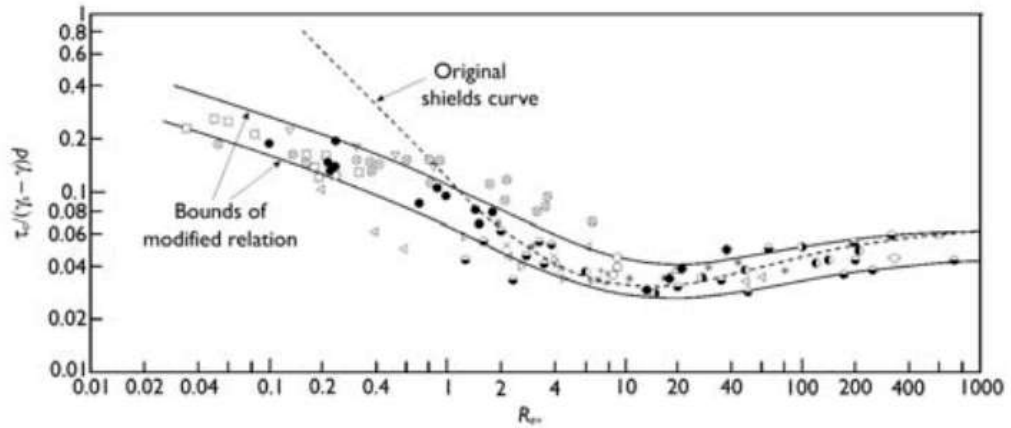range of data. One of these modifications done by Chien and Wan, can be found in Figure 3.5.

Figure 3.5 Shields curve modified by Chien and Wan (1983). (Wu, 2009).

Note that in Figure 3.5, the relation between Θ_c and R_{e*} is not explicit, therefore in order to obtain the critical shear stress for a given sediment size, iteration must be done. Instead of Figure 3.5 in order to obtain relation between Θ_c and the non-dimensional particle size $D_* = d\left[\left(\rho_s / \rho - 1\right) g / v^2\right]^{1/3}$, Equation (3.38), that suggested by (Wu and Wang, 1999) can be used.

$$\frac{\tau_c}{(\gamma_s - \gamma)d} = \begin{cases} 0.126 D_*^{-0.44} & D_* < 1.5 \\ 0.131 D_*^{-0.55} & 1.5 \leq D_* < 10 \\ 0.685 D_*^{-0.27} & 10 \leq D_* < 20 \\ 0.0173 D_*^{0.19} & 20 \leq D_* < 40 \\ 0.0115 D_*^{0.30} & 40 \leq D_* < 150 \\ 0.052 & D_* \geq 150 \end{cases} \tag{3.38}$$

where τ_c and d are in $N.m^{-2}$ and m, respectively.

3.3.4 Incipient Movement for Non- uniform Sediment Particles

Various size of non-uniform sediment particles in the bed load influence each other continuously. Generally coarse particles are more effected with water flow

instead of fine particles. Fine particles mostly hide between coarse ones. For this reason, considering the influence of these phenomena on non-uniform sediment transport is really important. Most of the researchers tried to suggest the correction factors for existing formulas in uniform sediment incipient motion and sediment transports.

3.3.4.1 Qin Equation (1980)

In order to determine the incipient motion of non-uniform sediment particles, Qin (1980) introduced the following equation.

$$U_{ck} = 0.786(\frac{h}{d_{90}})^{1/6}\sqrt{\frac{\gamma_s - \gamma}{\gamma}gd_k(1+2.5m\frac{d_m}{d_k})} \tag{3.39}$$

where U_{ck} is the critical average velocity for the incipient movement of the size of sediment particles in class k ($m.s^{-1}$), d_k is the diameter for the sediment particles in size class k(m), d_m is the arithmetic mean diameter of bed material (m), and m refers to the compactness for the bed material in non-uniform condition:

$$m = \begin{cases} 0.6 & \eta_d < 2 \\ 0.76059 - 0.68014/(\eta_d + 2.2353) & \eta_d \geq 2 \end{cases} \tag{3.40}$$

where $\eta_d = \dfrac{d_{60}}{d_{10}}$.

In order to determine the incipient motion of non-uniform sediment particles, many researchers like Egiazaroff (1965), Ashida and Michiue (1971), Hayashi et al. (1980), and Parker et al.(1982) proposed correction factors as functions of the non-dimensional sediment size $\dfrac{d_k}{d_m}$ or $\dfrac{d_k}{d_{50}}$.

3.3.4.2 Methods of Egiazaroff (1965)

The Egiazaroff formula can be written as

$$\frac{\Theta_{ck}}{\Theta_c} = \left[\frac{\log 19}{\log(19\frac{d_k}{d_m})}\right]^2 \tag{3.41}$$

where $\Theta_{ck} = \dfrac{\tau_{ck}}{[(\gamma_s - \gamma)d_k]}$, with τ_{ck} refers to the critical shear stress for the incipient movement of sediment particle d_k in bed material; and Θ_c is the critical Shields number that corresponding to *dm*. Egiazaroff suggested 0.06for the value of Θ_c , but Misri et al. (1984) modified this value and suggested it in the range of 0.023–0.0303 (Wu, 2007).

3.3.4.3 Ashida and Michiue (1971)

Ashida and Michiue (1971) suggested the modified form of Egiazaroff formula as:

$$\frac{\Theta_{ck}}{\Theta} = \begin{cases} [hog19/\log(19d_k/d_m)]^2 & d_k/d_m \geq 0.4 \\ d_m/d_k & d_k/d_m < 0.4 \end{cases} \tag{3.42}$$

3.3.4.4 Hayashi et al. (1980)

Hayashi *et al.* (1980) suggested a similar relation as:

$$\frac{\Theta_{ck}}{\Theta} = \begin{cases} [hog8/\log(8d_k/d_m)]^2 & d_k/d_m \geq 1 \\ d_m/d_k & d_k/d_m < 1 \end{cases} \tag{3.43}$$

3.3.4.5 Parker et al. (1982)

Parker *et al*. (1982) suggested the following:

$$\Theta_{ck} = \Theta_{c50}(\frac{d_k}{d_{50}})^{-m} \tag{3.44}$$

where Θ_{c50} is the critical Shields number by consider the medium size of sediment particles d_{50}, and *m* is an empirical coefficient in the range of 0.5–1.0.

3.3.4.6 Method of Wu et al (2000b)

The influence of drag and lift forces on sediment particles depends on three situations on the bed. Its position can be defined by apparent height which is defined between difference of top level of this sediment particle and upstream ones. This difference can be shown with Δ_e. If Δ_e is positive it means that particle is in exposed state. If it was negative it means that particle is in hidden station. In nature, distribution of sediment particles on bed is random. So Δ_e is a random variable .With assumption that Δ_e has a uniform probability distribution function can be written as:

$$f = \begin{cases} \dfrac{1}{d_k + d_j} & -d_j \leq \Delta_e \leq d_k \\ o & otherwise \end{cases} \tag{3.45}$$

where d_j is the diameter of the particle in upstream hand and d_k is the diameter of sediment particle. Illustration of mixture of sediment particles on the bed can be found in Figure (3.6).
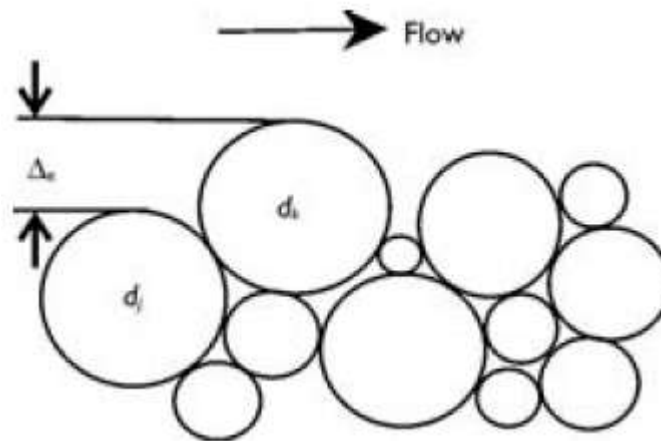
Figure 3.6 View of distribution of sediment particles. (Wu, 2007).

The probabilities of particles d_k that are hidden with upstream particles d_j is

$$P_{hk,j} = P_{bj} \frac{d_j}{d_k + d_j} \tag{3.46}$$

The probabilities of particles d_k that are exposed with upstream particle d_j is

$$P_{ek,j} = P_{bj} \frac{d_k}{d_k + d_j} \tag{3.47}$$

where P_{bj} is the probability of sediment particles d_j staying in front of particles d_k.

In order to find total hidden and exposed probabilities, P_{hk} and P_{ek}, of particles d_k, above equations over all size of classes must be accumulated.

$$P_{hk} = \sum_{j=1}^{N} P_{bj} \frac{d_j}{d_k + d_j} \tag{3.48}$$

$$P_{ek} = \sum_{j=1}^{N} P_{bj} \frac{d_k}{d_k + d_j} \tag{3.49}$$

where N is the total number of particle size classes in the non-uniform sediment mixture.

According to probability rules the sum of P_{hk} and P_{ek} must be equal to one. Whit uniform distribution of sediment particles, the hidden and exposed probabilities are equal, so $P_{hk} = P_{ek} = 0.5$. But in a non-uniform sediment mixture the governing station for coarse particles is $P_{hk} \leq P_{ek}$ and for fine particles is $P_{hk} \geq P_{ek}$.

By using the hidden and exposed probabilities, Wu *et al.* (2000) introduced hiding and exposure correction factor as:

$$\eta_k = (\frac{P_{ek}}{P_{hk}})^{-m} \tag{3.50}$$

where *m* is an empirical parameter.

The criterion for sediment incipient motion proposed by Shields (1936) is then modified as:

$$\frac{\tau_{ck}}{(\gamma_s - \gamma)d_k} = \Theta_c (\frac{P_{ek}}{P_{hk}})^{-m} \tag{3.51}$$

where $\Theta_c = 0.03$ and $m = 0.6$, which are found by laboratory and field measurements.

3.3.5 Incipient Motion of Sediment Particles on Slopes

On a sloped bed or bank the incipient motion of a sediment particle is influenced by the component of gravity along the slope.

Brooks (1963) suggested a method to determine $\tau_{c\varphi}$:

$$\frac{\tau_{c\varphi}}{\tau_c} = -\frac{\sin\varphi \sin\theta_s}{\tan\phi_r} + \sqrt{\cos^2\varphi - \frac{\sin^2\varphi \cos^2\theta_s}{\tan^2\phi_r}} \tag{3.52}$$

where φ is the angel of slope with positive values for down slope beds, θ_s is the angle between the flow direction and the horizontal line, and ϕ_r is the repose angle.

In order to determine the critical shear stress $\tau_{c\varphi}$ for the incipient motion of sediment on a sloped bed, Van Rijn (1989) also proposed this equation:

$$\tau_{c\varphi} = k_1 k_2 \tau_c \tag{3.53}$$

where k_1 is the correction factor for the streamwise-sloped bed (in the flow direction), determined by $k_1 = \sin(\phi_r - \varphi_L)/\sin\phi_r$; and k_2 is the correction factor for the sideward-sloped bed (normal to the flow direction), determined by $k_2 = \cos\varphi_T \sqrt{1 - \tan^2\varphi_T / \tan^2\phi_r}$. Here, φ_L and φ_T are the slope angles in the flow and sideward directions, respectively.

3.4 Roughness of Movable Bed

3.4.1 Bed forms

Bed forms in alluvial rivers are closely related to flow conditions. As the flow strength increases, a stationary flat bed may evolve to sand ripples, sand dunes, moving plane bed, anti-dunes, and chutes/pools (Richardson and Simons, 1967; Zhang *et al.*, 1989). Various form of bed changes can be found in figure 3.7
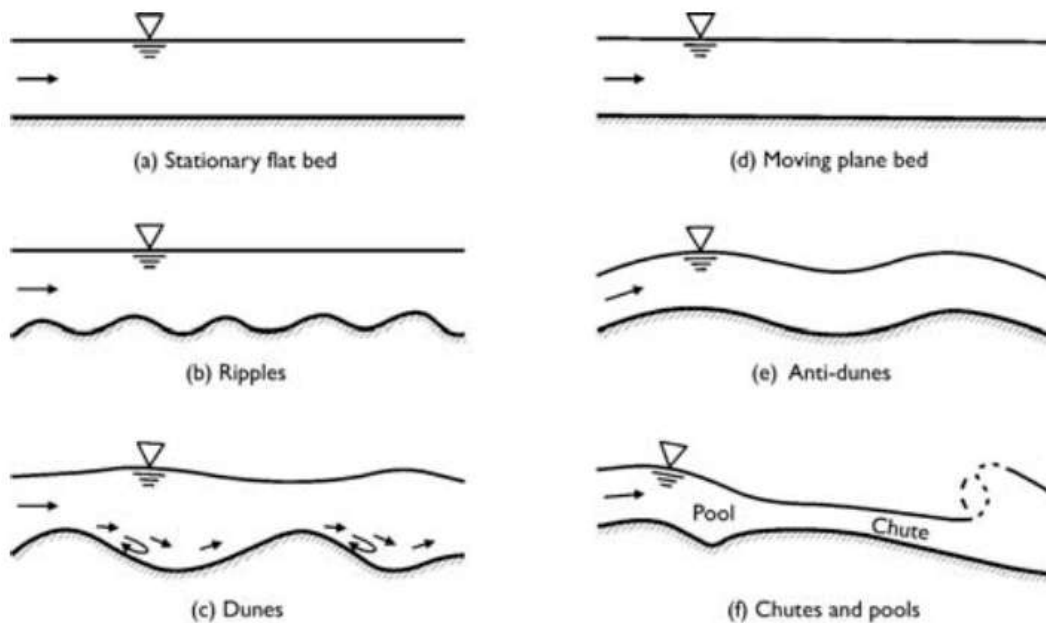
Figure 3.7 Bed forms in alluvial rivers (Zhang *et al.*, 1989).

The stationary flat bed, ripples, and dunes are mostly seen in lower flow, but moving plane bed, anti-dunes, and chutes/pools are usually happened in upper flow. Generally Anti-dunes and chutes/pools can happen in laboratory flumes but it is hard to face with it in nature.

3.4.2 Division of Grain and Form Resistances

The shear stress can be divided into two parts: 1 the grain (skin or frictional) shear stress τ'_b, 2. the bed forms (such as sand ripples and dunes) shear stress τ''_b:

$$\tau_b = \tau'_b + \tau''_b \tag{3.54}$$

The bed shear stress is generally determined by

$$\tau_b = \gamma R_b S_f \tag{3.55}$$

where R_b is the hydraulic radius of the channel bed.

Einstein (1942) proposed to divide shear stresses into two parts: grain roughness and form roughness, depending on hydraulic radius

$$\tau'_b = \gamma R'_b S_f \qquad\qquad \tau''_b = \gamma R''_b S_f \tag{3.56}$$

Considering Manning equations and in a equal velocity

$$U = \frac{R_b^{\frac{2}{3}} S_f^{\frac{1}{2}}}{n} \qquad U = \frac{R_b'^{\frac{2}{3}} S_f^{\frac{1}{2}}}{n'} \qquad\qquad U = \frac{R_b''^{\frac{2}{3}} S_f^{\frac{1}{2}}}{n''} \tag{3.57}$$

this relation between n, n' and n'' can be found.

$$R'_b = R_b (\frac{n'}{n})^{\frac{3}{2}} \text{ and } R''_b = R_b (\frac{n''}{n})^{\frac{3}{2}} \tag{3.58}$$

where U is the average flow velocity, n is the Manning roughness coefficient of channel bed flow velocity, n is the Manning roughness coefficient of channel bed,

and $n^{'}$ and $n^{''}$ are the Manning coefficients of grain and form roughness.

Accordingly, the following relations for the grain and shear stresses can be written.

$$\tau_b^{'} = (\frac{n^{'}}{n})^{3/2} \tau_b \qquad \tau_b^{''} = (\frac{n^{''}}{n})^{3/2} \tau_b \qquad\qquad (3.59)$$

The grain roughness coefficient can be determined by different methods. Some of these relations are:

$$n^{'} = \frac{d^{\frac{1}{6}}}{21.5} \qquad \text{(Strickler, 1923)} \qquad\qquad (3.60)$$

$$n^{'} = \frac{d_{90}^{\frac{1}{6}}}{26} \qquad \text{(Meyer-Peter and Mueller, 1948)} \qquad\qquad (3.61)$$

$$n^{'} = \frac{d_{65}^{\frac{1}{6}}}{24} \qquad \text{20 (Li and Liu, 1963; Wu and Wang, 1999)} \qquad\qquad (3.62)$$

where the unit of sediment size is m and unit of $n^{'}$ is $\frac{s}{m^{0.33}}$.

Substituting Equation (3.59) into Equation (3.50):

$$n^{\frac{3}{2}} = (n^{'})^{\frac{3}{2}} + (n^{''})^{\frac{3}{2}} \qquad\qquad (3.63)$$

In another approach, Engelund (1966) proposed that bed shear stress according to the energy slope can be divided and calculate the grain and form shear stresses can be calculated as:

$$\tau_b^{'} = \gamma R_b S_f^{'} \qquad\qquad \tau_b^{''} = \gamma R_b S_f^{''} \qquad\qquad (3.64)$$

where $S_f^{'}$ is the part of the energy slope for the grain roughness and $S_f^{''}$ is the part of the energy slope for the form roughness.

According to Manning's equation:

$$U = \frac{R_b^{2/3} S_f^{1/2}}{n} \;\; , U = \frac{R_b^{2/3} S_f^{(1/2)'}}{n'} \;\; , \;\; U = \frac{R_b^{2/3} S_f^{(1/2)''}}{n''} \tag{3.65}$$

Finally, the relation between S_f, S_f' and S_f'' can be written as:

$$S_f' = S_f (\frac{n'}{n})^2 \qquad , \; S_f'' = S_f (\frac{n''}{n})^2 \tag{3.66}$$

Substitute Equation (3.66) into Equation (3.64) and with many manipulation and using Equations (3.55) and (3.54) the following equation can be obtained as:

$$n^2 = (n')^2 + (n'')^2 \tag{3.67}$$

With paying attention can be found that Einstein's and Engelund's methods given the same relation for the Chezy coefficient:

$$\frac{1}{C_h^2} = \frac{1}{(C_h')^2} + \frac{1}{(C_h'')^2} \tag{3.68}$$

where C_h is the total Chezy coefficient; and C_h' and C_h' are the fractional Chezy coefficients for the grain and form roughness.

3.4.3 Relations of Movable Bed Roughness

In order to determine roughness coefficient of a movable bed level many of scientist suggested relations to determine the grain and form resistances separately, and some of them computed total roughness coefficient in a movable bed directly. Van Rijn (1984c) and Karim (1995) suggested empirical equation to predict the height of bed forms and then the roughness coefficient on a movable bed.

3.4.3.1 Van Rijn Relation (1984)

Van Rijn (1984), suggested the following relations for the sand-dune height:

$$\frac{\Delta}{h} = 0.11(\frac{d_{50}}{h})^{0.3}(1-e^{-0.5T})(25-T) \tag{3.69}$$

where T is the non-dimensional excess bed shear stress or the transport stage number, defined as

$$T = (\frac{U_*^{'}}{U_{*cr}})^2 - 1 \tag{3.70}$$

$U_*^{'}$ is the effective bed shear velocity related to grain roughness, determined by

$$U_*^2 = \frac{U_g^{0.5}}{C_h^{'}} \tag{3.71}$$

where

$$C_h^{'} = 18\log(\frac{4h}{d_{90}}) \tag{3.72}$$

U_{*cr} is the critical bed shear velocity for incipient movement of sediment particles, can be found in Shields diagram; and d_{50} and d_{90} are the characteristic diameters of sediment particles in bed level.

The relation above is expressed in curves of Figure (3.8) too.
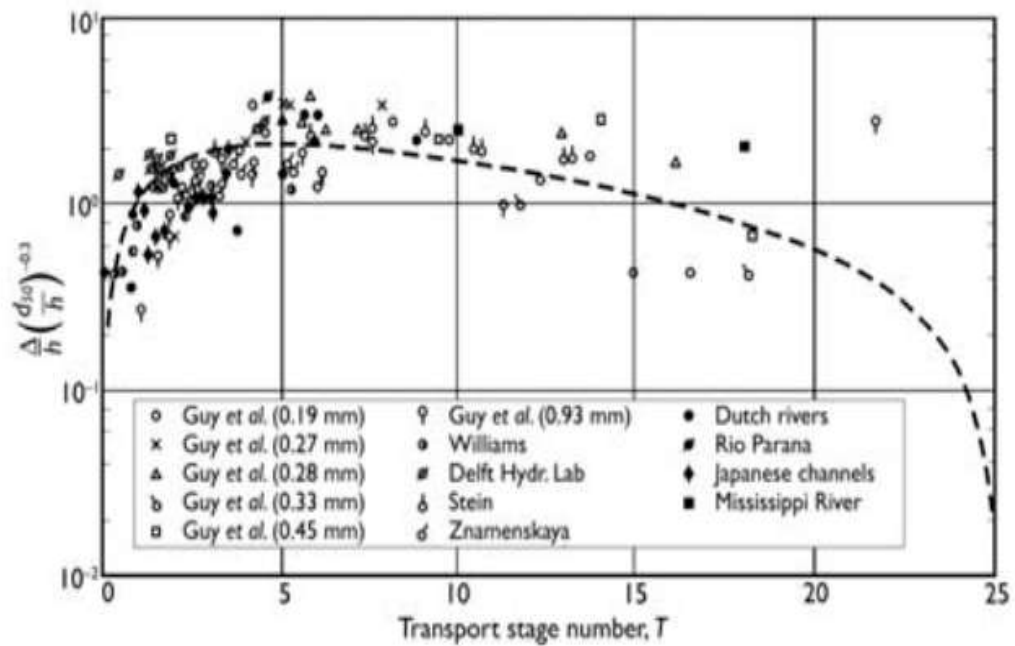
Figure 3.8 Relation of sand-dune height (van Rijn, 1984c).

In van Rijn's method, in order to calculate the length of sand dunes $\lambda_d = 7.3h$ can be use, and the grain roughness can be found by $3d_{90}$,moreover the form roughness can be found by $1.1\Delta\left(1-e^{-25\Delta/\lambda_d}\right)$. So the effective bed roughness can be determined by

$$k_s = 3d_{90} + 1.1\Delta(1-e^{-25\Delta/\lambda_d})$$ (3.73)

Therefore, the Chezy coefficient can be calculated by

$$C_h = 18\log(\frac{12R_b}{k_s})$$ (3.74)

where R_b can be computed using Vanoni and Brooks(1957) method.

3.4.3.2 Karim Equation (1995)

In order to compute the Manning roughness coefficient on a movable bed Karim (1995) suggested following relations

$$n = 0.037d_{50}^{0.126}(1.2 + 8.92\frac{\Delta}{h})^{0.465}$$ (3.75)

where dimension of Manning coefficient is $\dfrac{s}{m^{0.33}}$, and unit of d_{50} is meter. In this relation h is the hydraulic depth that can be calculated by dividing the flow area to water surface width.

For the value of $\dfrac{U_*}{\omega_s}$ in the range of (0.15-3.64), amount of Δ can be computed by following relations

$$\frac{\Delta}{h} = -0.04 + 0.294(\frac{U_*}{\omega_s}) + 0.00316(\frac{U_*}{\omega_s})^2 - 0.0319(\frac{U_*}{\omega_s})^3 + 0.00272(\frac{U_*}{\omega_s})^4 \qquad (3.76)$$

where ω_s is the settling velocity of sediment particles with size d_{50}. The graphic relation between Δ/h and $\dfrac{U_*}{\omega_s}$ can be found in Figure (3.9).
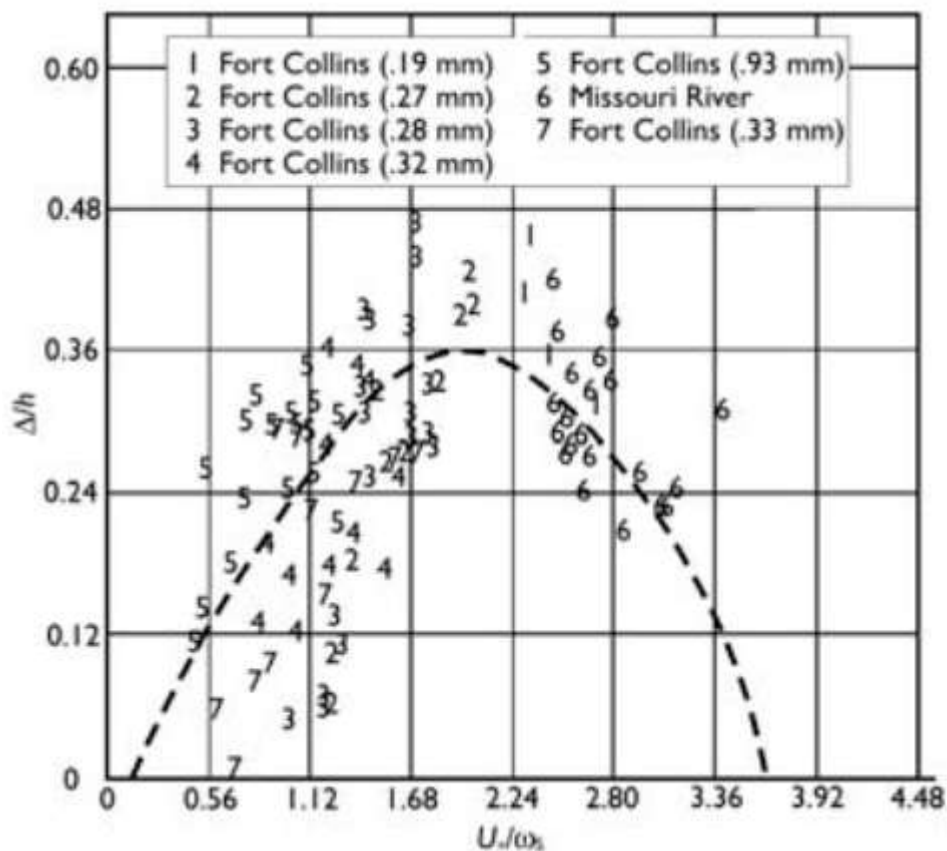
Figure 3.9 Relative roughness height as function of U_*/ω_s (Karim, 1995).

3.4.3.3 Wu-Wang Equation (1999)

Generally, for a movable bed, the Manning roughness coefficient can be related to the bed sediment size *d* by

$$n = \frac{d^{1/6}}{A_n} \qquad (3.77)$$

where A_n is a roughness parameter that depends to particle shape, flow conditions, bed forms, etc.

In a movable bed with sand waves, the influence of bed forms on A_n must be considerd .Li and Liu (1963), suggested the following relations for rivers.

$$A_n = \begin{cases} 20(\dfrac{U}{U_c})^{\frac{-3}{2}} & 1 < \dfrac{U}{U_c} \le 2.13 \\ 3.9(\dfrac{U}{U_c})^{\frac{2}{3}} & \dfrac{U}{U_c} > 2.13 \end{cases} \qquad (3.78)$$

Wu and Wang (1999), proposed the relation between $A_n/(g^{0.5}Fr^{0.33})$ and τ_b'/τ_{c50} in Figure (3.10) in order to improve equation (3.78).
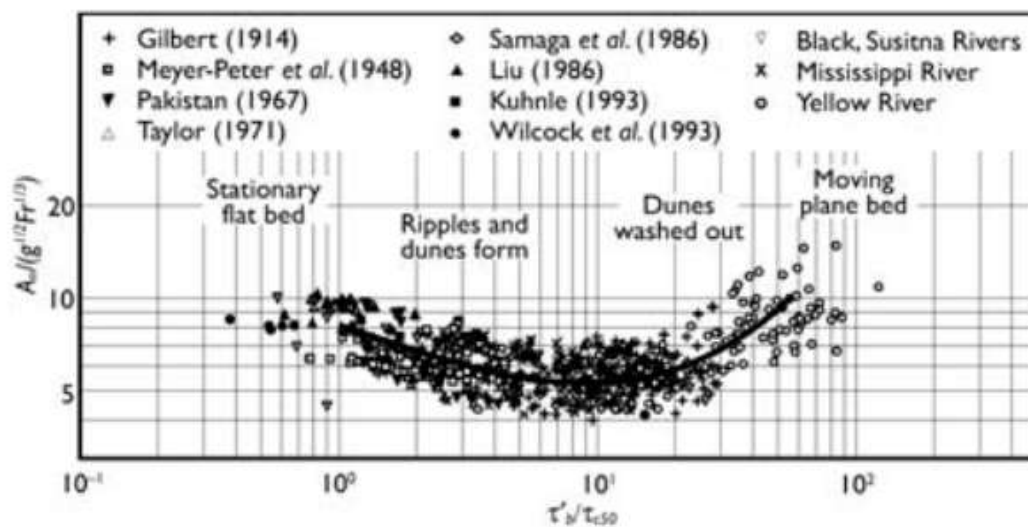
Figure 3.10 Relation between $A_n/(g^{0.5}Fr^{0.33})$ and τ_b'/τ_{c50} (Wu and Wang. 1999).

The values of $A_n/(g^{0.5}Fr^{0.33})$ decreases, and then, increases as τ_b'/τ_{c50} increases. Physically, this trend represents the fact that sand ripples and dunes are formed first, and then, washed away gradually. (Wu,2007)

In the range of (1-55) for value of τ_b'/τ_{c50} this curve can be formulated as:

$$\frac{A_n}{g^{0.5}Fr^{0.33}} = \frac{8[1+0.0235(\frac{\tau_b'}{\tau_{c50}})^{1.25}]}{(\frac{\tau_b'}{\tau_{c50}})^{0.33}} \qquad (3.79)$$

where Fr is the Froude number.

In order to calculate the critical shear stress the Shields curve modified by Chien and Wan (1983) can be used, n' can be determined by $n' = d_{50}^{1/6}/20$ and for value of τ_b and τ_b' (3.55) and (3.59) relations can be used.

The bed hydraulic radius can be calculated by following relation:

$$R_b = \frac{h}{1+0.055\dfrac{h}{B^2}} \qquad (3.80)$$

That is suggested by Williams (1970), where B is the channel width.

3.5 Bed-load Transport

Many of investigators, considering the field data and laboratory studies tried to develop various experimental formulas to determine bed-load transport in nature. Therefore, they used different approaches. Many of them divided sediment transport in two parts: Bed load sediment transport and suspended sediment transport. But another group tried to predict total of sediment transport together.

3.5.1 Computation of Total Sediment Transport in River

Many of researchers like Duboys (1879), Schoklitsch (1930), Meyer-Peter and Mueller (1948), Bagnold (1966, 1973), Dou (1964), Graf (1971), Yalin (1972), Engelund and Fredsøe (1976), and van Rijn (1984a) tried to proposed equations to predict total sediment transport .

3.5.1.1 Relation of Meyer, Peter, and Mueller (1948)

Meyer, Peter and Mueller (1948), suggested the following relation in order to express the bed-load transport rate

$$q_{b*} = 8.\gamma_s \sqrt{\Delta.g.d_{50}^3} (\tau_* - \tau_{*cr})^{3/2} \tag{3.81}$$

where q_{b*} is the bed-load transport rate that defined by weight per unit time and width ($N/m.s$), γ_s is the specific weight of sediment particles , d_{50} is the bed material size where 50% of the material is finer in mm, Δ is the relative specific gravity and, τ_* and τ_{*cr} are the dimensionless shear stress and dimensionless critical bed shear stresses.

Δ can be calculated as:

$$\Delta = \frac{(\gamma_s - \gamma)}{\gamma} \tag{3.82}$$

where γ_s and γ are the specific weights of sediment and water. It must be noted that Δ is a dimensionless parameter.

Bed shear stress can be obtain from

$$\tau_* = \frac{u_*^2}{g.\Delta.ds} \tag{3.83}$$

where ds is the diameter of sediment particle that can be use d_{50} of mixture of

sediment particles and u_* is critical shear velocity that is defined as

$$u_* = \sqrt{\frac{\tau_0}{\rho}} = \sqrt{g.R.S_f}$$

where τ_0 is the shear stress, ρ is the density of water, g is the gravity acceleration, R is the hydraulic radius and S_f is the friction slope. They suggested value of critical dimensionless bed shear stress as $\tau_{*cr} = 0.047$.

Many of researchers tried to improve this relation.

Note that in relations below, values of τ_* calculated by equation (3.83).

3.5.1.2 Relation of Ashida and Michue (1972)

Ashida and Michue (1972), give the following equation:

$$q_{b*} = 17.\gamma_s \sqrt{\Delta.g.d_{50}^3}(\tau_* - \tau_{*cr})(\sqrt{\tau_*} - \sqrt{\tau_{*cr}}) \tag{3.84}$$

They suggested the value of τ_{*cr} as 0.05.

3.5.1.3 Relation of Fernandez Luque and van Beek (1976)

Fernandez Luque and van Beek (1976), suggested:

$$q_{b*} = 5.7.\gamma_s \sqrt{\Delta.g.d_{50}^3}(\tau_* - \tau_{*cr})^{3/2} \tag{3.85}$$

They proposed a value between ranges of $\tau_{*cr} = 0.037 - 0.0445$

3.5.1.4 Relation of Engelund and Fredsøe (1976)

$$q_{b*} = 18.74 \cdot \gamma_s \sqrt{\Delta.g.d_{50}^3} (\tau_* - \tau_{*cr})(\sqrt{\tau_*} - 0.7\sqrt{\tau_{*cr}}) \tag{3.86}$$

They proposed the value of critical shear stress as $\tau_{*cr} = 0.05$.

3.5.1.5 Relation of Parker (1979)

$$q_{b*} = 11.2 \cdot \gamma_s \sqrt{\Delta.g.d_{50}^3} \frac{(\tau_* - \tau_{*cr})^{4.5}}{\tau_*^3} \tag{3.87}$$

where $\tau_{*cr} = 0.03$.

3.5.1.6 Relation of Wong (2003)

Wong (2003), suggested this formula

$$q_{b*} = 4.93 \cdot \gamma_s \sqrt{\Delta.g.d_{50}^3} (\tau_* - \tau_{*cr})^{1.6} \tag{3.88}$$

He proposed $\tau_{*cr} = 0.047$ for equation above.

3.5.1.7 Relation of Wong and Parker(2006)

$$q_{b*} = 3.97 \cdot \gamma_s \sqrt{\Delta.g.d_{50}^3} (\tau_* - \tau_{*cr})^{1.5} \tag{3.89}$$

where $\tau_{*cr} = 0.0495$.

3.5.1.8 Relation of Tayfur and Singh(2006)

Tayfur and Singh (2006), proposed the following relations to predict sediment transports in alluvial channels.

$$q_{b*} = \gamma_s.pv_s z \left[1 - \frac{z}{z_{max}} \right] \tag{3.90}$$

where p is the porosity of sediment layer, v_s is the velocity of sediment particles as concentration approaches zero(L/s), z refers to thickness of bed layer and $z_{\max}$ is the maximum thickness of bed layer.

In order to determine the value of velocity of sediment particles, researchers suggested different relations. For example, Kalinske (1947) suggested the fallowing relations.

$$v_s = b(u - u_c) \tag{3.91}$$

where b is a constant coefficient that is near to unit, u_c is the critical fall velocity at incipient motion, v_s is the sudden velocity of sediment particles and u is the sudden velocity of fluid .

As an another approach, the value of velocity of sediment particles v_s as $0.01 m/s$ can be selected.

3.5.1.8 Bagnold Relation(1966, 1973)

Bagnold (1966, 1973), suggested bed-load transport formula as below

$$q_{b*} = \frac{\rho_s}{\rho_s - \rho} \frac{\tau_b U}{\tan \alpha} \frac{U_* - U_{*c}}{U_*} (1 - \frac{5.75 U_* \log(\frac{0.37h}{n_d}) + \omega_s}{U}) \tag{3.92}$$

where q_{bs} is the bed-load transport rate that defined by weight per unit time and width ($N/m.s$), $\tan \alpha$ is the friction coefficient of about 0.63, d is the sediment size (m), n_d is the average height of acting force during a saltation and τ_b is the bed shear stress (Wu, 2007).

The value of n can be computed by

$$n = 1.4\left(\frac{U_*}{U_{*c}}\right)^{0.6} \tag{3.93}$$

Equation (3.93) makes a relation between sediment transport and steam power.

3.5.1.9 Dou Relation(1964)

Dou (1964), proposed the following equation

$$q_{b*} = k_0 \frac{\rho_s}{\rho_s - \rho} \tau_b (U - U_c') \frac{U}{g\omega_s} \tag{3.94}$$

where unit of q_{b*} in this relation is mass per unit time per width ($kg/m.s$), U_c' is the critical average velocity for sediment particles to cease motion, and k_0 is an empirical coefficient . amount of $k_0 = 0.01$ for sand can be used.

3.5.1.10 Yalin Relation(1972)

Yalin (1972), by paying attention to bed-load velocity and weight suggested the following relation:

$$\frac{q_{b*}}{\gamma_s dU_*} = 0.635s\left[1 - \frac{1}{as}\ln(1+as)\right] \tag{3.95}$$

where q_{b*} is the bed-load transport rate that defined by weight per unit time and width ($N.m^{-1}.s^{-1}$).

The value of s can be calculated by

$$s = \frac{\Theta - \Theta_c}{\Theta_c} \tag{3.96}$$

The value of a can be determined by

$$a = 2.45\sqrt{\Theta_c}(\frac{\gamma}{\gamma_s})^{0.4} \tag{3.97}$$

where Θ is the Shields number.

3.5.2 Fractional Transport Rate of Bed Load

Many of investigators like Einstein (1950), Ashida and Michiue (1972), Parker et al.(1982), Misri et al. (1984), Samaga et al. (1986a), etc. studied about fractional transport rate of non-uniform sediments and suggested several methods and formulas about it. Some of these methods and relations are introduced below.

3.5.2.1 Einstein Relation (1942, 1950)

Einstein (1942, 1950), considered the probability of sediment transport due to the fluctuation of turbulent flow and established sediment transport functions based on fluid mechanics and probability theory. (Wu, 2007) .Einstein bed-load function is graphically given in Figure 3.11 and expressed as

$$1 - \frac{1}{\sqrt{\pi}} \int_{\frac{-1}{7}\Psi_{*k}^{-2}}^{\frac{1}{7}\Psi_{*k}^{-2}} e^{-t^2} dt = \frac{43.5\Phi_{*k}}{1+43.5\Phi_{*k}} \tag{3.98}$$

where vales of Φ_{*k}, Ψ_{*k}, Ψ, β, β_x, Δ_x, X and δ can be determined by

$$\Phi_{*k} = \frac{q_{b*k}}{\left[P_{bk}\gamma_s\sqrt{\frac{\gamma_s}{\gamma-1}gd_k^3}\right]} \tag{3.99}$$

$$\Psi_{*k} = \xi_b Y(\frac{\beta^2}{\beta_x^2})\Psi \tag{3.100}$$

$$\Psi = \frac{(\gamma_s - \gamma)d_k}{\gamma R'S_f} \tag{3.101}$$

$$\beta = \log 10.6 \tag{3.102}$$

$$\beta_x = \log(\frac{10.6X}{\Delta_s}) \tag{3.103}$$

$$\Delta_s = \frac{k_s}{\chi_s} \tag{3.104}$$

$$X = \begin{cases} 0.77\Delta_s & \dfrac{\Delta_s}{\delta} > 1.8 \\ X = 1.39\delta & \dfrac{\Delta_s}{\delta} \leq 1.8 \end{cases} \tag{3.105}$$

$$\delta = \frac{11.6v}{U_*^{'}} \tag{3.106}$$

where q_{b*k} is the bed-load transport rate of size class k by weight per unit time and width($N/m.s$), Y and ξ_b are the pressure and hiding correction factors for non-uniform sediment, $R^{'}$ is the hydraulic radius due to grain roughness, that can be calculated by using Einstein's movable bed roughness method. In order to determine the value of apparent roughness of bed surface (Δ_s), the amount of k_s is d_{65} and vale of χ_s can be computed by Equation (3.36), where δ is the laminar sub-layer thickness.
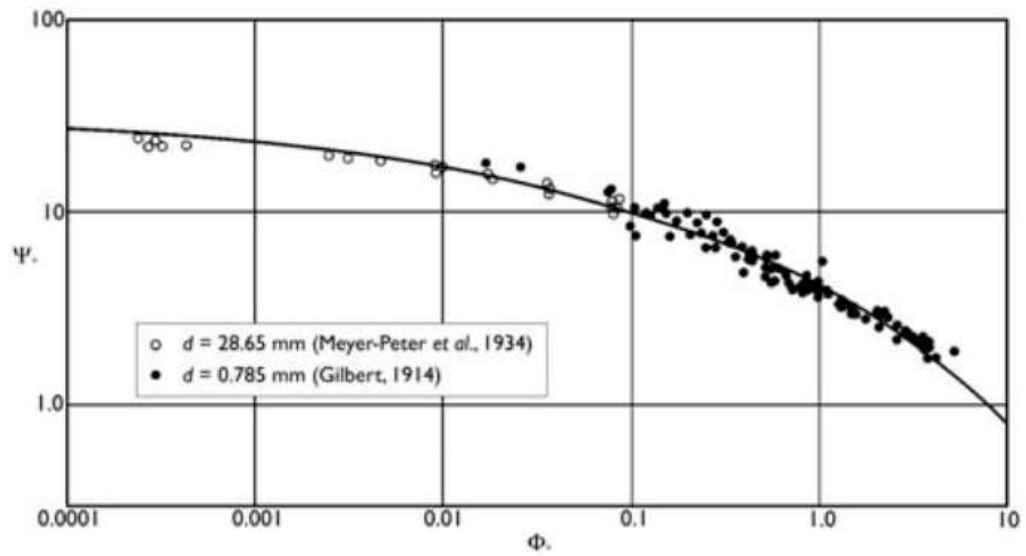
Figure 3.11 Einstein's (1950) bed-load function compared with uniform sediment data. (Wu, 2007).

3.5.2.2 Parker et al. Relation (1982)

Parker *et al.* (1982), developed a gravel transport equation that can be found in Figure 3.12. The basic concept of this relation is equal mobility of sediment particles. The dimensionless bed load transport rate that proposed by Parker W_k^* is defined in Equation (3.31) and the dimensionless shear stress θ_k is

$$\theta_k = \frac{hS_f}{(\frac{\rho_s}{\rho-1})d_k\tau_{rk}^*} \tag{3.107}$$

where

$$\tau_{rk}^* = 0.0875\frac{d_{50}}{d_k} \tag{3.108}$$
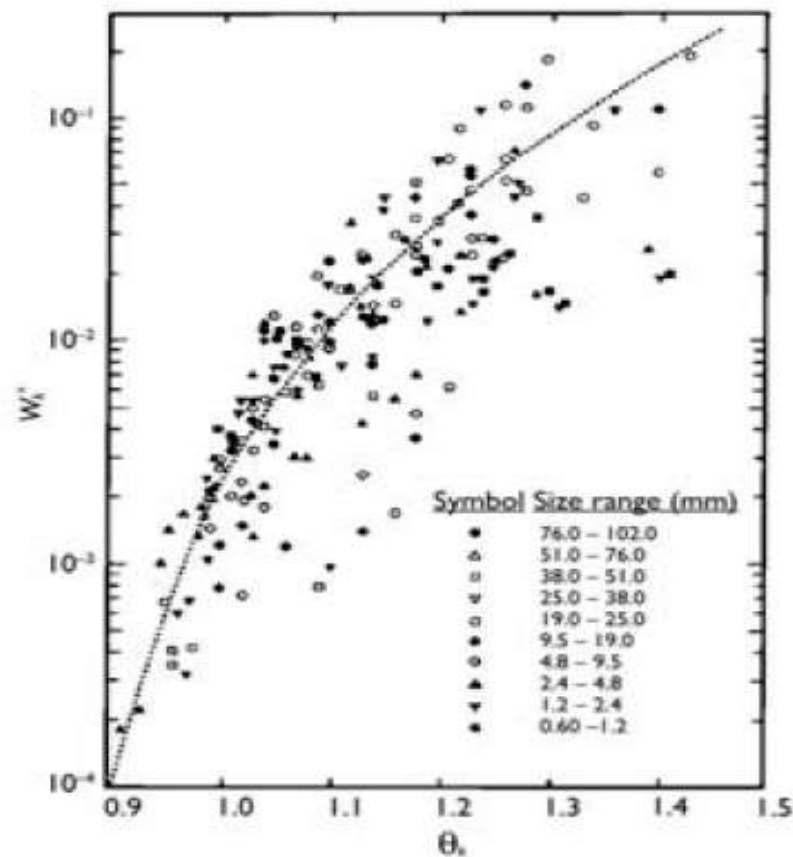
Figure 3.12 Gravel transport function of Parker et al. (1982).(Wu, 2007)

By considering equal mobility for all grain size, only value of d_{50} is used to characterize the bed-load transport rate as

$$W_k^* = \begin{cases} 0.0025\exp[14.2(\theta_{50}-1)-9.28(\theta_{50}-1)^2 & 0.95 < \theta_{50} < 1.65 \\ 11.2(1-\dfrac{0.822}{\theta_{50}})^{4.5} & \theta_{50} \geq 1.65 \end{cases} \quad (3.109)$$

where θ_{50} is the dimensionless shear stress with paying attention to sub-pavement size d_{50}.

3.5.2.3 Hsu and Holly's Relation (1992)

Hsu and Holly (1992), in order to calculate whole of sediment transport rate, initially compute the size of transported sediment distribution. The amount of each size of carried sediment depends to two things. Firstly the govern hydraulic condition,

and secondly, the availability of that size of sediment particles on bed surface. With assumption that the Gaussian probability distribution is the govern probability distribution, the mobility of size of class k can be determined by

$$P_{mo,k} = \frac{1}{\sigma\sqrt{2\pi}} \int\limits_{\frac{U_{ck}}{\bar{U}}-1}^{\infty} \exp(-\frac{x^2}{2\sigma^2})dx \tag{3.110}$$

where $\bar{U}$ is the mean velocity of flow; σ is the standard deviation of the normalized fluctuating velocity that can be calculated by $U'/\bar{U}$,but usually can use a value of 0.2 for it. U_{ck} is the incipient velocity of size class k that can be computed by Qin relation (3.39) that modified by recalibrating the coefficient 0.786 as 1.5.

The proportion of size of class k in the transported material can be written by

$$P_k = \frac{P_{m0,k}P_{bk}}{\sum\limits_{d\min}^{d\max} P_{mo,k}P_{bk}} \tag{3.111}$$

where P_{bk} is the ratio of size class k on the bed surface.

Finally, in order to calculate the total bed-load transport rate can be used the modified form of Shamov equation

$$q_{b*} = 12.5\sqrt{d_{mt}}(\bar{U}-U_{c\min})(\frac{\bar{U}}{U_{ct}})^3(\frac{d_{mt}}{h})^{1/4} \tag{3.112}$$

where d_{mt} is the mean size, U_{ct} is the mean incipient velocity, q_{b*} is defined by total transport rate of bed load per width o unit channel($kg.m^{-1}.s^{-1}$) and $U_{c\min}$ is the incipient velocity of the smallest size class ($m.s^{-1}$).

3.5.2.4 Ranga Raju et.al Relation (1996)

In order to calculate the fractional transport rate of non-uniform bed load Ranga Raju and his co-workers (Misri et al., 1984; Samaga et al., 1986a; Patel and Ranga

Raju, 1996) reformed the uniform bed-load equation that suggested by Paintal (1971). Patel and Ranga Raju revised hiding-exposure correction factor that proposed by Misri *et al*. (1984).

$$\Phi_{bk} = \frac{q_{b*k}}{P_{bk}\gamma_s \sqrt{(\frac{\gamma_s}{\gamma}-1)gd_k^3}} \tag{3.113}$$

$$\tau_{eff} = \xi_b \tau_b' \tag{3.114}$$

where Φ_{bk} is the dimensionless bed-load transport rate, τ_{eff} is the effective shear stress and ξ_b is the hiding-exposure correction factor ξ_b.

The values of τ_b', R_b' and n' are

$$\tau_b' = \gamma R_b' S_f \quad , R_b' = (\frac{Un'}{S_f^{1/2}})^{\frac{3}{2}} \quad , n' = \frac{d_{65}^{\frac{1}{6}}}{24} \tag{3.115}$$

ξ_b for the effective shear stress determined by

$$C_m \xi_b = 0.0713(C_s \tau_{*k}')^{-0.75144} \tag{3.116}$$

$$\tau_{*k}' = \frac{\tau_b'}{(\gamma_s - \gamma)d_k} \tag{3.117}$$

$$\log C_s = -0.1957 - 0.9571\log\frac{\tau_b'}{\tau_c} - 0.1949\left[\log\frac{\tau_b'}{\tau_c}\right]^2 + 0.0644\left[\log\frac{\tau_b'}{\tau_c}\right]^3 \tag{3.118}$$

$$C_m = \begin{cases} 1 & M > 0.38 \\ 0.7092\log M + 1.293 & 0.05 < M \leq 0.38 \end{cases} \tag{3.119}$$

where τ_c is the critical shear stress for the arithmetic mean size d_m, and M is the Kramer uniformity coefficient.
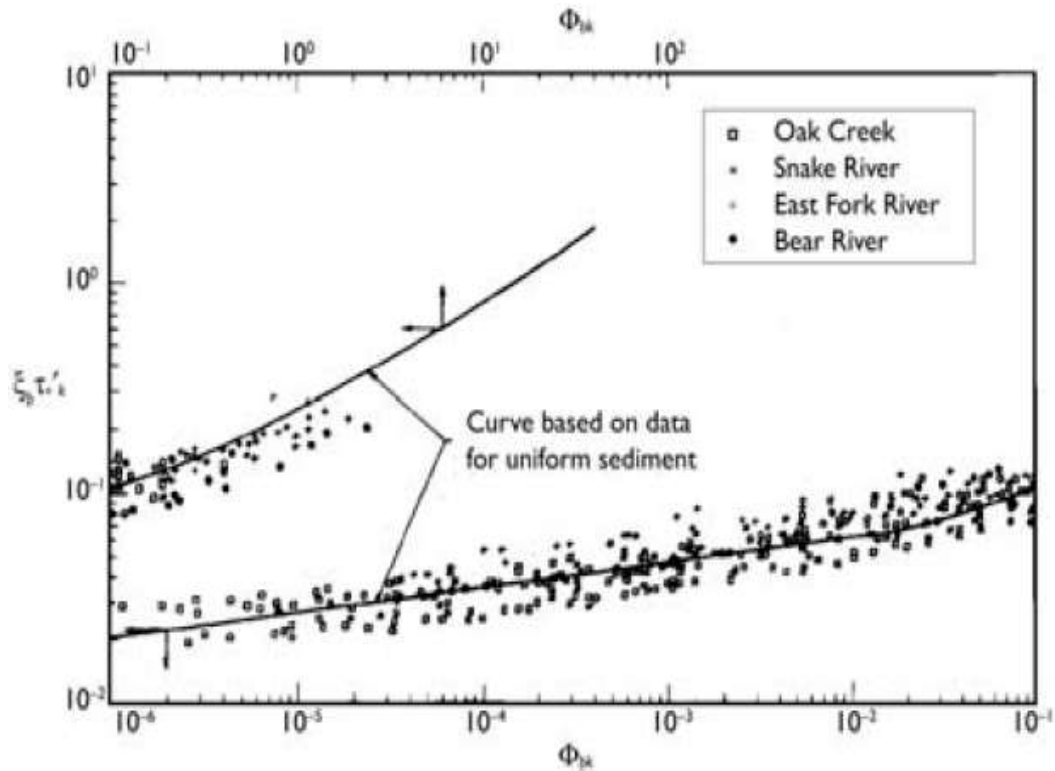
Figure 3.13 Fractional bed-load function (Patel and Ranga Raju, 1996).

3.5.2.5 Wu et al. Relation (2000)

In order to calculate the fractional transport rate of non-uniform bed load Wu *et al.* (2000), suggested the following relation and graphically curve in Figure 3.14

$$\Phi_{bk} = 0.0053\left[(\frac{n'}{n})^{\frac{3}{2}} \frac{\tau_b}{\tau_{ck}} - 1 \right]^{2.2} \tag{3.120}$$

where $\Phi_{bk} = q_{b*k} / \left[P_{bk} \sqrt{(\gamma_s / \gamma - 1)g d_k^3} \right]$, q_{b*k} is by volume per unit time and width $m^2 s^{-1}$, $n' = d_{50}^{1/6} / 20$, and *n* is the Manning roughness coefficient of channel bed.
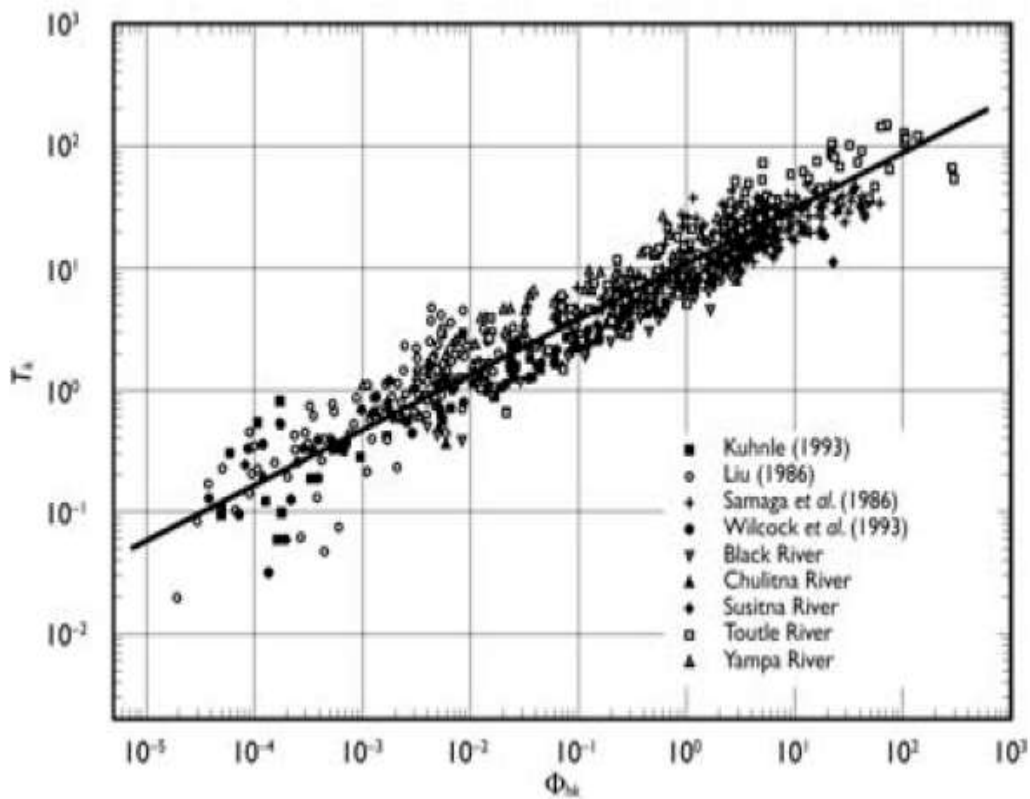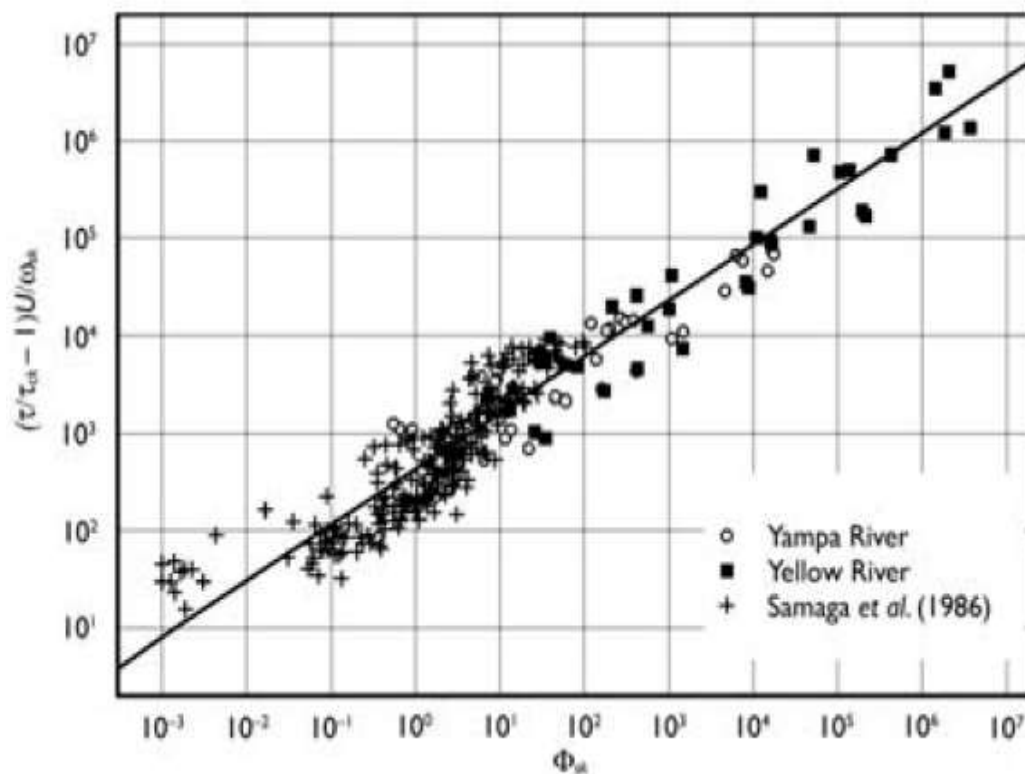
Figure 3.14 Relation of fractional bed-load transport rate (Wu et al., 2000b).

3.6 Suspended-load Transport

3.6.1 Concentration of Suspended Load on Near Bed

Many of investigators like Einstein, van Rijn, and Zyserman-Fredsøe etc. suggested formulas for predict concentration of single or multi size of suspended load in near bed level.

3.6.1.1 Einstein Relation (1950)

Einstein (1950), set the reference level of suspended-load concentration at two grain diameters above the channel bed and related the near-bed concentration of suspended load to the bed-load transport rate q_{b*k} as follows(Wu, 2007)

$$c_{b*k} = \frac{1}{11.6} \frac{q_{b*k}}{\delta U_*^{'}}$$
(3.121)

where c_{b*k} is the concentration at the reference level δ *for* the k th size of sediment particles (by weight per unit volume), and $U_*^{'}$ is the friction velocity on skin level.

3.6.1.2 Van Rijn Relation

Van Rijn (1984), suggested the following relation.

$$c_{b*} = 0.015 \frac{d_{50} T^{1.5}}{\delta D_*^{0.3}} \tag{3.122}$$

where δ is the reference level at the equivalent roughness height k_s, c_{b*} is the volumetric concentration of suspended load at the reference level, values of T can be calculated by Van Rijn relations(3.69) and D_* can be determined by

$$q_{b*} = 0.053((\rho_s - \rho)g / \rho)^{0.5} (d_{50}^{1.5} T^{2.1} / D_*^{0.3})$$

3.6.1.3 Zyserman-Fredsøe Relation (1994)

Zyserman and Fredsøe (1994), set the reference level at two grain diameters above the bed and determined the near-bed volumetric concentration of suspended load as: (Wu, 2007)

$$c_{b*} = \frac{0.331(\Theta^{'} - 0.045)^{1.75}}{1 + 0.72(\Theta^{'} - 0.045)^{1.75}} \tag{3.123}$$

where

$$\Theta^{'} = \frac{U_*^{2^{'}}}{\left[(\frac{\rho_s}{\rho - 1})gd \right]} \tag{3.124}$$

3.6.2 Suspended-load Transport Rate

3.6.2.1 Einstein Relation (1950)

In order to compute the suspended-load transport rate Einstein (1950), suggested a method that use integration of product of local sediment concentration c_k and flow velocity u over the suspended-load zone from δ $(=2d)$ to h :

$$q_{s*k} = \int_{\delta}^{h} c_k u dz \tag{3.125}$$

where q_{s*k} is the transport rate of suspended load in the k th size class.

With considering the govern of Rouse distribution to the concentration of sediment ($\sigma_s = 1$) and the logarithmic distribution of flow velocity in Equation (3.35) (substitute U_* by U'_*) yields

$$q_{s*k} = \int_{\delta}^{h} c_{b*k} (\frac{\frac{h}{z}-1}{\frac{h}{z}-1})^{\frac{\omega_{sk}}{kU_*}} * 5.75 U'_* \log(30.2\frac{z}{\Delta_s}) dz$$

$$= 11.6 U'_* c_{b*k} \delta \left[2.303 \log(\frac{30.2h}{\Delta_s}) * I_{1k} + I_{2k} \right] \tag{3.126}$$

$$I_{1k} = 0.216 \frac{\xi_b^{r_k-1}}{(1-\xi_b)^{r_k}} \int_{\xi_b}^{1} (\frac{1-\xi}{\xi})^{r_k} d\xi \tag{3.127}$$

$$I_{2k} = 0.216 \frac{\xi_b^{r_k-1}}{(1-\xi_b)^{r_k}} \int_{\xi_b}^{1} (\frac{1-\xi}{\xi})^{r_k} \ln \xi d\xi \tag{3.128}$$

$$\xi = \frac{z}{h} \qquad \xi = \frac{\delta}{h} \qquad r_k = \frac{\omega_{sk}}{kU_*} \tag{3.129}$$

With substitute Equation (3.115) into Equation (3.120) can be found that

$$q_{s*k} = q_{b*k} \left[2.303 \log(\frac{30.2h}{\Delta_s}) * I_{1k} + I_{2k} \right] \tag{3.130}$$

Consequently q_{t*k} is

$$q_{t*k} = q_{b*k} + q_{s*k} \tag{3.131}$$

3.6.2.2 Bagnold Relation (1966)

Bagnold (1966), relation is

$$q_{s*} = 0.01 \frac{\rho_s}{\rho_s - \rho} \frac{\tau_b U^2}{\omega_s} \tag{3.132}$$

where q_{s*} is the suspended-load transport rate ($N.m^{-1}.s^{-1}$)

3.6.2.3 Zhang Relation (1961)

Zhang (1961), with considering the concept of the energy balance of sediment-laden flow, suggested the following relation as:

$$C_* = \frac{1}{20} (\frac{U^3}{gR\omega_s})^{1.5} \left/ \left[1 + (\frac{1}{45} \frac{U^3}{gR\omega_s})^{1.15} \right] \right. \tag{3.133}$$

Also can be found the graphic model of this relation in Figure (3.15) which show the relation between suspended-load transport capacity C_* and parameter $U^3 / gR\omega_s$.
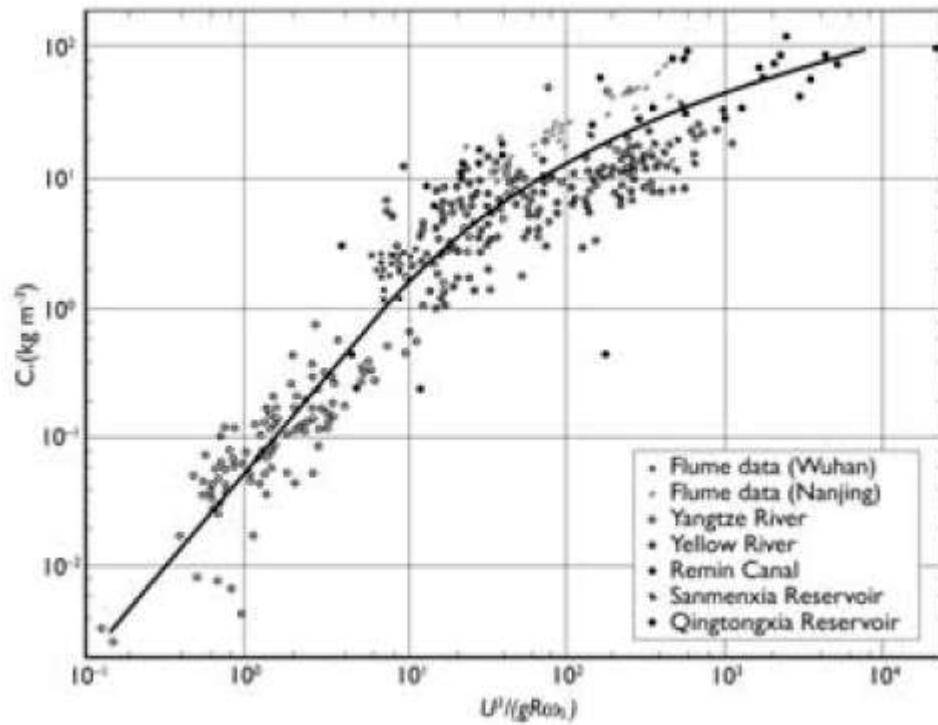
Figure 3.15 Relation of C_* and $U^3 \big/ (gR\omega_s)$ (Zhang, 1961).

3.6. 2.4 Wu et al. Relation (2000)

With considering concept of stream power that suggested by Bagnold's (1966) and by using laboratory data that measured by Samaga *et al*. (1986) and two sets of field data that evaluate in Yampa and Yellow Rivers Wu (2000b) suggested the following relation

$$\Phi_{sk} = 0.0000262 \left[(\frac{\tau}{\tau_{ck}} - 1) \frac{U}{\omega_{sk}} \right]^{1.74} \tag{3.134}$$

$$\Phi_{sk} = \frac{q_{s*k}}{\left[P_{bk} \sqrt{(\frac{\gamma_s}{\gamma - 1}) g d_k^3} \right]} \tag{3.135}$$

where q_{s*k} is the suspended-load transport rate ($m^2.s^{-1}$).

In addition can be used the curve of Figure (3.16).instead of relation above.

Figure 3.16 Relation of fractional suspended-load transport rate (Wu *et al.*, 2000b).

3.7 Bed and Suspended Load Transport

3.7.1 Total Transported Material

3.7.1.1 Laursen Relation (1958)

In order to predict the total average concentration of material that transported by flow, with considering the size of sediment particles Laursen (1958) suggested the following relation.

$$C_{t*} = 0.01 \sum_{k=1}^{N} P_k (\frac{d_k}{h})^{\frac{7}{6}} (\frac{\tau_b^{'}}{\tau_{ck}} - 1) f(\frac{U_*}{\omega_{sk}}) \tag{3.136}$$

where C_{t*} is the concentration of sediment by weight per unit volume; P_k is ratio of sediment size k between sediment particles in bed surface level; N is the all kind of

sediment classes size; τ_{ck} is the critical shear stress for the incipient motion of size classes d_k, that can be determined by the Shields diagram; and $\tau_b^{'}$ can be computed by

$$\tau_b^{'} = \frac{\rho U^2}{58}(\frac{d_{50}}{h})^{1/3}$$

(3.137)

The function $f(U_*/\omega_s)$ can find in curves of Figure (3.17)
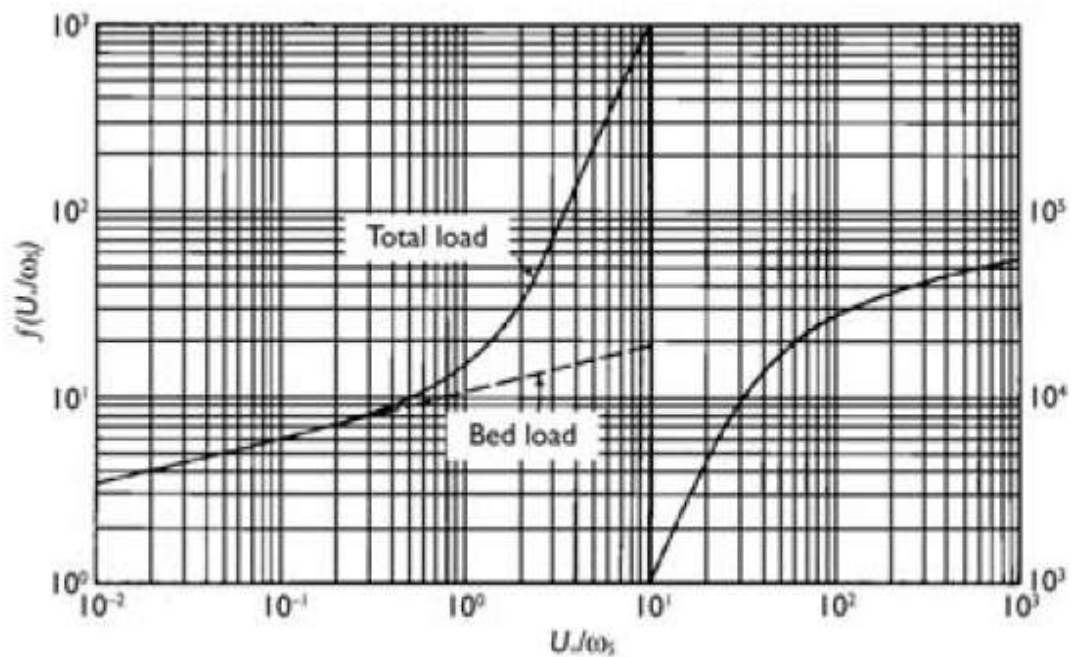
Figure 3.17 Function $f\left(U_*/\omega_s\right)$ in the Laursen (1958) relation. (Wu, 2007)

3.7.1.2 Engelund-Hansen Relation (1967)

Engelund and Hansen (1967), suggested the following relation to calculate sediment transport.

$$f^{'}\Phi_t = 0.1\Theta^{5/2}$$

(3.138)

where $f^{'} = \dfrac{2gRS_f}{U^2}$ and $\Phi_t = \dfrac{q_{t*}}{\left[\gamma_s\sqrt{\dfrac{\gamma_s}{\gamma-1}gd^3}\right]}$

3.7.1.3 Yang Relation (1973, 1984)

Yang (1973, 1984), calculated the suspended and bed load transport for the unit stream power as follows

$$\log C_{t*} = M + N \log \left(\frac{US_f}{\omega_s} - \frac{U_c S_f}{\omega_s} \right) \tag{3.139}$$

where M and N are coefficients and calculated by

For sand $d \leq 2mm$

$$M = 5.435 - 0.286l \, og \frac{\omega_s d}{v} - 0.457l \, og \frac{U_*}{\omega_s}$$
$$N = 1.799 - 0.409l \, og \frac{\omega_s d}{v} - 0.314l \, og \frac{U_*}{\omega_s} \tag{3.140}$$

For gravel $2mm < d < 10mm$

$$M = 6.681 - 0.633l \, og \frac{\omega_s d}{v} - 4.816l \, og \frac{U_*}{\omega_s}$$
$$N = 2.784 - 0.305l \, og \frac{\omega_s d}{v} - 0.282l \, og \frac{U_*}{\omega_s} \tag{3.141}$$

where C_{t*} is the concentration of sediment in parts per million (ppm) by weight.

3.7.1.4 Ackers-White Relation (1973)

The transport of coarse sediments, which are mainly in bed load, is attributed to the Stream power corresponding to the grain shear stress, $\tau_b' U$, while the transport of fine Sediments, which are mainly in suspended load, is related to the turbulence intensity and in turn the total stream power, $\tau_b U$.(Wu, 2007)

With considering the concept that explained above Ackers and White (1973) proposed a mobility factor of sediment transport:

$$F_{gr} = \frac{U_*^n}{\left[\frac{\gamma_s}{\gamma-1}gd\right]^{1/2}} \left[\frac{U}{\sqrt{32}\log(\frac{10h}{d})}\right]^{1-n} \tag{3.142}$$

$$G_{gr} = \frac{C_{t*}h}{d\frac{\gamma_s}{\gamma}}\left(\frac{U_*}{U}\right)^n = \Lambda\left(\frac{F_{gr}}{A_c}-1\right)^m \tag{3.143}$$

where C_{t*} is the concentration of sediment particles by weight, Λ and m are empirical coefficients, n is the transition exponent, and A_c may be interpreted as the critical value of F_{gr} for sediment incipient motion. Coefficients Λ, A_c, m, and n were proportional with the dimensionless grain diameter $D_* = d\left[(\rho_s/\rho-1)g /v^2\right]^{1/3}$, as listed in Table (3.4)

Table 3.4 Coefficients of the Ackers-White equation

	$D_* \geq 60$	$1 < D_* < 60$
n	0.0	$1.00 - 0.56\log D_*$
A_c	0.17	$0.23D_*^{-1/2} + 0.14$
m	1.50	$9.66D_*^{-1} + 1.34$
Λ	0.025	$\log\Lambda = -3.53 + 2.86\log D_* - (\log D_*)^2$

3.7.2 Fractional Transport Rate of Suspended and Bed Load

3.7.2.1 Modified Ackers-White Relation

Day (1980) and Proffitt and Sutherland (1983), modified the Ackers-White (1973) relations to determine the fractional suspended and bed load transport rate:

$$G_{gr,k} = \Lambda\left(\frac{F_{gr,k}}{A_c}-1\right)^m \tag{3.144}$$

$$F_{gr,k} = \eta_k \frac{U_*^n}{\left[\frac{\gamma_s}{\gamma-1}gd_k\right]^{1/2}} \left[\frac{U}{\sqrt{32}\log\left(\frac{10h}{d_k}\right)}\right]^{1-n} \tag{3.145}$$

$$G_{gr,k} = \frac{C_{t*k}h}{P_{bk}d_k\frac{\gamma_s}{\gamma}}\left(\frac{U_*}{U}\right)^n \tag{3.146}$$

With C_{t*k} refers to concentration of sediment by weight of size class k, and η_k the hiding and exposure correction factor. Day's correction factor is

$$\eta_k = \frac{1}{0.4\left(\frac{d_k}{d_A}\right)^{-0.5}+0.6} \tag{3.147}$$

where d_A is the reference diameter and calculated by

$$\frac{d_A}{d_{50}} = 1.6\left(\frac{d_{84}}{d_{16}}\right)^{-0.28} \tag{3.148}$$

and Proffitt and Sutherland suggested the following correction factor

$$\eta_k = \begin{cases} 0.40 & \frac{d_k}{d_u} \leq 0.075 \\ 0.53\log\left(\frac{d_k}{d_u}\right)+1.0 & 0.075 < \frac{d_k}{d_u} \leq 3.7 \\ 1.30 & \frac{d_k}{d_u} > 3.7 \end{cases} \tag{3.149}$$

where d_u is the reference diameter used by Proffitt and Sutherland (1983).

3.7.2.2 SEDTRA Module (Garbrecht et al., 1995)

Garbrecht *et al.*(1995), proposed the SEDTRA module. This module use three equations to compute the fractional sediment transport rates: the Laursen (1958) relation for classes of size from 0.01 to 0.25 mm, the Yang (1973) relation for classes of size from 0.25 to 2.0 mm, and the Meyer-Peter-Mueller (1948) relation for classes of size from 2.0 to 50.0 mm. The total sediment concentration can be determined by

$$C_{t*} = \sum_k P_k C_{t*k} \tag{3.150}$$

where P_k is the fraction of the k th, the size of class of sediment in bed load surface, usually set as the suspended and bed load gradation.

The hiding and exposure effect in non-uniform bed load can be computed by

$$d_{ek} = d_k \left(\frac{d_k}{d_m} \right)^{-x} \tag{3.151}$$

where x is an empirical parameter that can be calculated by $x = 1.7 / B_m$, d_m is the mean diameter of bed load; and B_m can be calculated by

$$B_m = \left(\frac{d_c}{d_f} \right)^{1/2} \sum P_m \tag{3.152}$$

where d_c and d_f refers to diameters of coarse and fine modes, and P_m is the ratio of the sediment mixture contained in the two modes.

The mixture names for Wilcock and Southard's (1988) data refer to the standard deviation of bed material, and those for Kuhnle's (1993) data refer to the percentage of gravel in bed material, SG25 for the mixture with 25% gravel and 75% sand (Wu, 2007).

Note that this module may not be suitable in the case of low sediment transport,

because the situation that they used in order to calculate incipient motion of sediment particles are difference.

Table(3.5) lists the values of *x* that introduced by Kuhnle *et al.* (1996).

Mixture name	Reference	$d_m(mm)$	Mixture type	B_m	x
SG10(lab.)	Kulnle(1993)	0.616	Bimodal	2.49	0.7
SG25(lab.)	Kulnle(1993)	0.927	Bimodal	2.60	0.7
SG45(lab.)	Kulnle(1993)	1.454	Bimodal	2.73	0.6
$1/2\psi$ (lab.)	Wilcock & S.(1988)	1.82	Unimodal	0.67	1
ψ (lab.)	Wilcock & S.(1988)	1.85	Unimodal	0.37	1
Goodwin Creek	Kulnle(1993)	1.189	Bimodal	3.10	0.5

3.7.2.2 Karim Relation (1998)

Karim (1998), in order to predict the fractional transport rate of suspended and bed load suggested the following relation

$$\frac{q_{t*k}}{\sqrt{\frac{\gamma_s}{\gamma-1}gd_k^3}} = 0.00139\left[\frac{U}{\sqrt{\frac{\gamma_s}{\gamma-1}gd_k}}\right]\left(\frac{U_*}{\omega_{sk}}\right)^{1.47}P_{ak}\eta_k \tag{3.153}$$

where unit of q_{t*k} is $m^2.s^{-1}$; P_{ak} is the real fraction of suspended and bed load, depends to the volumetric fraction of suspended and bed load, P_{bk}, by

$$P_{ak} = \frac{\frac{P_{bk}}{d_k}}{\sum_{k=1}^{N}\frac{P_{bk}}{d_k}} \tag{3.154}$$

and η_k is the correction factor of hiding and exposure:

$$\eta_k = C_1\left(\frac{d_k}{d_{50}}\right)^{C_2} \tag{3.155}$$

where C_1 and C_2 are

$$C_1 = 1.15 \frac{\omega_{s50}}{U_*}$$ (3.156)

$$C_2 = 0.60 \frac{\omega_{s50}}{U_*}$$ (3.157)

where ω_{s50} is the settling velocity for d_{50}.

CHAPTER FOUR
GOVERNING EQUATIONS OF SEDIMENT TRANSPORT

4.1 The Saint Venant Equations (SVE):

4.1.1 Main Assumptions and Derivation

The Navier-Stocks Equations are basic relations which can be used in investigate the treat of flow. Because in the most channels the length of horizontal scale is much larger than vertical ones, so using the shallow water equations can be sufficient. The main idea of this chapter is to present the one-dimensional continuity and momentum equations that are usually referred to as the Saint Venant equations.

4.1.2 Basic Hypothesis for the SVE

The main concepts and assumptions of unsteady flow, formalized in the Navier-Stokes equations.

The governing equations of unsteady flow condition in open channel can be described by de Saint Venant equations. In order to define the flow condition in unsteady condition must be compute two flow variables, such as the flow depth and velocity or the flow depth and the rate of flow. The Saint Venant defined cantinuity and momentom equations with many assumptions.

●the streamlines do not have sharp curves, so that the pressure distribution is hydrostatic.

●As the channel bottom slope is small, the measured lateral and vertical velocity are approximately same, so the lateral velocity and acceleration component can be neglected.

●No lateral, secondary circulation occurs. The flow velocity distribution is

uniform over any channel cross section.

●The channel is prismatic with the same cross section and slope thorough out the distance.

●The head losses in unsteady flow can be simulated by using the steady – state resistance laws, so Chezy and Manning equations can be used also in unsteady flow model. Water has uniform density and flow is generally sub-critical (Chaudhry, 1993).

4.1.3 The derivation of the Continuity Equation

The law of conservation of mass, states that in a closed system the mass of substances will not exchange, without paying attention what kind of processes are acting inside the system.
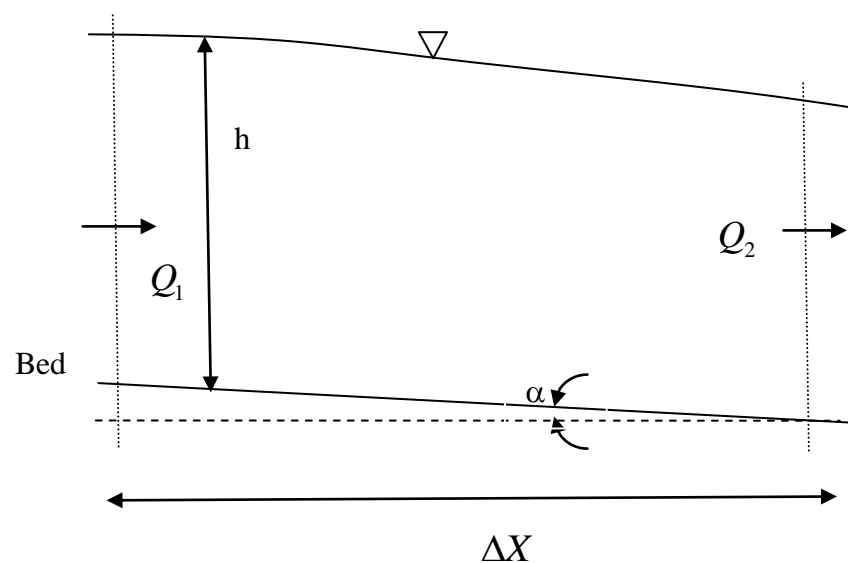
Figure 4.1 View of continuity equations of mass

Whit refer to law of conservation of mass and with assuming that there is no lateral inflow or outflow, then

$$Q_2 - Q_1 = \frac{\partial Q}{\partial x} \Delta x \tag{4.1}$$

where, Q is the discharge at the section, x is the position of the section measured from the upstream end.

The volume of mass of water in control volume with consider a time steps between section 1 and 2 can be shown as

$$b.\frac{\partial h}{\partial t} \Delta x \tag{4.2}$$

where b is the width of volume.

With substitute Equation (4-2) into Equation (4-1), can be rewritten as

$$\frac{\partial Q}{\partial x} \Delta x + b.\frac{\partial h}{\partial t} \Delta x = 0 \tag{4.3}$$

Now with divided Equation (4-3) to width of channel can be rewritten as

$$\frac{\partial h.u}{\partial x} \Delta x + \frac{\partial h}{\partial t} \Delta x = 0 \tag{4.4}$$

Finally with some simplification can be write continuity equation as

$$h.\frac{\partial u}{\partial x} + u.\frac{\partial h}{\partial x} + \frac{\partial h}{\partial t} = 0 \tag{4.5}$$

where, h is the depth of flow at the section, u *is the* mean velocity at the section, *t is the* time.

4.1.4 The Derivation of the Dynamic or Momentum Equation.

According to Newton's second law the acceleration of an object is directly proportional to the net force acting on it, and inversely proportional to its mass. By applying this rule to control volume of channel in Figure 4.1 can be written as:

Force= Mass. Acceleration

$$F = \rho A \Delta x \frac{du}{dt} \qquad (4.6)$$

$$F = \rho A \Delta x [u \frac{\partial u}{\partial x} + \frac{\partial u}{\partial t}] \qquad (4.7)$$

The external forces which cause this acceleration in the simplest case are three: Change in static pressure that shown as $\frac{\partial H}{\partial x}$, Frictional resistance of channel walls and bed that shown as F and Gravity force (the weight) that shown as ρg .The sum of these forces is

$$\frac{\partial H}{\partial x} . \Delta x . cos \propto -F. \Delta x + \rho. g. A. \Delta x. sin \propto \qquad (4.8)$$

where, α $\square$ is the $\square$ bed slope (measured positive as the bed rises from downstream to up)

If the bed slope is smaller then 6 ($\alpha \le 6^\circ$) then $\cos\alpha = 0$ and $\sin\alpha = \alpha = S_0$

Whit some manipulation about static pressure changes and frictional resistance can be written

$$\frac{\partial H}{\partial x} = -\rho.g.A.\frac{\partial h}{\partial x} \qquad (4.9)$$

$$F = \rho.g.A.S_f \qquad (4.10)$$

where, S_f is lose of energy per unit length of channel per unit weight of fluid.

With substitute (4-8), (4-9) and (4-10) equations in (4-7) can be shown that

$$\rho.A.\Delta x [u.\frac{\partial u}{\partial x} + \frac{\partial u}{\partial t}] = -\rho.g.A.\frac{\partial h}{\partial x}.\Delta x - \rho.g.A.S_f.\Delta x + \rho.g.A.S_0.\Delta x \qquad (4.11)$$

Whit some rearranging, consequently can be write dynamic or momentum equation.

$$g.\frac{\partial h}{\partial x} + u.\frac{\partial u}{\partial x} + \frac{\partial u}{\partial t} = g(S_0 - S_f) \tag{4.12}$$

4.2 Governing Equations

The bed profile evolution and movement in alluvial channels can be represented, as shown in Figure 4.2, as a system involving two layers: water flow layer and movable bed layer. The water flow layer may contain suspended sediment. The movable bed layer consists of water and sediment particles and therefore has porosity. There may be an exchange of sediment between the two layers, depending upon the flow transport capacity and sediment rate in suspension. (Tayfur and Singh, 2006).
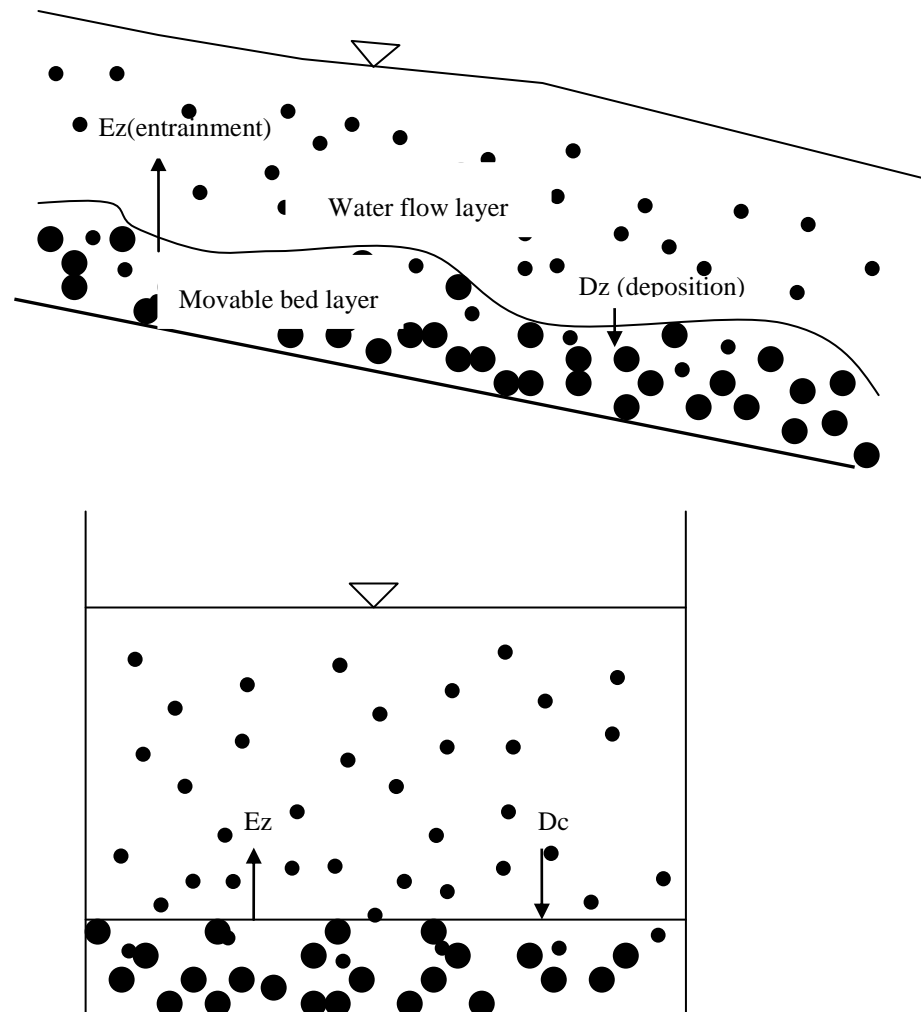
Figure 4.2. Schematic representation of two layer systems (Tayfur and Singh, 2007)

With considering the concentration of suspended and bed load and flux of flow into sediment porosity the equation of conservation of mass for water in a wide rectangular channel with constant width can rearrange as(Tayfur and Singh, 2007):

$$\frac{\partial h(1-c)}{\partial t} + \frac{\partial hu(1-c)}{\partial x} + p\frac{\partial z}{\partial t} = q_{lw} \tag{4.13}$$

$$\frac{\partial hc}{\partial t} + \frac{\partial huc}{\partial x} = q_{lsus} + \frac{1}{\rho_s}\left[E_z - D_c\right] \tag{4.14.a}$$

$$(1-p)\frac{\partial z}{\partial t} + \frac{\partial q_{bs}}{\partial x} = q_{lbed} + \frac{1}{\rho_s}\left[D_c - E_z\right] \tag{4.14.b}$$

$$\frac{\partial hc}{\partial t} + \frac{\partial huc}{\partial x} + (1-p)\frac{\partial z}{\partial t} + \frac{\partial q_{bs}}{\partial x} = q_{ls} \tag{4.15}$$

where h is the flow height (L), u is the velocity of flow (L/T), c is the volumetric concentration of sediment in suspension (L^3/L^3), p is the porosity of   sediment in bed level(L^3/L^3), z is the movable bed layer elevation (L), q_{lw} is the lateral water flux (L/T), q_{bs} is the sediment flux in the movable bed layer (L^2/T), q_{lsus} is the lateral suspended sediment (L/T), q_{lbed} is the lateral bed load sediment (L/T), ρ_s is the sediment mass density (M/L3), E_z is the entrainment rate ($M/L^2/T$), and D_c is the deposition rate ($M/L^2/T$).

Note that the equations that refer to conservation of mass write two form: equilibrium ($D_c = E_z$) (4.15) and non-equilibrium ($D_c \neq E_z$) (4.14.a and b) form. In non-equilibrium case when ($E_z > D_c$) there is entrainment from the bed layer, that cause to decrease bed load but increase the concentration of suspended load sediments. In the opposite of this situation ($E_z < D_c$) can be seen the gathering in bed load and reducing in suspended load of sediments.

In order to compute the values of E_z and D_c Yang (1996) proposed the following

relations

$$E_z = \sigma T_c = \sigma \left[\Phi \left(\tau - \tau_{cr} \right)^k \right] \tag{4.16}$$

$$\tau = \gamma_w h S_0 \tag{4.17}$$

$$\tau_{cr} = \kappa \left(\gamma_s - \gamma_w \right) d_s \tag{4.18}$$

where σ is the coefficient of transfer rate (1/L), T_c is the flow transport capacity ($M/L/T$), Φ is the soil erodibility coefficient, τ is the shear stress (M/L^2), k an exponent, κ a constant, γ_w and γ_s is the specific weight of water and sediment (M/L^3), d_s is the sediment particle diameter (L).

The value of deposition rate D_c can be determined by

$$D_c = \sigma \rho_s q_{ss} = \sigma \left[\rho_s h u c \right] \tag{4.19}$$

where q_{ss} is the unit of suspended sediment discharge (M/L/T).

Easily can be seen that when $E_z = D_c$, with adding of Equations (4.14) and (4.15) can be found equilibrium form of these equations.

In laboratory flume that used in study, there is no lateral of sediment or flow influence, so q_{lw} and q_{ls} are equal to zero.

Note that there are five unknown in continuity equations of sediment and water (h, u, c, z, and q_{bs}). Therefore we need three aide equations to solve set of equations above.

Instead of third equation can be use Momentum equation. With considering the flux of flow into sediment porosity can be rearrange Equation (4.12) as follow.

$$\frac{\partial u}{\partial t} + u.\frac{\partial u}{\partial x} + g\frac{\partial h}{\partial x} + g\frac{\partial z}{\partial x} = g(So - Sf) \tag{4.20}$$

where g is the gravitational acceleration (L/T^2), S_0 is the bed slope and S_f is the friction slope.

The forth equation obtains from suspended sediment concentration that represented by Velikanov (1954)

$$c = \delta u^3 h^{-1} \tag{4.21}$$

In equation above the value of δ can be substitute form relations below

$$\delta = \frac{\kappa}{gv_f} \tag{4.22}$$

where v_f is the average fall velocity of sediments (L/T) and κ is the coefficient of sediment transport capacity. ($\kappa = 0.756 \times 10^{-4}$)

As a last one must be represent relations for q_{bs}. This symbol represents a relation for the sediment flux in the movable bed layer. There are various empirical equations that given by investigators .Some of them represent in here.

Note that in solution with Kinematic wave model instead of velocity u should be used the following relations

$$u = \alpha h^{\beta - 1} \tag{4.23}$$

$$\alpha = C_z S_f^{0.5} \tag{4.24}$$

where $\beta = 1.5$

CHAPTER FIVE
EXPERIMENTAL INSTRUMENTS

Experimental investigations carried out in a rectangular channel with 18.6 m length and 80 cm width. The walls in the right and left hand of channel made from Plexiglas with 75 cm high. The slope of channel could be changed in the ranges of 0.001 to 0.01 from horizontal. The water is circulated continuously. The volume of the water supply reservoir (main tank) is 27 m^3. The general view of experimental set up is shown in Figure 5.1.a and Figure 5.1.b. (Bombar, 2009).

Figure 5.1(a and b) The general view of the experimental set-up. (Bombar, 2009)

In this system used a kind of pump (figure 5.2 a) with maximum 100 lit/s capacity ,that connected with pump rotational speed control unit(figure 5.2 b). By using the pump rotational speed control unit we can program the system for hydrograph generation and control the flow rate.
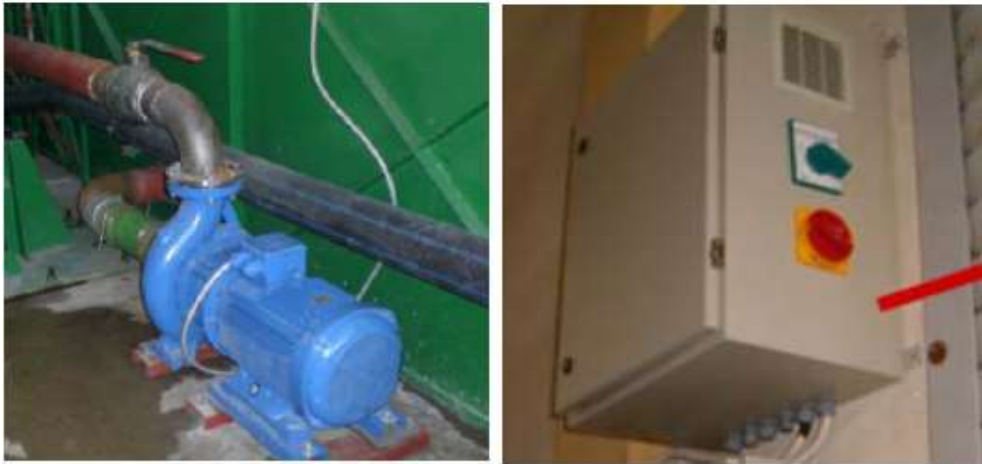
Figure 5.2 (a) Pump that used in this study, (b) pump rotational speed control unit (Bombar, 2009).

In the end of the channel there is a tail gate(figure 5.3) that uses for control the depth of water. For collecting the bed load that coming from channel there are set of baskets that located at the downstream part of the flume.

Figure 5.3 tail gate. (Bombar, 2009)

5.1 Instrument

5.1.1 Baskets

In the end of channel set up a movable part that can move by human force. In order to measure the suspended and bed load sediments that come from the flume,

get baskets on this movable part and change it in fixed time distance. View of baskets and movable system can be found in Figure 5.4 (a and b) (Bombar, 2009).
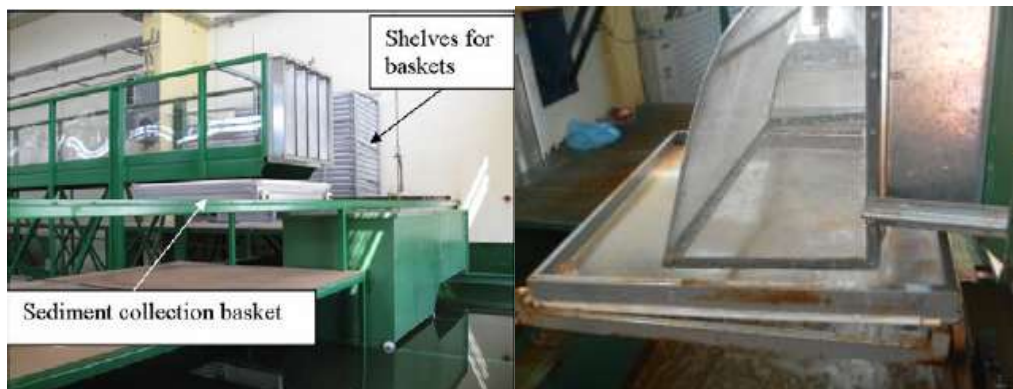
Figure 5.4 (a). Place of baskets on platform, (b) basket on movable set. (Bombar, 2009)

5.1.2 Ultrasonic Velocity Profiler (UVP)

The general view of UVP are given in figures 5.5(a) and 5.5(b).

Figure 5.5 (a and b) Ultrasonic Velocity Profiler (UVP) (Bombar, 2009).

The velocities are measured by using UVP given in figure 5.6.a (manufactured by Met-Flow SA). The velocity profile along the ultrasonic beam axis is measured by detecting the doppler shift frequency. The measurement principle is as follows; the UVP DUO transducer transmits a short emission of ultrasound, which travels along the measurement axis, and then switches over to receiving. When the ultrasound pulse hits a small particle in the liquid, part of the ultrasound energy scatters on the particle and echoes back. The echo reaches the transducer after a time delay. If the

scattering particle is moving with a non-zero velocity component into the acoustic axis of the transducer, doppler shift of echoed frequency takes place, and received signal frequency becomes 'doppler-shifted'. By using the time delay and doppler shift frequency, it is then possible to calculate both position and velocity of a particle on the measuring axis, i.e. velocity profile over the measuring axis, as depicted in figure 5.6.b (Met-Flow, 2002).
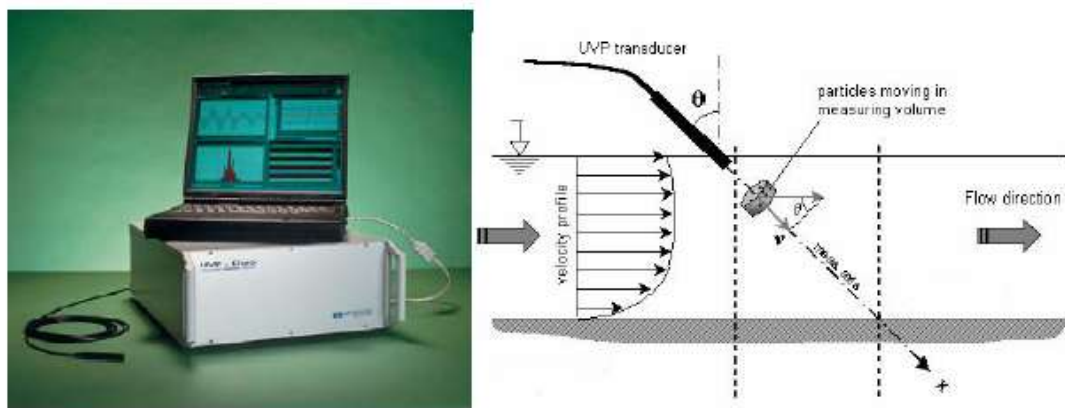
Figure 5.6(a) Ultrasonic Velocity Profiler (UVP), (b) UVP working system. (Bombar, 2009)

During the study for measurement of velocity used two UVP sensor in the begin of the channel. These sensors established in the fix part of bed profiles in first 3 meters.

5.1.3 Level Meter

The IMP+ level monitoring system (Pulsar Process Measurement Limited) is a highly developed ultrasonic level measurement system which provides noncontacting level measurement for a wide variety of applications in both liquids and solids (figure 5.7). It operates on the principle of timing the echo received from a measured pulse of sound transmitted in air and utilizes echo extraction technology. IMP 3 madel has a range from 0.15m to 3.00m. The otput voltage 4-20mA is transmitted by a RS232 connection to the data recorder. Whilst in the Run Mode, the 4 digit LCD can display the current level reading in mm (Bombar, 2009).

Figure 5.7 Level meter. (Bombar, 2009).

5.1.4 Flow Meter

The OPTIFLUX 1000 (manufactured by Krohne) is an electromagnetic flow sensor which works according to the Faraday Law and is mounted on the pipe before the entrance of the channel (figure 5.8). It can measure both the steady and unsteady flow rates with a precision of 0.01 l/s. The measured data is sent to the data recorder, with 6 channels (Bombar, 2009).

Figure 5.8 Flow meter (Bombar, 2009).

5.1.5 Data Recorder

The data from the flow-meter and level-meter is recorded and stored by the data recorder as shown in figure 5.9. The data recorder has 6 channels which can acquire the data with a frequency of 1s. The data is both displayed on the screen and stored simultaneously and can be transferred to the computer by the help of the CF card

after the experiments (Bombar, 2009).

Figure 5.9 Data recorder (Bombar, 2009).

5.1.6 Ultaralab ULS

Figure 5.10 Ultaralab ULS.

ULS (figure 5.10) is an instrument that use for measurement of distance in laboratory. The benefit of using this instrument is obviously clear: particularly in small-scale experimental set-ups, it is imperative to avoid any mechanical intervention that may affect the experiment, but at the same time, parameters must be

measured and evaluated.

General Acoustics ULS ultrasound sensors permit distance measurement from 30 mm to 3.4 m and, thanks to high-resolution propagation time measurement, measure with sub-millimeters resolution.

The *ULTRALAB*® ULS sends out an acoustic pulse via the ultrasound sensor. The ultrasound pulse emitted is reflected on the measurement object and is received back as an echo. A key aspect when it comes to measuring distances is the time required for the transmitted pulse to cover the distance to the respective measurement object and back. This sound propagation time is measured by the *ULTRALAB*® ULS with high resolution.

The measured propagation times are averaged. A tolerance band (expectation range) is set around the average propagation time. Only measurement values that lie within the expectation range are admitted for further calculation of the measurement value. The average value is modified according to changes in distance.

The measured distance is converted to a voltage signal (0-10V) proportional to the distance. The sound propagation time and the measured distance obtained from it will depend to a certain extent on the following environmental conditions: air temperature, humidity, air pressure, air currents.

5.1.7 Laser Meter

In studies, for measurement of sediment elevation codes Bosch DLE 70 laser meter (figure 5.11.a) used. The measuring rang of this equipment is (0.05 – 70) meters. This is the smallest laser-meter in the world and it can be measure with 1.5 mm accuracy in a compact unit.

Before begin to research, the level of sediment in bed made smooth and used laser meter for measure this level. After finished the research for finding final deformation

of bed profiles, again should be used this instrument to get the last form of level codes. In order to use this equipment easily and rapidly set a moveable system that could be found in Figure 5.11.b.

Figure 5.11 (a) General view of Laser meter, (b) moveable set of Laser meter.

5.1.8 The Property of Bed Load Sediments

In this study in order to simulate the nature condition as more as possible used a composed of uniform graded material with $d_{50} = 3.4$ mm (Table1). The average grain size distribution is given in Figure 5.12. The sort of material is quarts.

Investigators in order to calculate the channel bottom roughness, generally use two equations. These relations are given below.

Chezy Relations

$$Cz = \frac{Q}{A\sqrt{R.S}}$$ (5.1)

Manning relations

$$n = \frac{A\sqrt{R}.S^{2/3}}{Q}$$ (5.2)

Table 1.Analysis of sample of sediment

Size of sediment particles (mm)	Weight (gr)	Percent in weight	Cumulative percentage
6.5	0	0	100.00
6.3	50.21	2.87	97.13
4.75	360.83	20.61	76.52
3.35	498.50	28.48	48.04
2.36	98.93	5.65	42.39
1.7	18.14	1.04	41.35
1.18	2.69	0.15	41.20
0.85	4.72	0.27	40.93
0.6	200.60	11.46	29.47
0.425	458.75	26.21	3.26
0.3	54.33	3.10	0.15
0.25	2.71	0.15	0
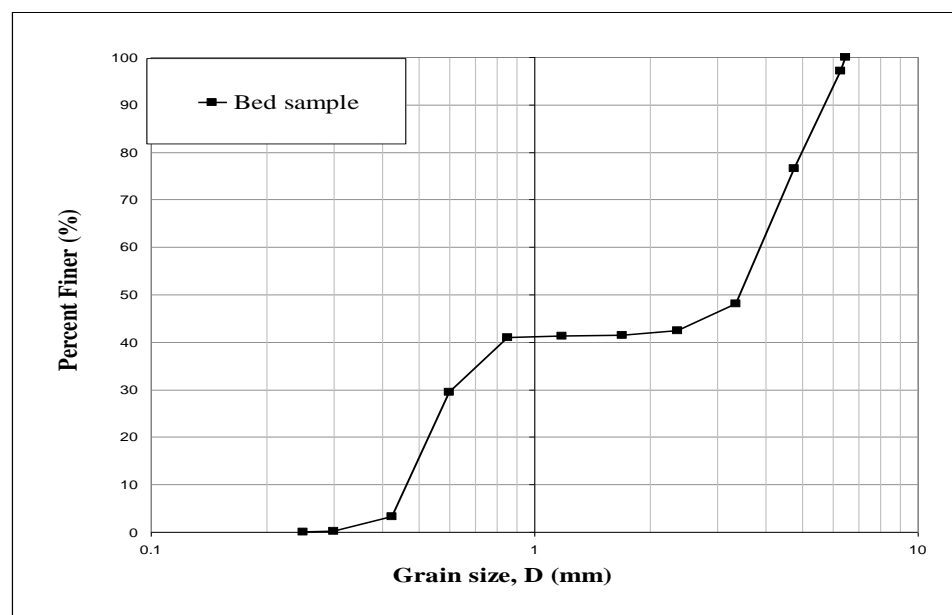
Figure 5.12 Distribution of bed material.

where Q is flow rate (m^3/s), A is area (m^2), R is hydraulic radius that can be found by proportional of area to wetted cross, S is energy slope, Cz is Chezy coefficient and n is Manning coefficient.

In this research applied Chezy coefficient. Note that this value is depend to flow rate and depth of flow. So in unsteady flow it would be changed. In order to find the correct value of Chezy coefficient, this value calculated for the minimum and maximum points of all of hydrographs. The biggest difference found in third hydrograph, so used these values in model to see the influence of Chezy coefficient in models prediction. The percentage of difference graph is given in Figure below.

(zmax-zmin)/zmin*100
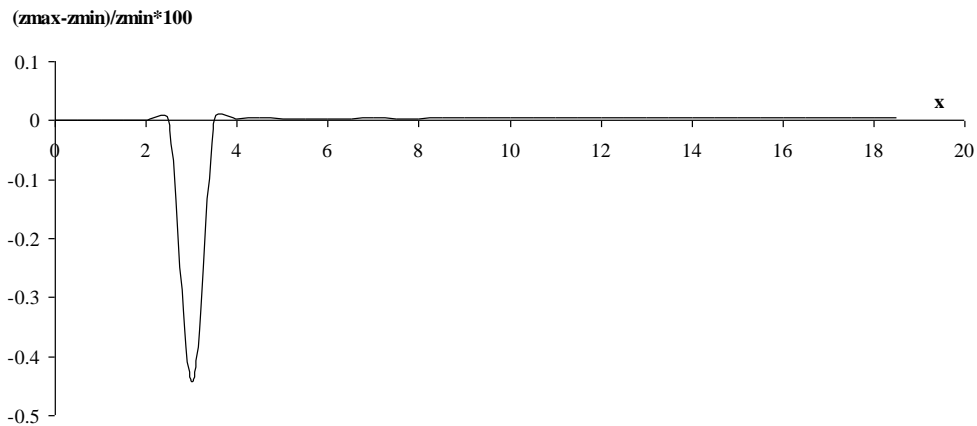
Figure 5.13 Difference of bed load predication for the max. and min. Chezy coefficient in percent for the third hydrograph .

It can be seen that, differences are not really important. Finally, the value of Chezy coefficient selected as 27.3 that is the average value of all of hydrographs.

5.2 Experimental Procedure

First of all, the bed materials should be mixed to get homogeneous sediments and after that with using a mobile system that shown if Figure 5.14 make a smooth surface of sediments in vertical and stream-wise direction.

Before to start the experiments, with using the Laser-meter, should be measured the elevation of initial bed profiles that help to compare changes of geometry between before and after passing the flow.

Figure 5.14 System to make a fix bed level. (Bombar, 2009)

At the beginning of the study, flow rate increases slowly to the basic value which is below the sediment inception threshold condition in order to not disturb the sediments and instrument that placed in channel start to measurement. While demand hydrograph begin to pass the channel length, the shape of bottom level begin to change.

For collect the bed loads that carry out with flow rate, baskets that located at the downstream part of the flume used.

Finally after past the hydrograph, with using the Laser-meter measure the final bed profile code that is useful for compare between before and after bottom changes.

CHAPTER SIX
FINITE VOLUME METHOD

6.1. Introduction

The finite volume method is a method for representing and evaluating partial differential equations in the form of algebraic equations (LeVeque, 2002; Toro, 1999).

Finite Volume method is one of the finite family methods used frequently in recent years.

The most important advantage of Finite Volume Method is its ability to conservative of quantities such as mass, momentum, energy, and species in solution. The Finite volume approach guarantees local conservation of a fluid property for each control volume (Versteeg & Malalasekera, 1995). So, FVM is the useful method for computing flow problems.

6.2. Finite Volume Method for One Dimensional Equations

Consider of a property ϕ in a one-dimensional domain shown in Figure (6.1).
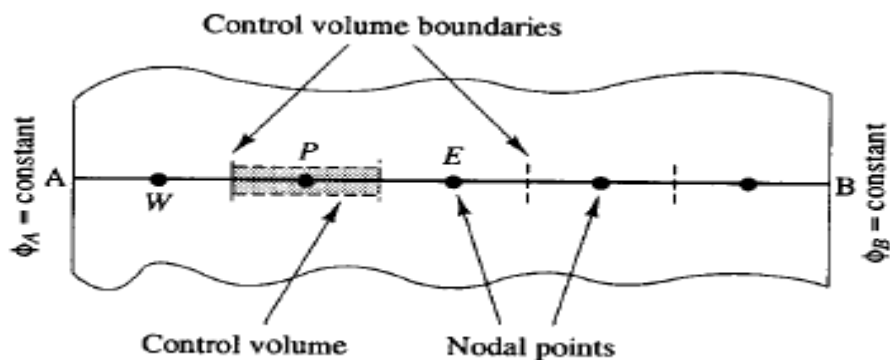
Figure 6.1 View of 1D Control volume notation. (Versteeg & Malalasekera, 1995)

Solution with finite volume method consists of three stages.

Step 1: Grid generation.

The first step of the solution with finite volume method consists of dividing the domain into discrete control volumes. Number of nodal points are placed in space between A and B. The boundaries of control volumes are placed between these nodal points so each node is surrounded by a control volume. Generally, these control volumes are set up near the edge of the domain in such away that the real physical boundaries adapt to the control volume boundaries.

Consider the value of P as a nodal point that should be calculated. In a one-dimensional geometry the neighborhood nodal points called as east and west nodal points and for identify these points can be used E and W symbols. In order to show distance between P and E nodal points, can be used δx_{PE} and as a same way for distance between P and W, can be use δx_{WP} symbols. The west side face of control volume is refer to w and the east side control volumes face refer to e. Similarly the distances between face w and point P and between P and face e are denoted by δx_{wp} and δx_{pe} respectively. The view of this system can be found in Figure (6.2).
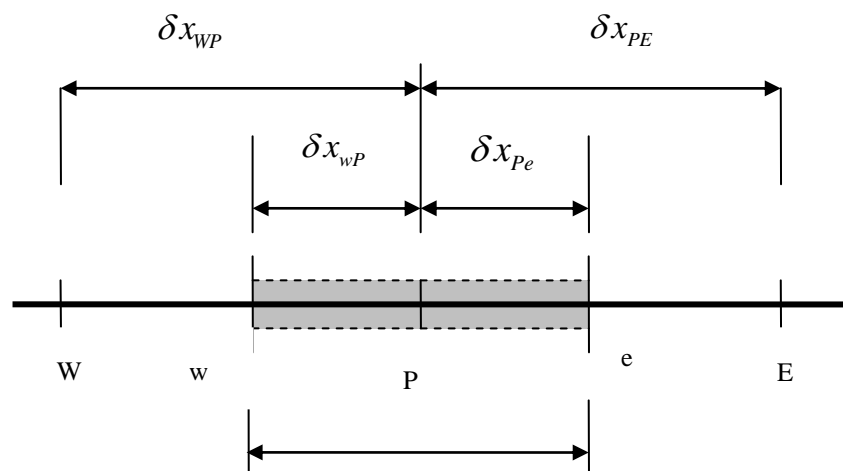
Figure 6.2 View of one Control volume. (Versteeg & Malalasekera, 1995)

Step 2. Discretisation.

The key step of the finite volume method is the integration of the governing equation (or equations) over a control volume to yield a discretised equation as its

nodal point P (Versteeg & Malalasekera, 1995). Maybe the most interesting property of the finite volume method is that the discretised equation has an exactly physical concept.

For constitute a suitable form of discretisation equation, the values of diffusion coefficient Γ and the gradient $d\phi/dx$ at east e and west w are required. In order to calculate gradients at the control volume faces an approach of distribution of properties between nodal points is used. Maybe in point of simplicity and visibility way for calculating interface values and the gradients the linear approximations are better then others .In this part introduce some of simple and useful linear ways: 1.Central scheme. 2. Upwind scheme.

6.2.1. Central Scheme

In the central method a uniform grid linearly interpolated values for Γ_e and Γ_w are given by

$$\Gamma_w = \frac{\Gamma_W + \Gamma_P}{2} \tag{6.1.a}$$

$$\Gamma_e = \frac{\Gamma_E + \Gamma_P}{2} \tag{6.1.b}$$

and the diffusive flux terms are evaluated as:

$$(\Gamma A \frac{d\phi}{dx})_e = \Gamma_e A_e (\frac{\phi_E - \phi_P}{\delta x_{PE}}) \tag{6.2}$$

$$(\Gamma A \frac{d\phi}{dx})_w = \Gamma_w A_w (\frac{\phi_P - \phi_W}{\delta x_{WP}}) \tag{6.3}$$

where A_e and A_w are the face areas of the control volumes.

6.2.2. Upwind Scheme

One of the most important restrictions about central difference scheme is its incapability to identify flow direction. In central method the values of property ϕ at the west cell faces is always influenced by both neighbor nodal points (ϕ_P and ϕ_W) as a same weights. In a case of flow diffusion from west to east, this assumption is unsuitable because the influence of node W in the west cell face is much stronger than node P.

The upwind differencing or donor cell differencing scheme can solve this problem with paying attention to the effect of flow direction when determining to the value at the cell face. The value of ϕ at a cell is taken to be equal to the value at the upstream node. In Figure (6.3) can be found a view of upwind method.
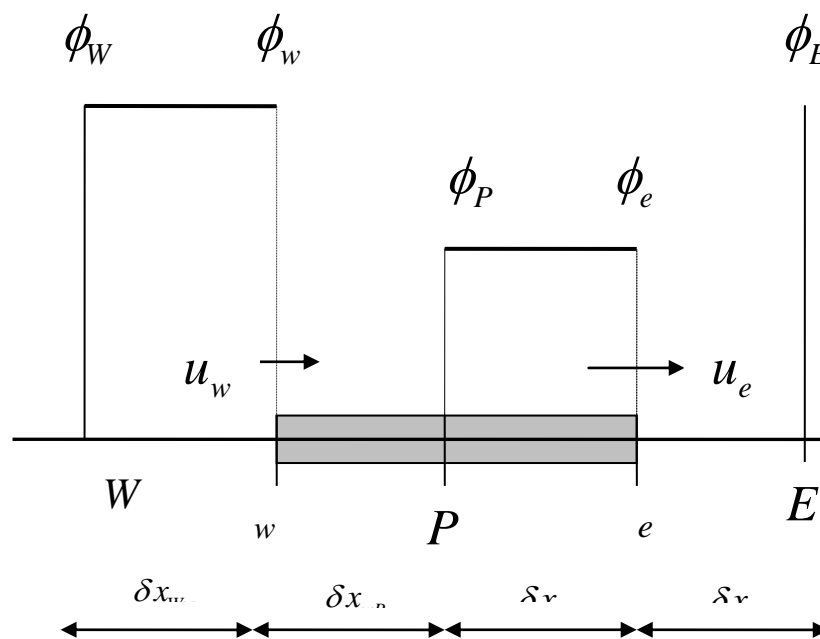
Figure 6.3 View of upwind scheme. (Versteeg & Malalasekera, 1995)

When the flow is in the positive direction (from west to east) with applying upwind method for ϕ can be written as:

$$\phi_w = \phi_W \quad \text{And} \quad \phi_e = \phi_P . \tag{6.4}$$

Step 3: Solution of equations.

In the end of all in order to solve a problem discretised form, must be applied for each of the nodal points. In order to see the effect of boundary conditions, the general discretised form for control volumes that are neighbor with domain boundaries must be modified.

Consequently the collection of these linear algebraic equations should be solved to obtain the distribution of the property ϕ at nodal points.

6.3 Solution of Sediment Transport Equations with Finite Volume Method

In order to shown better, use the following form for Equations (4.13), (4.15) and (4.20).

$$W_t = -F_x + S \tag{6.5}$$

where $W = \begin{bmatrix} h(1-c)+pz \\ hc+(1-p)z \\ u \end{bmatrix}$ $F = \begin{bmatrix} hu(1-c) \\ huc+q_{bs} \\ \dfrac{1}{2}u^2+g(h+z) \end{bmatrix}$ $S = \begin{bmatrix} 0 \\ 0 \\ g(So-Sf) \end{bmatrix}$.

With integration of Equation (6.5) can be seen that

$$\int_{CV}\int_t^{t+\Delta t} \frac{\partial W}{\partial t} dt.dV = -\int_{CV}\int_t^{t+\Delta t} \frac{\partial F}{\partial x} dt.dV + \int_{CV}\int_t^{t+\Delta t} Sdt.dV \tag{6.6}$$

If the values of P at Figure (6.2) at a node are assumed to govern over the whole control volume, the left hand side of Equation (6.5) can be written as

$$\int_{CV}\left[\int_t^{t+\Delta t} \frac{\partial W}{\partial t} dt\right]dV = (W_p - W_p^o)\Delta V \tag{6.7}$$

In equation above superscript 0 refers to value of unknown at time t, but values of unknown at time $_{t+\Delta t}$ are not superscripted. With insert relation (6.7) into Equation (6.6) and with integration of F order to location (x) can be rearrange Equation (6.6) as follows

$$(W_p - W_p^o)\Delta V = -\left(A_e.F_e - A_w.F_w\right)\Delta t + S.\Delta t.\Delta V \tag{6.8}$$

where A_e and A_w are the face areas of the control volumes, ΔV is the volume of control volume which is written as $A_e \Delta x$ and $A_w \Delta x$ where Δx called as the width of the control volume.

In order to solve the right hand side of this equation, should be make an assumption about the value of unknowns in point p with respect to time. Depending on the way of solution can be select these values at time t or time $t + \Delta t$ or combination of these at time t and $t + \Delta t$. The general form of unknowns with respect to weighting parameter θ can be written between 0 and 1

$$I_T = \int_t^{t+\Delta t} W_p dt = \left[\theta W_p + (1-\theta)W_p^0\right]\Delta t \tag{6.9}$$

Hence

Table 6.1 Value of θ in different schemes

θ	0	$1/2$	1
I_T	$W_p^0 \Delta t$	$\dfrac{1}{2}\left(W_p + W_p^0\right)\Delta t$	$W_p \Delta t$

With paying attention to Equation (6.9) can rearrange Equation (6.8) as follow

$$(W_p - W_p^o)\Delta V = (1-\theta)\left[-\left(A^0_e.F^0_e - A^0_w.F^0_w\right)\Delta t\right] + \theta\left[-\left(A_e.F_e - A_w.F_w\right)\Delta t\right] + S.\Delta t.\Delta V \tag{6.10}$$

Note that by selecting θ as zeros only use values of unknowns at old time level t; this scheme called as explicit method. When θ selected in the range of zero and one ($0 < \theta \le 1$) the values of unknown at the new time level are used; the resulting schemes are called implicit method. The extreme case of $\theta = 1$ is termed fully implicit method and the name of scheme that used $\theta = 1/2$ is Crank-Nicolson scheme.

6.3.1 Explicit Scheme

Substituting the value of θ as zero in Equation (6.10) is given the explicit solution.

$$(W_p - W_p^o)\Delta V = -\left(A^0_e.F^0_e - A^0_w.F^0_w\right)\Delta t + S.\Delta t.\Delta V \tag{6.11}$$

Note that by select the value of θ as zero, the value of unknowns at old time level can be used.

6.3.2 Crank-Nicolson Scheme

Whit substitute the value of θ as 1/2 in Equation (6.10) Crank-Nicolson scheme would be found.

$$\begin{aligned}(W_p - W_p^o)\Delta V &= (1/2)\left[-\left(A^0_e.F^0_e - A^0_w.F^0_w\right)\Delta t\right] + \\ &(1/2)\left[-\left(A_e.F_e - A_w.F_w\right)\Delta t\right] + S.\Delta t.\Delta V\end{aligned} \tag{6.12}$$

6.3.3 The Fully Implicit Scheme

With selecting the value of θ as one, can be obtained the fully implicit scheme. In this scheme the new time step $(t + \Delta t)$ value of unknowns should be used in both side of equation. In order to obtain a solution with this scheme a system of algebraic equations must be solved at each time level. The solution procedure begins with using given initial field of unknowns with paying attention to selected time step Δt. In the next level the new find value for F and W substitute in F^0 and W^o and procedure is repeated to progress the solution by a further time step.

Since the accuracy of the implicit scheme is only first order in time, small time steps are needed to insure the accuracy of results. The implicit method is recommended for general purpose transient calculations because of its robustness and unconditional stability (Versteeg & Malalasekera, 1995).

In this study in order to determine the values of F, applied upwind scheme. The Figure of upwind scheme can be seen in Figure 6.3.

With applying upwind method in Equation (6.10) with considering fully implicit method can be written

$$(W_p - W_p^o)\Delta V = \left[-\left(A_P.F_P - A_W.F_W\right)\Delta t\right] + S.\Delta t.\Delta V \tag{6.13}$$

6.4 Equilibrium

6.4.1 Kinematic Wave Model

In the solution of one dimensional equations for equilibrium sediment transport processes in unsteady flow conditions there are the six following unknowns:
h: depth of flow, u: velocity of water, z: sediment thickness , c: the volumetric concentration of sediment in suspension, q_{b*}: flux of sediment particles and S_f: frictional slope.

In kinematic wave model the required six equations are:

●Continuity equations of water (Eq. 4.13) (to find h and z).

●Continuity equations of sediment (Eq. 4.15) (to find h and z).

●(4.23-4.24) relations (to find velocity of water).

●Velikanov equation (Eq. 4.21) (to find volumetric concentration of sediment in suspension).

●Engelund and Fredsøe relation (Eq. 3.86 divided by γ_s to find flux of sediment particles).

●Momentum equation which is written as (S_f=S_0).

6.4.1.1 Explicit Scheme

Continuity equation of water is

$$a.h_p - m.a.h_p^{1.5} + P.a.z_p + s1 = 0$$

$$s1 = -h_p^0.a + m.a.h_p^{0^{1.5}} - P.a.\frac{z_E^0 + z_W^0}{2} +$$

$$(((\frac{h_p^0 + h_E^0}{2})^{2.5}) - ((\frac{h_p^0 + h_W^0}{2})^{2.5})) - ((n(\frac{h_p^0 + h_E^0}{2})^3) - (n(\frac{h_p^0 + h_E^0}{2})^3))$$

$$(6.14)$$

Continuity equation of sediment is

$$m.a.h_P^{1.5} + (1-p).a.z_p + s2 = 0$$

$$s2 = -m.a.h_P^{0^{1.5}} - (1-p).a.\frac{z_E^0 + z_W^0}{2} + (\,(n(\frac{h_P^0 + h_E^0}{2})^3) - (n(\frac{h_W^0 + h_P^0}{2})^3))$$

$$+(\frac{h_P^0 + h_E^0}{2}.qbs_e^0 - \frac{h_W^0 + h_P^0}{2}.qbs_w^0)$$

$$(6.15)$$

where $m = \delta.\alpha^3$, $n = \delta.\alpha^4$.

6.4.1.2 Fully Implicit Scheme

Continuity equation of water is

$$ah_p - ma.h_p^{1.5} + P.a.z_p + ((\frac{h_P + h_E}{2})^{2.5}) - ((\frac{h_P + h_W}{2})^{2.5}) -$$

$$((n(\frac{h_P + h_W}{2})^3) - (n(\frac{h_P + h_W}{2})^3)) + s1 = 0$$

$$s1 = -h_p^0.a + ma(\frac{h_E^0 + h_W^0}{2})^{1.5} - P.a.\frac{z_E^0 + z_W^0}{2}$$

$$(6.16)$$

Continuity equation of sediment is

$$m.a.h_P^{1.5} + (1-p).a.z_p + (\,(n(\frac{h_P + h_E}{2})^3) - (n(\frac{h_W + h_P}{2})^3)) + (\frac{h_P + h_E}{2}).(\frac{qbs_P + qbs_P}{2}) -$$

$$(\frac{h_W + h_P}{2}).(\frac{qbs_P + qbs_W}{2}) + s2 = 0$$

$$s2 = -m.a.(\frac{h_E^0 + h_W^0}{2})^{1.5} - (1-p).a.\frac{z_E^0 + z_W^0}{2}$$

$$(6.17)$$

where $m = \delta.\alpha^3$, $n = \delta.\alpha^4$.

6.4.2 Dynamic Wave Model

In dynamic wave model the first five equations are the same. Only the last equation is substituted by the momentum equation in general form (4.20).

6.4.2.1 Explicit Scheme

The momentum equation is

$$k.a.u_p + s1 = 0$$

$$s1 = g.Sf.\Delta A - k.a.u_p^0 + h^0_{\,P}.u^{02}_{\,P}.(\frac{k}{2}) - h^0_{\,W}.u^{02}_{\,W}.(\frac{k}{2}) + \qquad (6.18)$$

$$g.(h^{02}_{\,P} - h^{02}_{\,W} + h^0_{\,P}.z^0_P - h^0_{\,W}.z^0_W - S_0.\Delta A)$$

Continuity equation of water is

$$a.h_p - a.\delta.u_p^3 + p.a.z_p + s2 = 0$$

$$s2 = -a.h_p^0 + a.\delta.u_p^{0^3} - p.a.z_p^0 + u_p^0.h_p^{0^2} - \qquad (6.19)$$

$$u_W^0.h_p^0.h_W^0 + h_p^{0^2}.u_p^0 - u_p^0.h_p^0.h_W^0 + u_p^{0^4}.\delta.h_p^0 - u_W^{0^4}.\delta.h_W^0$$

Continuity equation of sediment is

$$\delta.a.u_p^3 + a.z_p(1-p) + s3 = 0$$

$$s3 = -\delta.a.u_p^{o^3} + a.z_p^0.(p-1) + h^0_{\,P}.u_P^{4^0}.(\delta) - h^0_{\,W}u_W^{4^0}.\delta + h^0_{\,P}.qbs \qquad (6.20)$$

where $dA = h.\Delta x$, $a=dA/dt$ and k is a coefficient that depend to the solution. The value of k in fully implicit scheme is equal to 1 and in crank-Nicolson scheme is equal to 1/2. In other equations the value of k is the same.

6.5 Non Equilibrium

In this case the continuity equation of sediment must be modified. Instead of (Eq. 4.15), two equations (Eqs. 4.14.a and b) are used with two unknowns which are

entrainment rate E_z and deposition rate D_c.

Gessler (1965) suggested a value of 0.047 for K for most flow conditions. The value of transfer rate can be calculated in flumes by $\sigma = 1/(7h)$, where h is flow depth, parameter Φ has a range of $0.0 - 1.0$ and exponent k has a range of $1.0 - 2.5$ in literature (Foster 1982, Tayfur 2002, Yange 1996). This study applied value of k as 1 and value of Φ as 0.001.

6.5.1 Kinematic Wave Model

6.5.1.1 Explicit Scheme

Continuity equation of water is

$$h_p(1+\frac{c_E^0+c_W^0}{2})-2.c_p.h_p+p.z_p+c_p.h_p^0+\frac{s1}{a}=0$$

$$s1=-a.h_p^0-p.a.\frac{z_E^0+z_W^0}{2}+\alpha(h_e^{2.5^0}-h_w^{2.5^0})-$$

$$\alpha.\frac{c_E^0+c_W^0}{2}(h_P^{2.5^0}-h_W^{2.5^0})-\alpha.h_p^{1.5^0}(h_P^0\frac{c_E^0+c_W^0}{2}-h_W^0c_W^0)$$

(6.21)

Conservation of mass for suspended sediment in the water flow layer:

$$2.h_p.c_p-c_p.h_p^0-h_p.\frac{c_E^0+c_W^0}{2}+\frac{s2}{a}=0$$

$$s2=-\frac{1}{\rho_s}[E_z^0-D_c^0]\Delta A+\alpha(h_p^{1.5^0}h_P^0.\frac{c_E^0+c_W^0}{2}-h_W^0.c_W^0)+$$

$$\alpha\frac{c_E^0+c_W^0}{2}(h_{\ P}^{2.5^0}-h_{\ W}^{2.5^0})$$

(6.22)

Conservation of mass for bed sediment in the movable bed layer:

$$(1\text{-}p)z_p+\frac{s3}{a}=0$$

$$s3=\text{-}(1\text{-}p).a.\frac{z_{i+1}^0+z_{i-1}^0}{2}+(h_{\ P}^0.qbs_{\ P}^0-h_{\ W}^0.qbs_{\ W}^0)-\frac{1}{\rho_s}[D_c^0-E_z^0]\Delta A$$

(6.23)

6.5.1.2 Fully Implicit Scheme

Continuity equation of water is

$$a.h_p - 2.a.c_p.h_p + a.c_p.h_p^0 + a.h_p.c_p^0 + p.a.z_p$$
$$+\alpha(1-c_P)(h_P^{2.5} - h_W^{2.5}) - \alpha.h_p^{1.5}(h_P c_P - h_W c_W) + s1 = 0 \tag{6.24}$$
$$s1 = -a.h_p^0 - p.a.\frac{z_E^0 + z_W^0}{2}$$

Conservation of mass for suspended sediment in the water flow layer:

$$2.c_p.a.h_p - c_p.a.h_p^0 - h_p.a.c_p^0 + \alpha h_p^{1.5}(h_P.c_P - h_W.c_W) + \alpha c_p(h^{2.5}{}_P - h^{2.5}{}_W) - n1 = 0$$
$$n1 = \frac{1}{\rho_s}[E^0{}_z - D^0{}_c]\Delta A \tag{6.25}$$

Conservation of mass for bed sediment in the movable bed layer:

$$(1\text{-}p).a.z_p + h_P.qbs_P - h_W.qbs_W + s3 = 0$$
$$s3 = -(1\text{-}p).a.\frac{z^0_{i+1} + z^0_{i-1}}{2} + n1 \tag{6.26}$$

6.5.2 Dynamic Wave Model

6.5.2.1 Explicit Scheme

Continuity equation of water is

$$h_P - 2c_P h_P + c_P h_P^0 + h_P c_P^0 + p.z_P + \frac{s1}{a} = 0$$
$$S1 = -ah_P^0 - pa\frac{z_E^0 + z_W^0}{2} + (1-2c_P^0)u_P^0(h^{0^2}{}_P - h^{0^2}{}_W) \tag{6.27}$$
$$+(1-2c_P^0)h_P^0(h_P^0.u^0{}_P - h_W^0 u^0{}_W) - 2u_P^0 h_P^0(h_P^0.c^0{}_P - h_W^0 c^0{}_W)$$

Conservation of mass for suspended sediment in the water flow layer:

$$2c_P.h_P - c_P.h_P^0 - h_P.c_P^0 + \frac{s2}{a} = 0$$

$$s2 = 2h_P^0 u_P^0 (h_P^0 c_P^0 - h_W^0 c_W^0) + 2h_P^0 c_P^0 (h_P^0 u_P^0 - h_W^0 u_W^0)$$

$$+2u_P^0 c_P^0 (h_P^{2^0} - h_W^{2^0}) - \frac{1}{\rho_s}[E_z^0 - D_c^0]$$

(6.28)

Conservation of mass for bed sediment in the movable bed layer:

$$(1\text{-}p)z_p + \frac{s3}{a} = 0$$

$$s3 = -(1\text{-}p).a.\frac{z_{i+1}^0 + z_{i-1}^0}{2} + (h_P^0.qbs_P^0 - h_W^0.qbs_W^0) + \frac{1}{\rho_s}[E_z^0 - D_c^0]\Delta A$$

(6.29)

The momentum equation is

$$k.a.u_p + S4 = 0$$

$$S4 = g.S_f.\Delta A - k.a.u_p^0 + h_P^0.u_P^{02}.(\frac{k}{2}) - h_W^0.u_W^{02}.(\frac{k}{2})$$

$$+g.(h_P^{02} - h_W^{02} + h_P^0.\frac{z_E^0 + z_W^0}{2} - h_W^0.z_W^0 - S_0.\Delta A)$$

(6.30)

It must be noted that instead of value of bed profile z in time t in point P used average of values of east E and west W point (LAX scheme).

The important mater is that must be attention in working with numerical solution about stability conditions. In order to satisfy this condition Courant − Friedrichs − Lewy (CFL) condition can be used.

$$C_n = \frac{\left(u + \sqrt{gh}\right)\Delta t}{\Delta x} \leq 1$$

(6.31)

where C_n is Courant number, u is velocity of flow ($m.s^{-1}$), g is gravity acceleration ($m.s^{-2}$) and h refers to depth of flow (m).

CHAPTER SEVEN
TEST OF MODELS

7.1. Introduction

This study is realized in the scope of the research project TUBİTAK (109M637) titled "Experimental and theoretical investigation of two dimensional sediment transport resulting from flood wave propagation in open channels; determination of local scours at bridges abutments and around interior piers due to this motion-design and tests of counter-measures". Numerous experiments are carried out by using the experimental system designed and built in hydraulics laboratory (Güney et al., 2011a, Güney et al. 2011b).

The numerical results are compared with these experimental findings obtained by generating the following six input hydrographs.
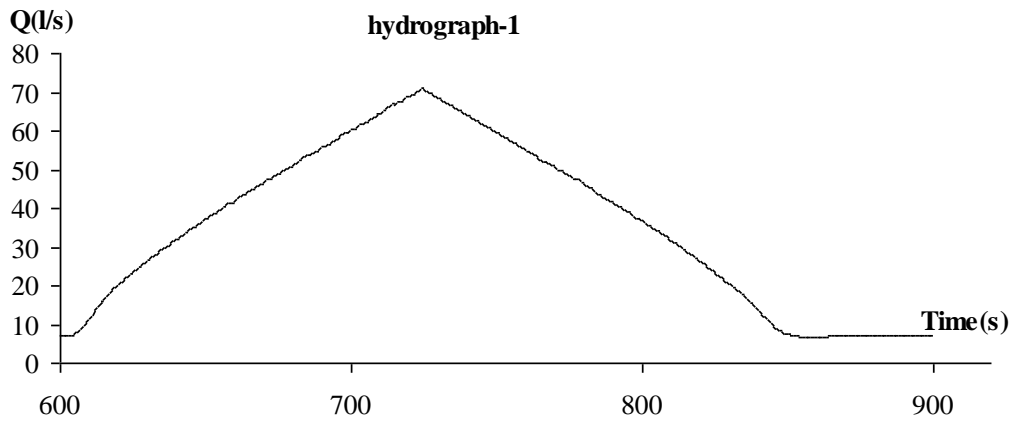
Figure 7.1 Inflow hydrograph 1.
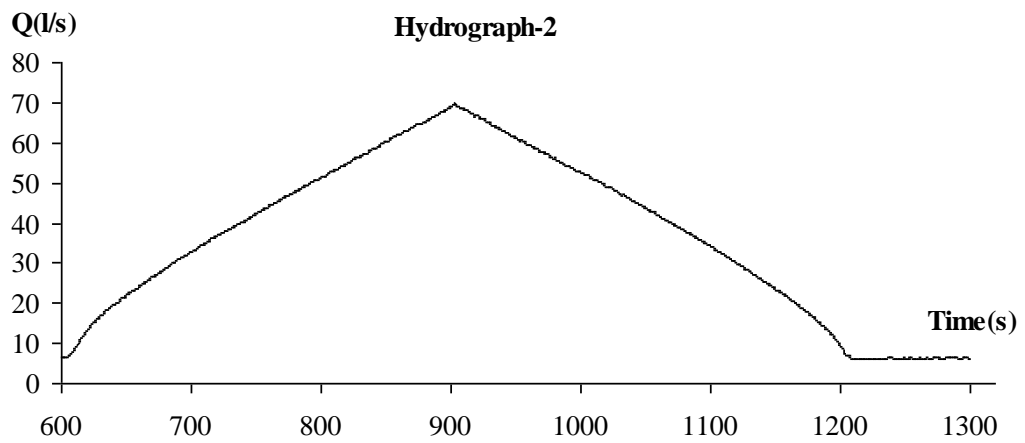
Figure 7.2 Inflow hydrograph 2.
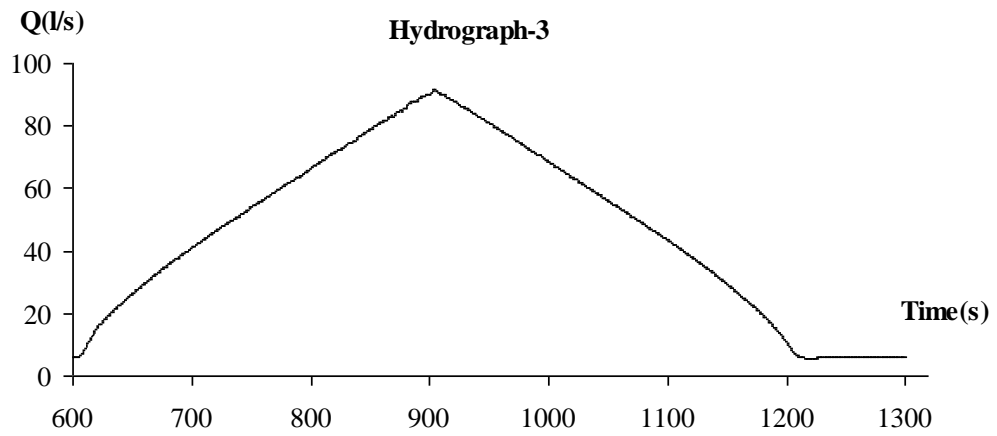
Figure 7.3 Inflow hydrograph 3.
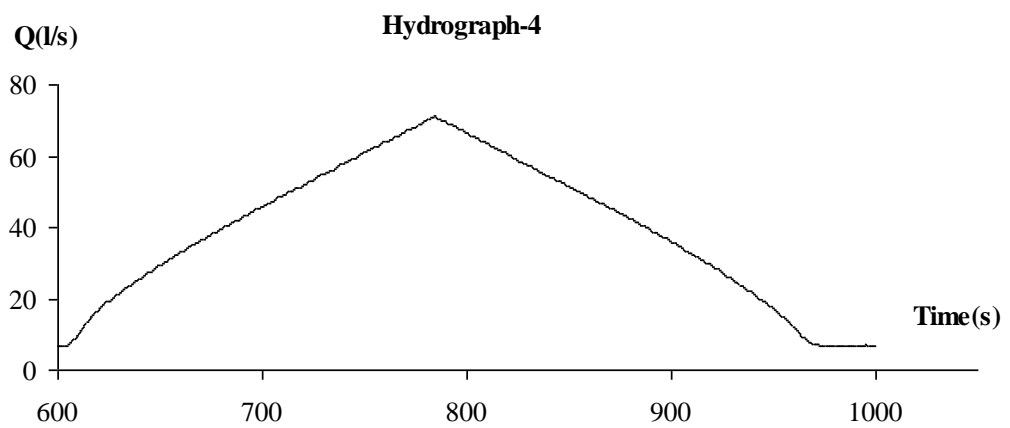
Figure 7.4 Inflow hydrograph 4.
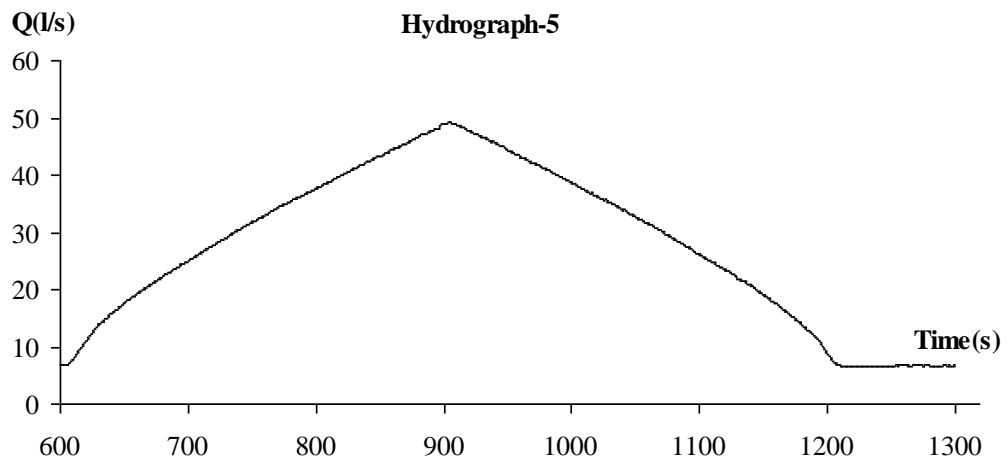
Figure 7.5 Inflow hydrograph 5.
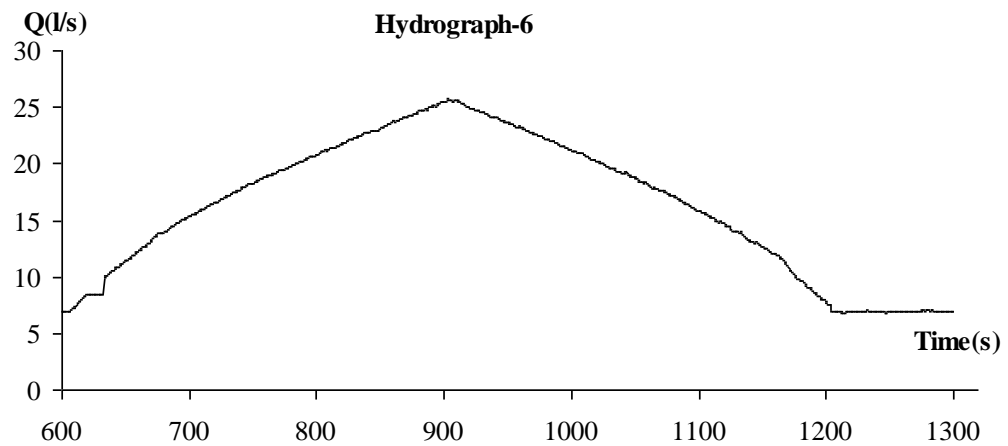
Figure 7.6 Inflow hydrograph 6.

Note that the unit of time is second and the unit of flow rate (Q) is liter per second. Before begin to pass the hydrographs made a smooth surface of sediments in vertical and stream-wise direction. The elevation of this bed level measured in longitude and latitude directions. But because the aim of this thesis is developed a one dimensional models, the average value of bed level elevations in latitude directions used. One and two dimensional forms of bed can be found profiles in Figures below.
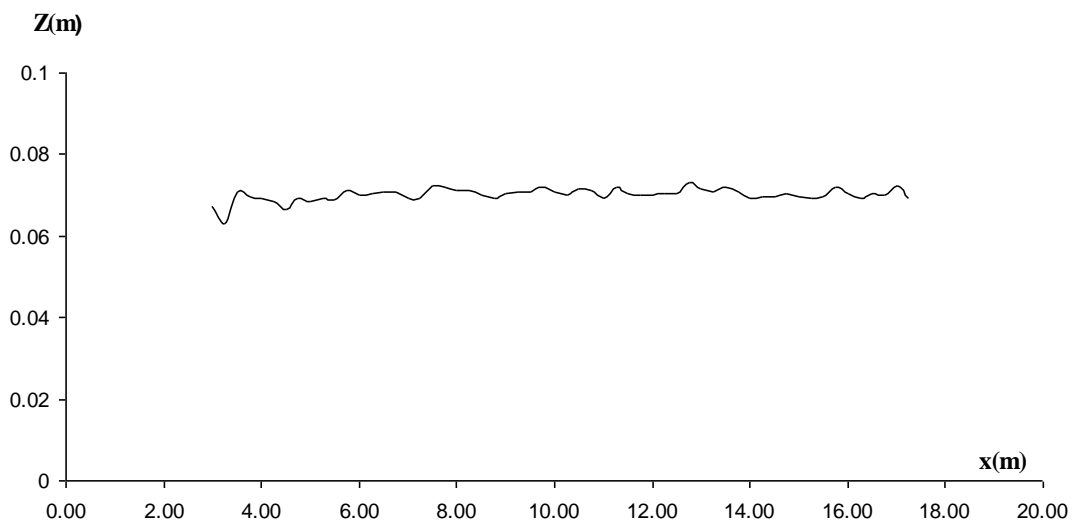
Figure 7.7 Average of initial view of one dimensional bed profile
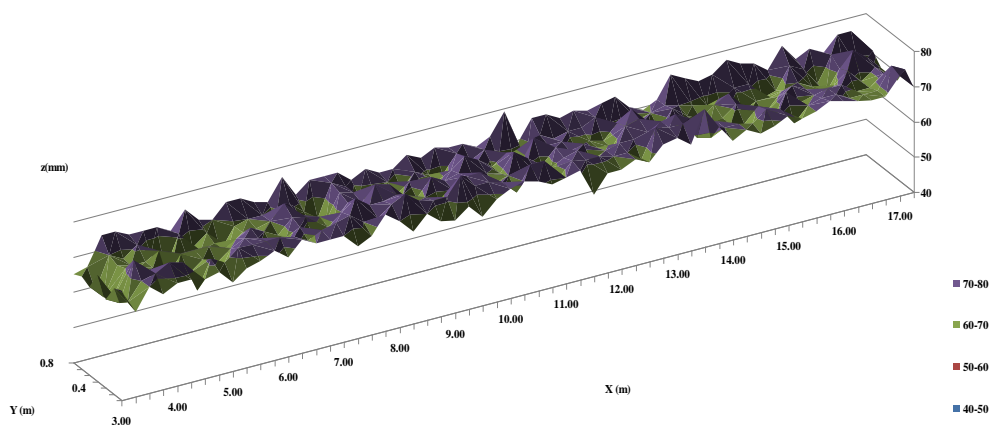
Figure 7.8 view of Initial two dimensional bed profile

Now in this part initially will be given the measurement values of bed profiles for hydrographs and after that the bed profile comparison between results of models and measurements in one dimensional are given.
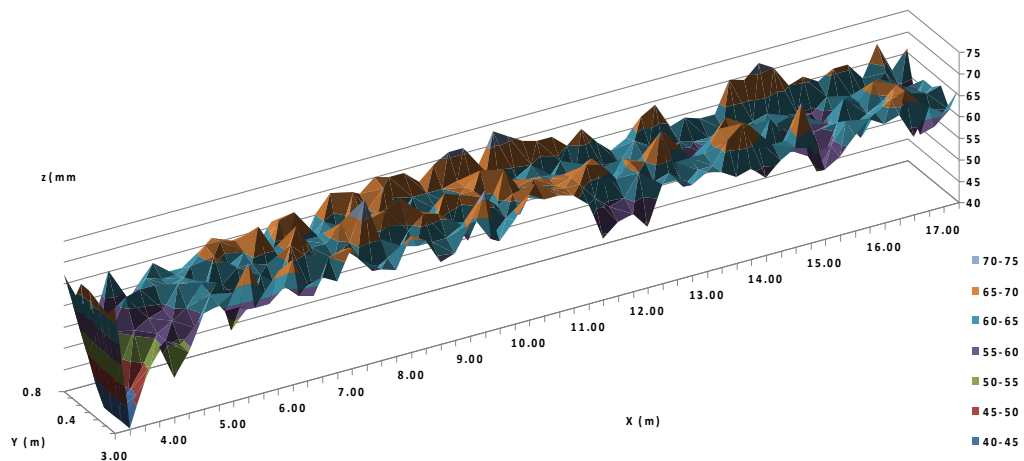
Figure 7.9 View of 2 dimensional bed profile after passing the flow for Hydrograph 1.
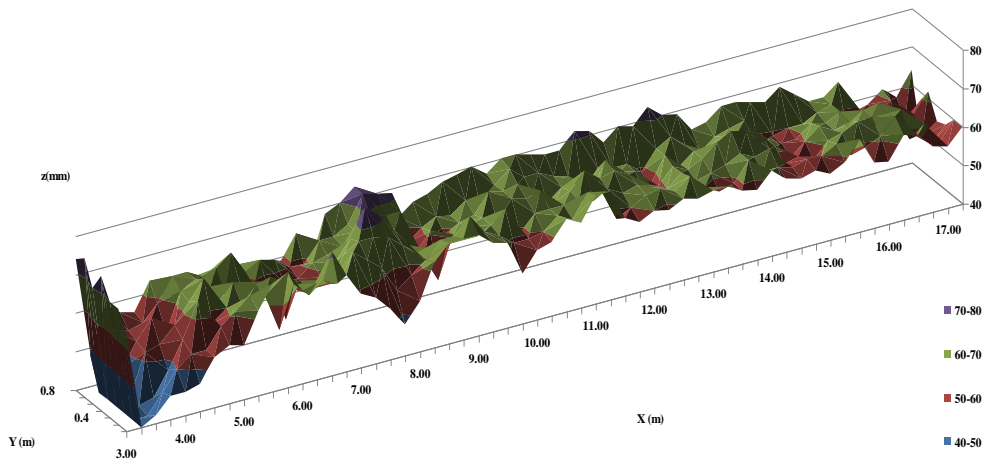
Figure 7.10 View of 2 dimensional bed profile after passing the flow for Hydrograph 2.
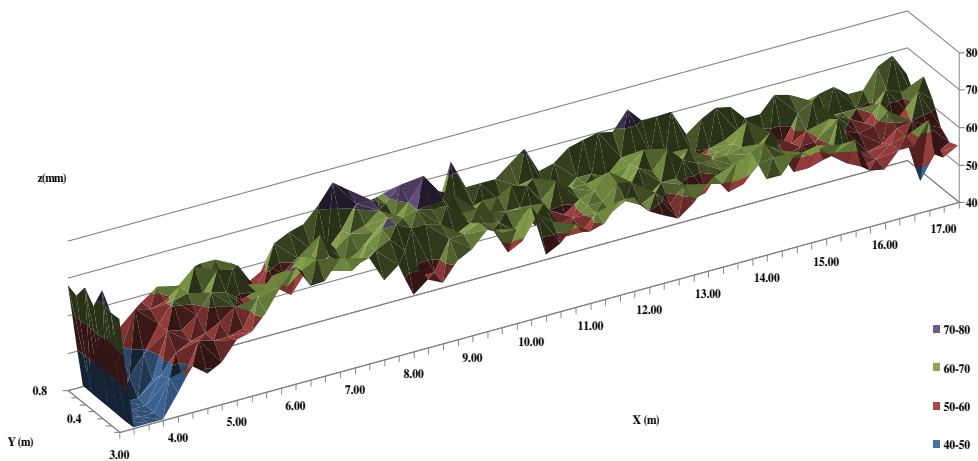
Figure 7.11 View of 2 dimensional bed profile after passing the flow for Hydrograph 3.
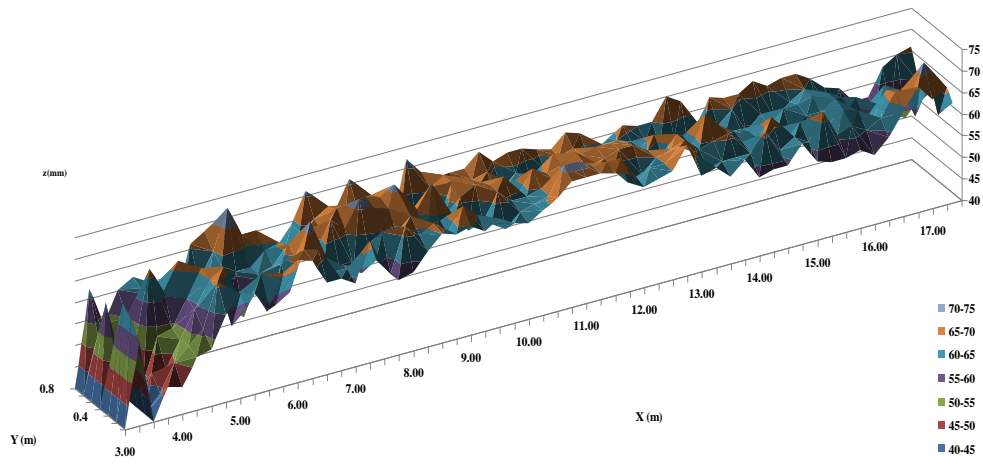
Figure 7.12 View of 2 dimensional bed profile after passing the flow for Hydrograph 4.
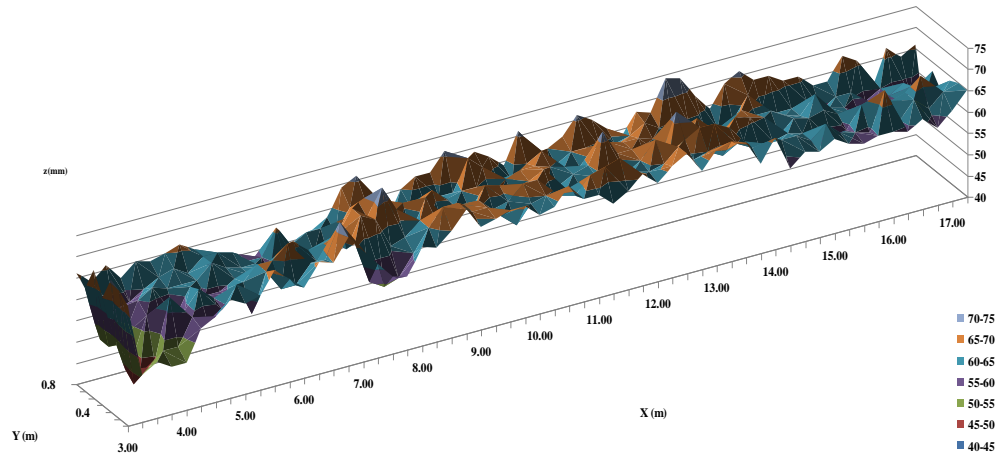
Figure 7.13 View of 2 dimensional bed profile after passing the flow for Hydrograph 5.
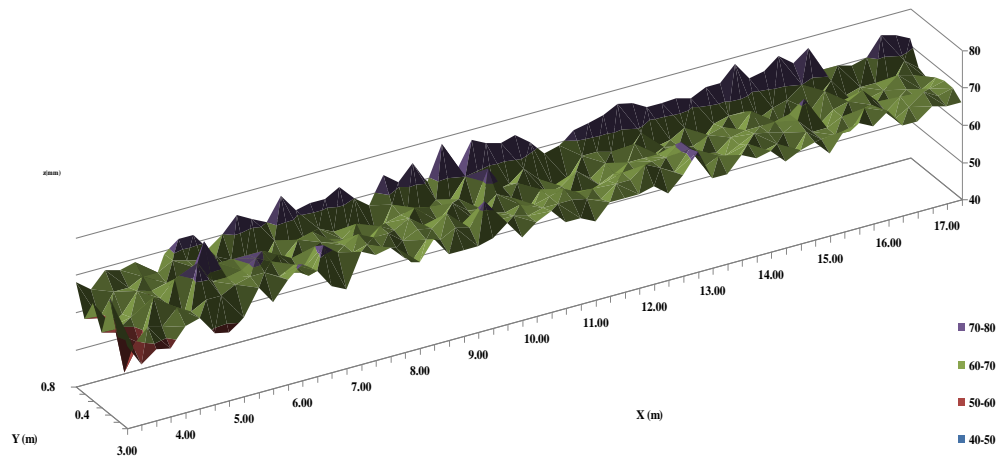
Figure 7.14 View of 2 dimensional bed profile after passing the flow for Hydrograph 6.

Note that first three meters of channel is fixed bed. In this research in order to understand the influence of sediment flux relations (q_{bs}), three empirical relations that suggested by difference investigators, applied. The comparison of results between these relations (Luque and Van Beek 1976,Wong and Parker 2006, Engelund and Fredsøe 1976), shown there is not really important difference in simulation of bed profiles, but between these relations Engelund and Fredsøe (1976) relation's yield the best results in predict of sediment flux. The results of these comparisons are given in Figures below.
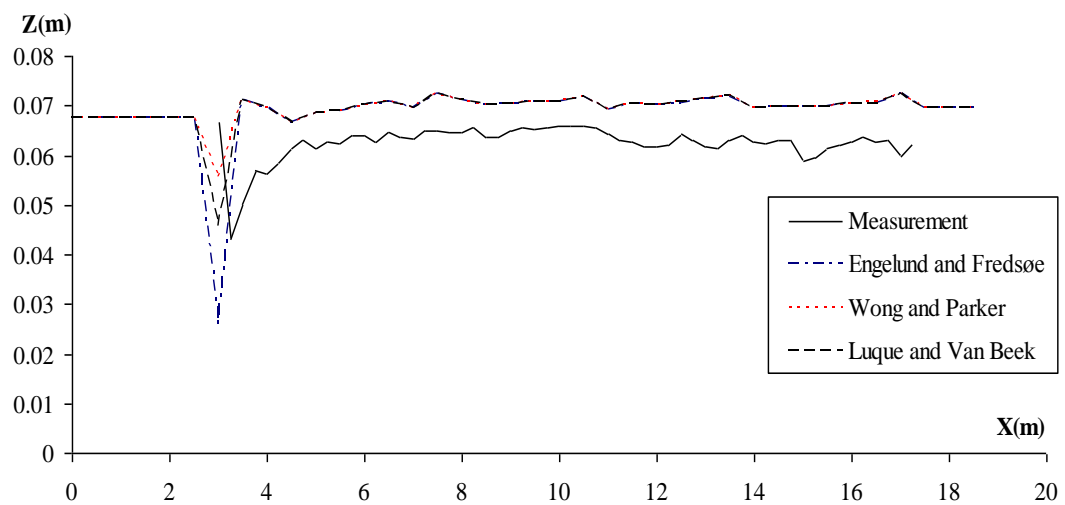
Figure 7.15 Comparison of bed profiles by difference relations in Eq, Ex, Kwm, Hydrograph 1.
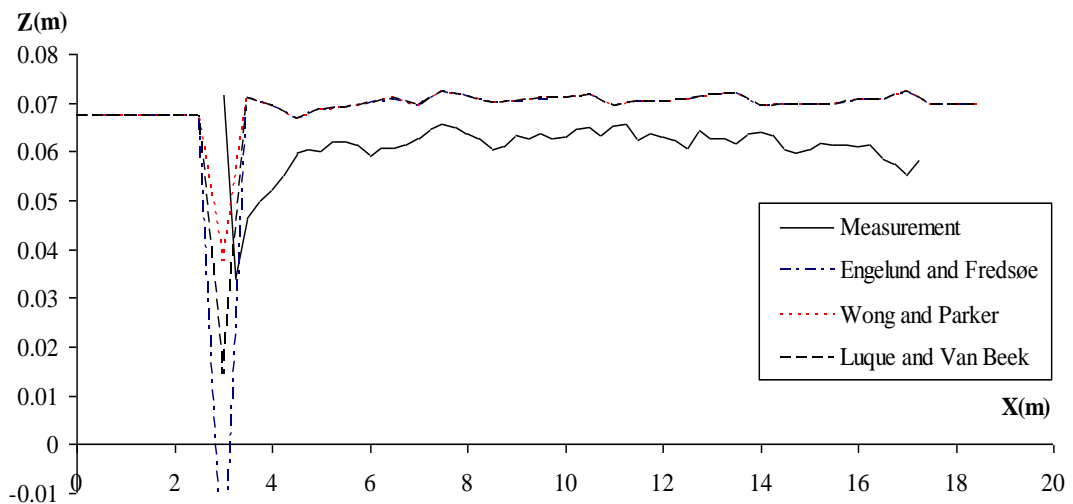
Figure 7.16 Comparison of bed profiles by difference relations in Eq, Ex, Kwm Hydrograph 2.
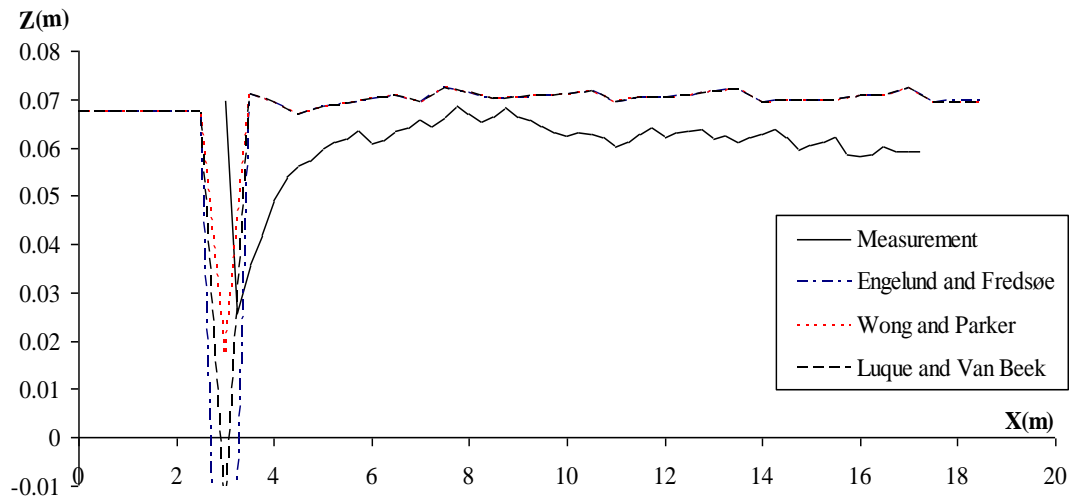
Figure 7.17 Comparison of bed profiles by difference relations in Eq, Ex, Kwm, Hydrograph 3.
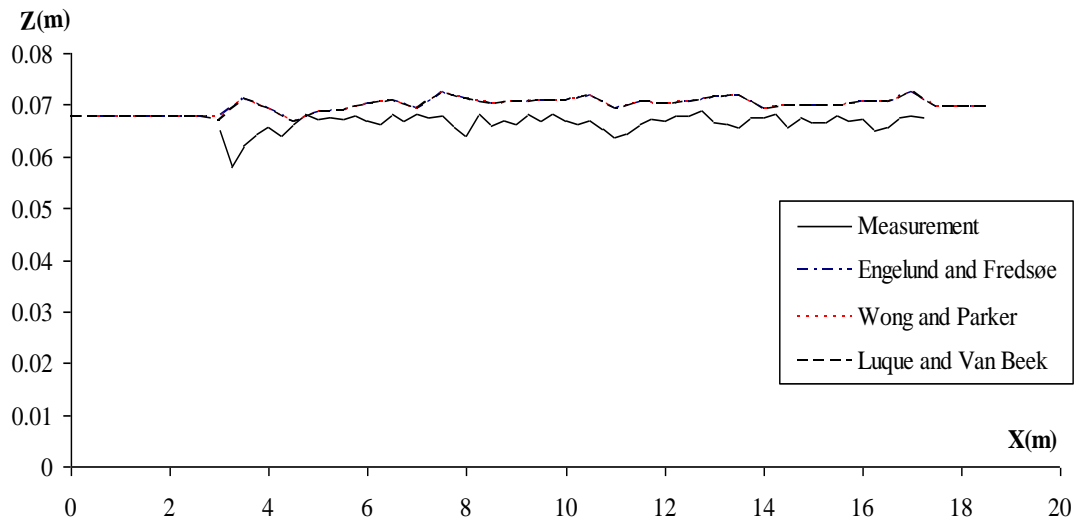
Figure 7.18 Comparison of bed profiles by difference relations in Eq, Ex, Kwm Hydrograph 6.
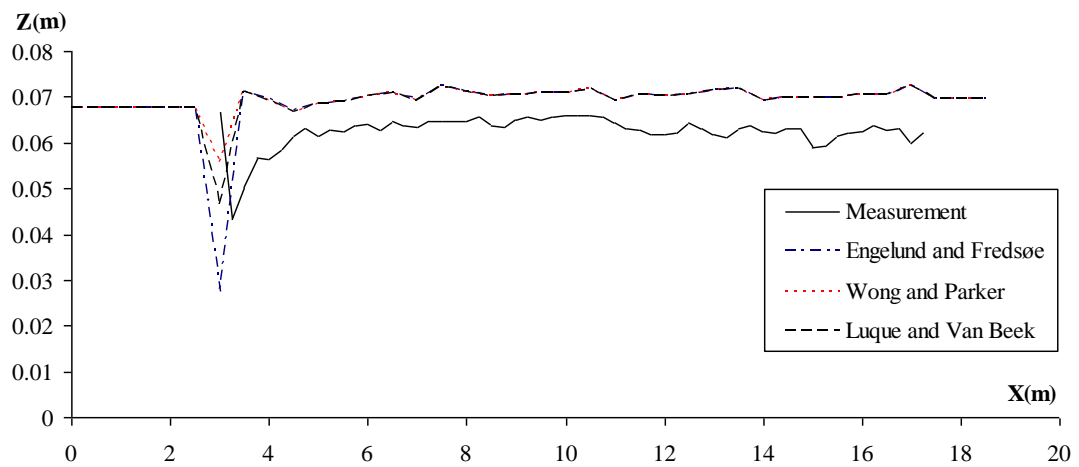
Figure 7.19 Comparison of bed profiles by difference relations in Eq, Ex, Dwm, Hydrograph 1.
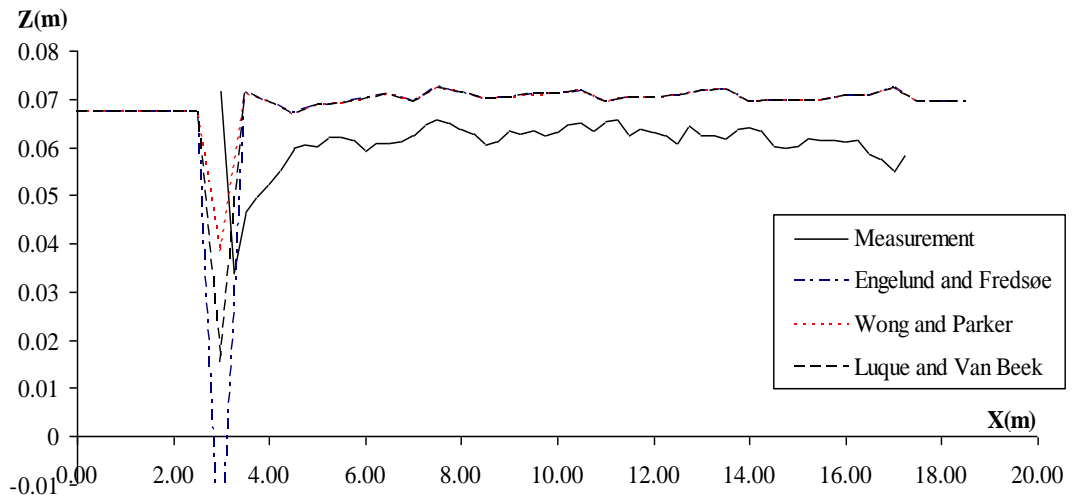
Figure 7.20 Comparison of bed profiles by difference relations in Eq, Ex, Dwm, Hydrograph 2.
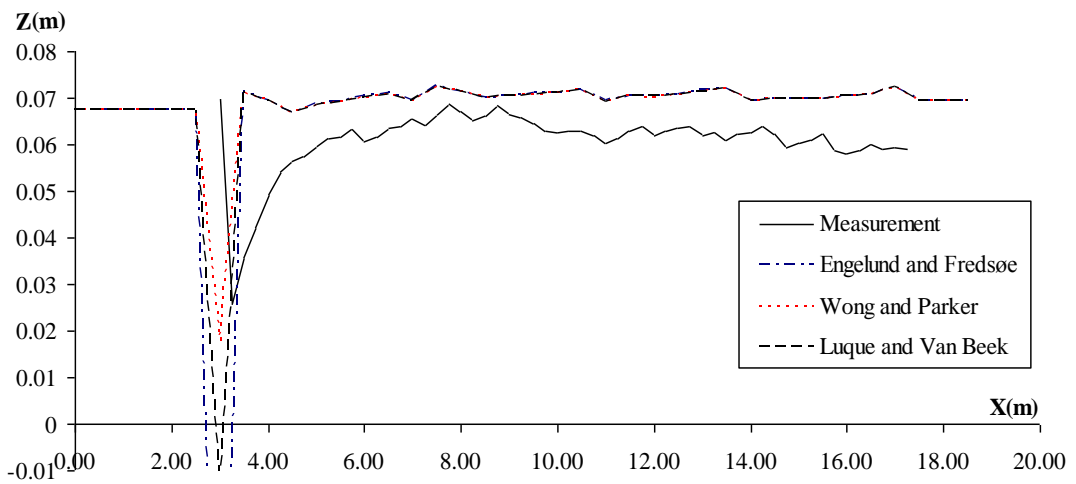
Figure 7.21 Comparison of bed profiles by difference relations in Eq, Ex, Dwm, Hydrograph 3.
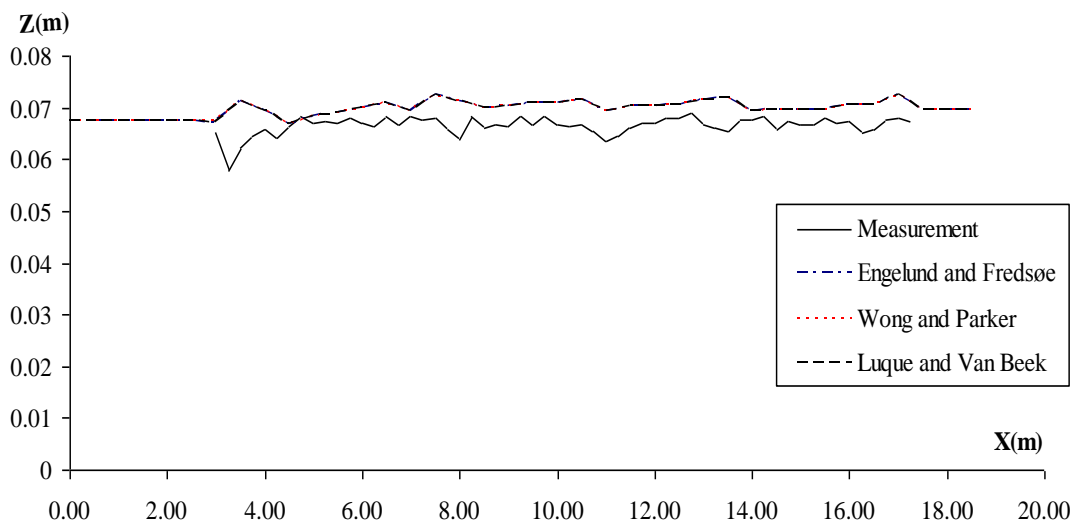
Figure 7.22 Comparison of bed profiles by difference relations in Eq, Ex, Dwm, Hydrograph 6.

Some incompatibilities exist between the experimental findings and numerical results due to the selected empirical relations and the different approaches used in numerical solutions. The hydrograph durations and the peak discharge values also affect this phenomenon.

Views of sediment flux for example hydrographs are given in figure 7.23 to 7.30.
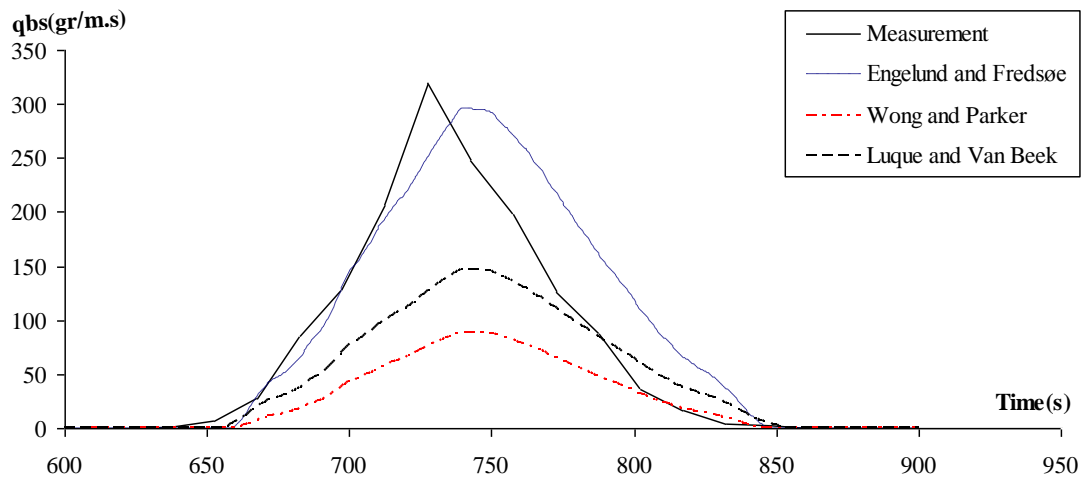
Figure 7.23 Comparison of sediment weights in Eq.,Ex., Kinematic wave model, Hydrograph 1.
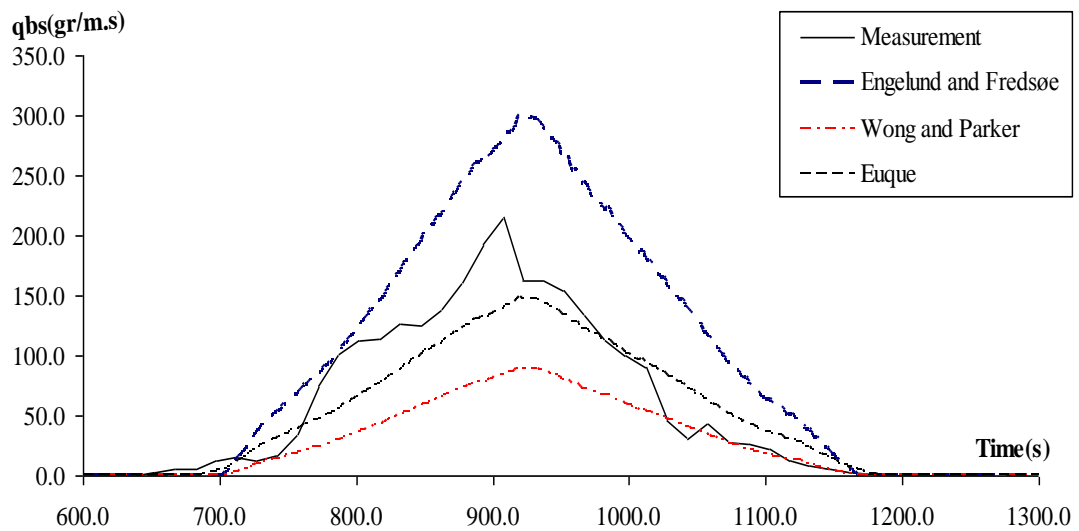
Figure 7.24 Comparison of sediment weights in Eq.,Ex., Kinematic wave model, Hydrograph 2.
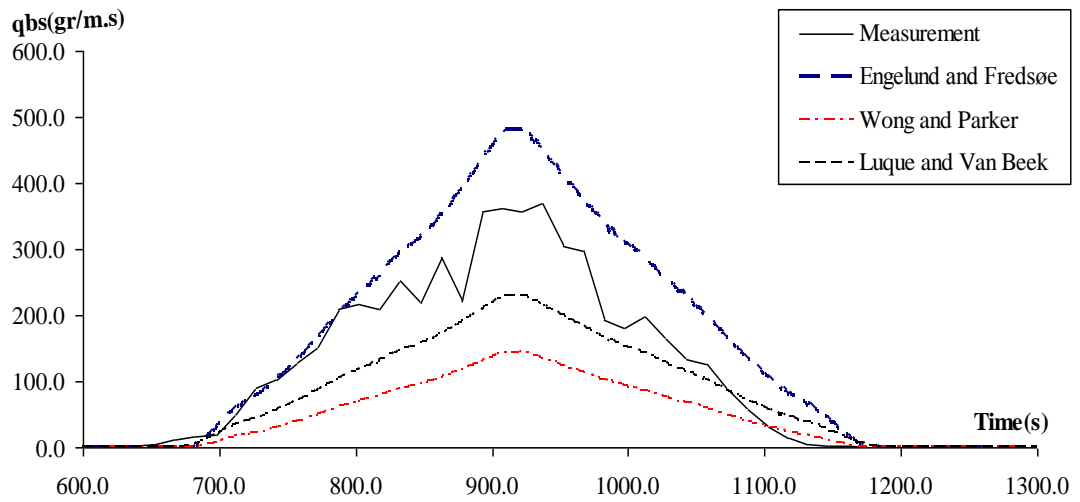
Figure 7.25 Comparison of sediment weights in Eq.,Ex., Kinematic wave model, Hydrograph 3.
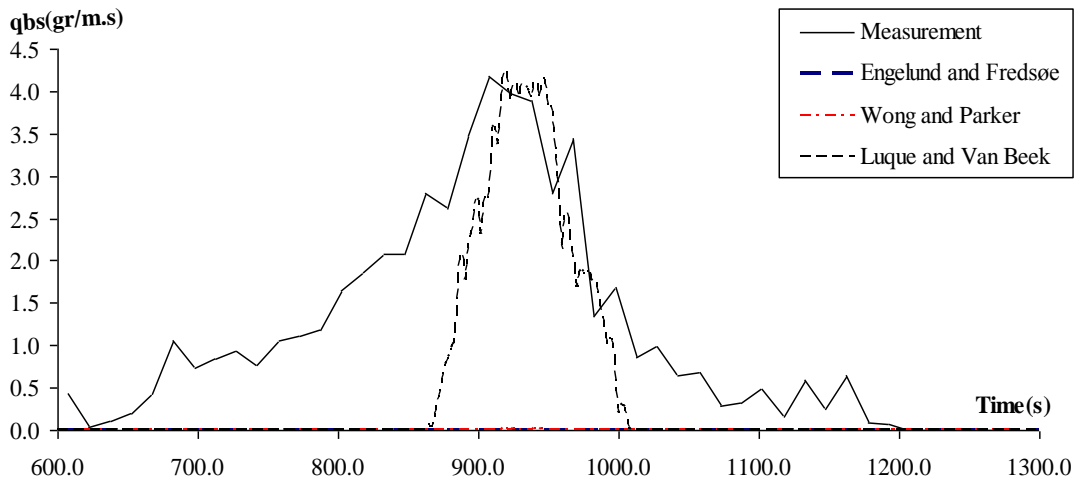
Figure 7.26 Comparison of sediment weights in Eq.,Ex., Kinematic wave model, Hydrograph 6.
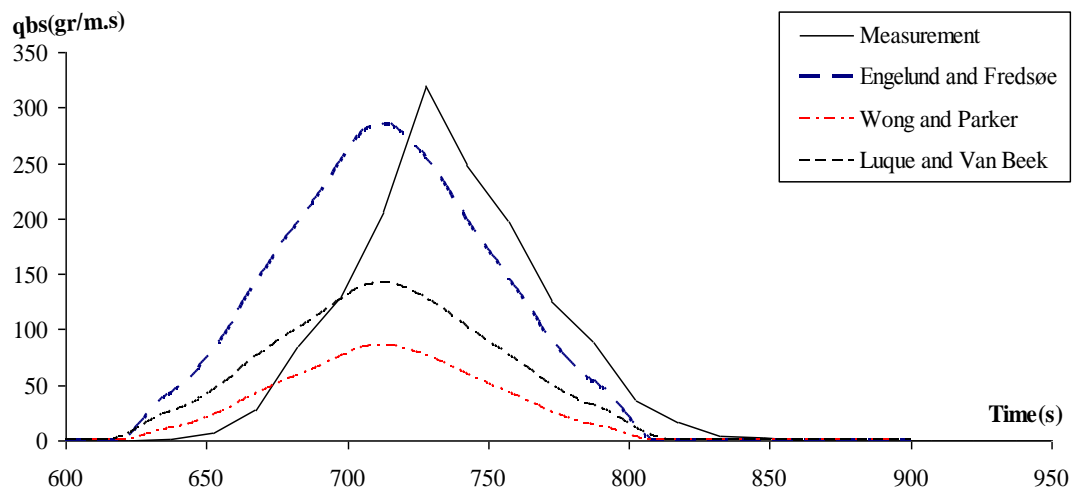
Figure 7.27 Comparison of sediment weights in Eq.,Ex., Dynamic wave model, Hydrograph 1.
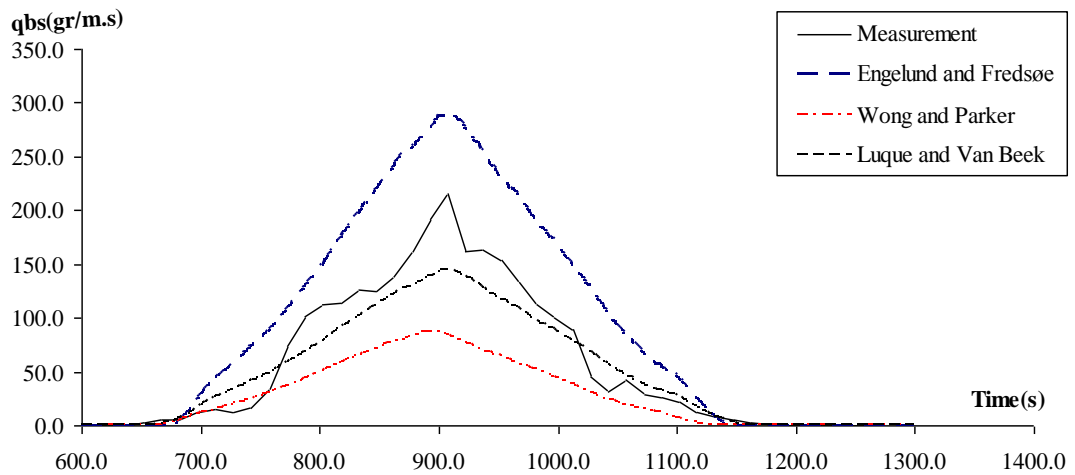
Figure 7.28 Comparison of sediment weights in Eq.,Ex., Dynamic wave model, Hydrograph 2.
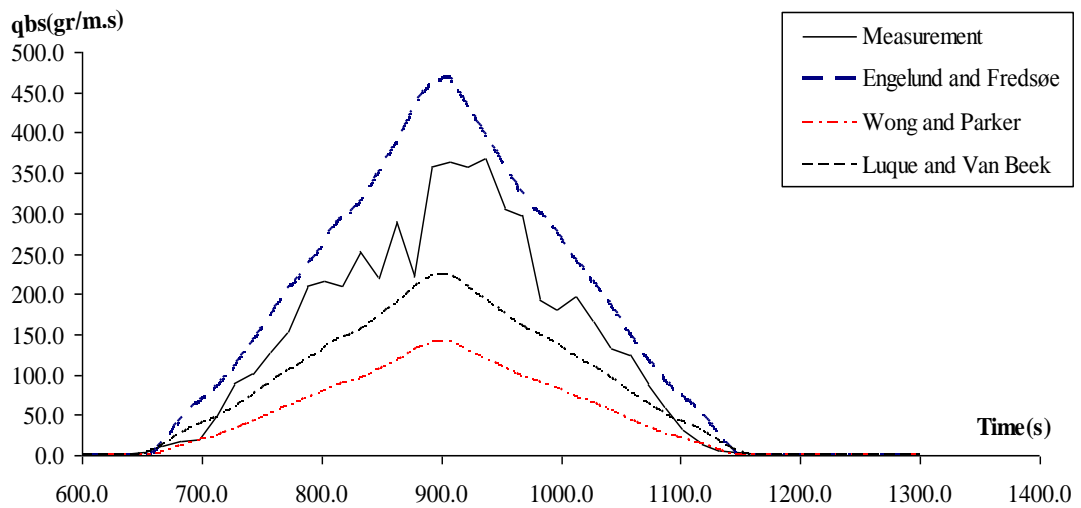
Figure 7.29 Comparison of sediment weights in Eq.,Ex., Dynamic wave model, Hydrograph 3.
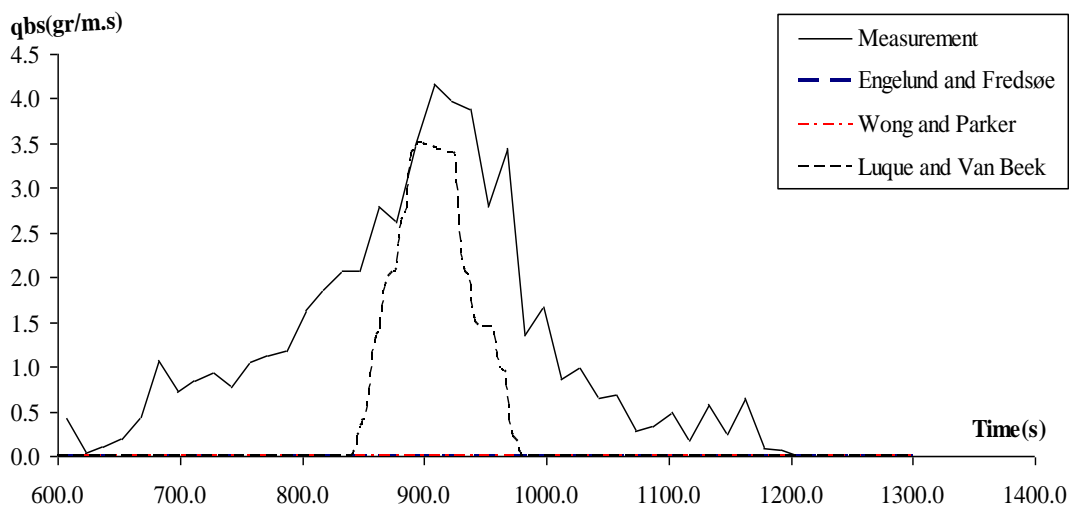
Figure 7.30 Comparison of sediment weights in Eq.,Ex., Dynamic wave model, Hydrograph 6.

Three empirical relations are used to calculate the sediment flux. The calculated value is smaller compared to the measured one (hydrograph 6). In this case the relation proposed by Luque and van Beek is more suitable. When all hydrographs are considered together the relation of Engelund and Fredsoe seems to be the most compatible.

7.2 Comparison of Kinematic Wave Models

In different sections (5m, 8m, 11m, 13.5m, 15m and 17m.) for the six hygrographs h values depending on time are given in Figures 7.31 − 7.66 for the kinematic wave models. z values after carried out hydrographs at the last time are given in Figure 7.67 - 7.72.
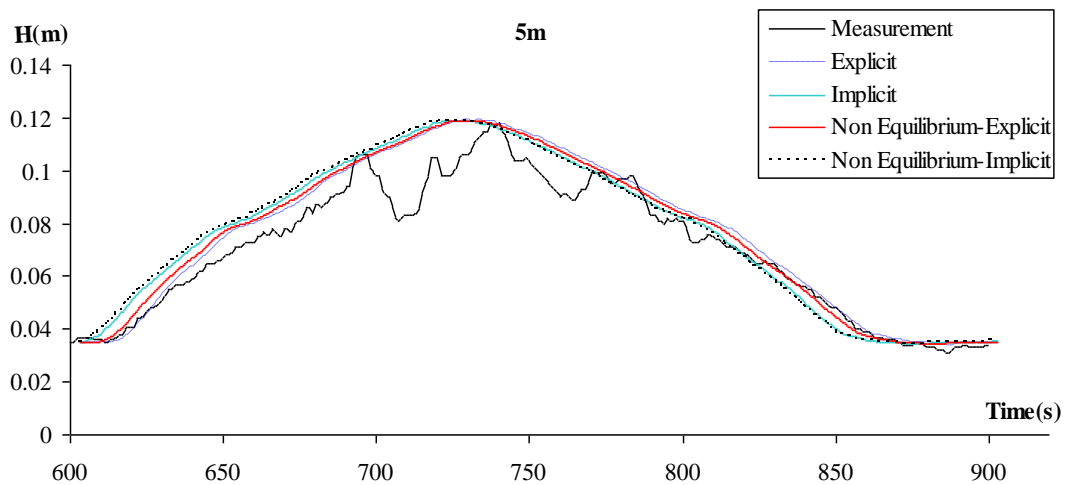
Figure 7.31 View of comparison between measurement and predict flow depth in 5.m –Hyd. 1
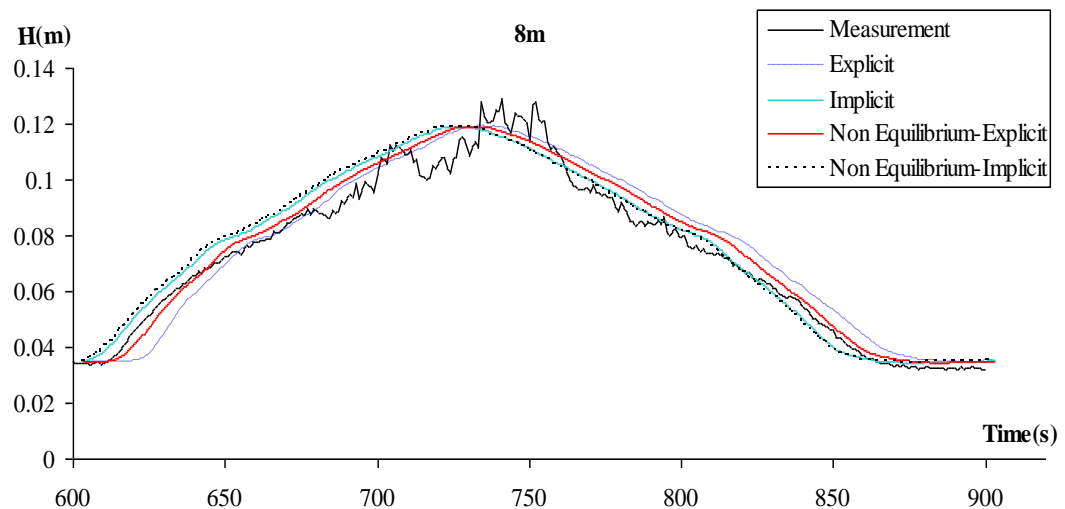
Figure 7.32 View of comparison between measurement and predict flow depth in 8.m –Hyd. 1
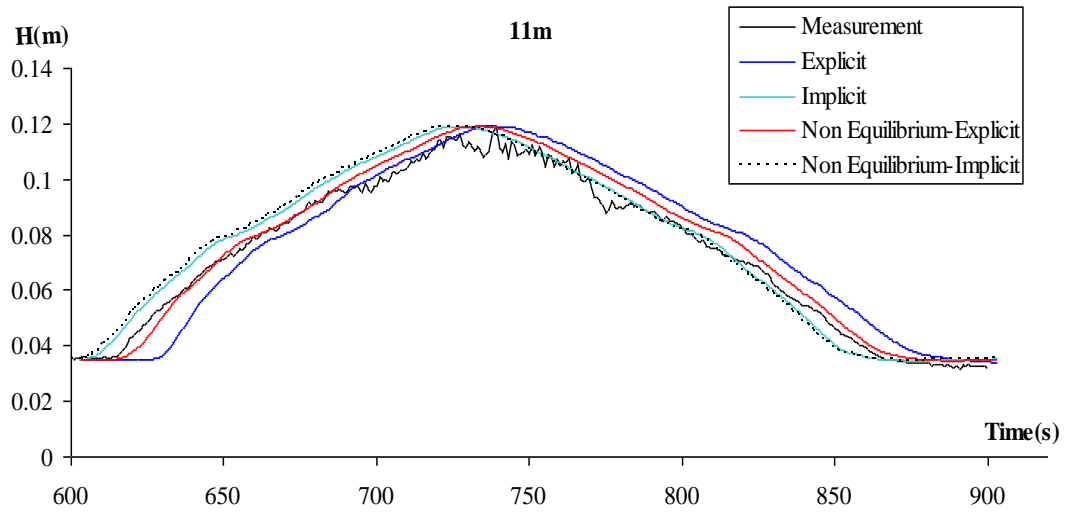
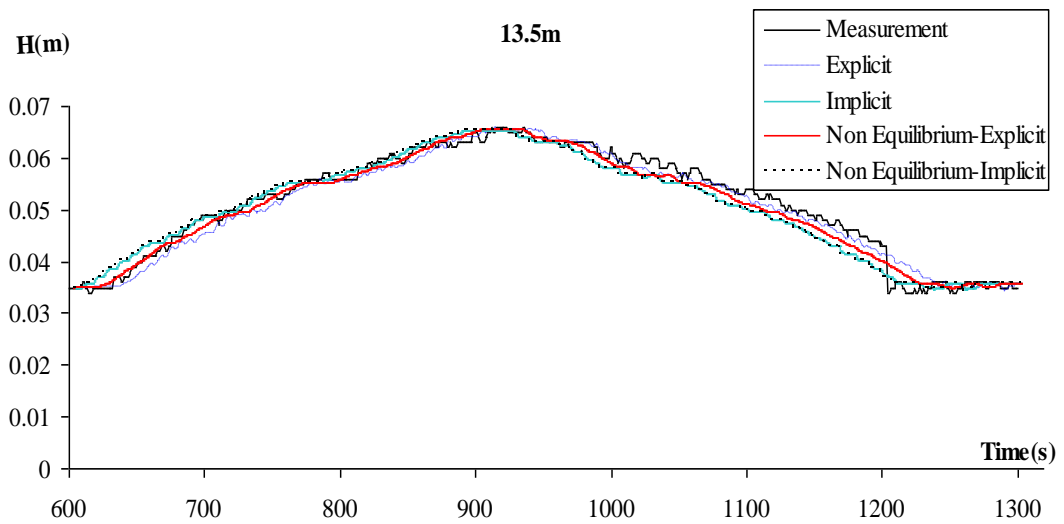Figure 7.33 View of comparison between measurement and predict flow depth in 11.m –Hyd. 1
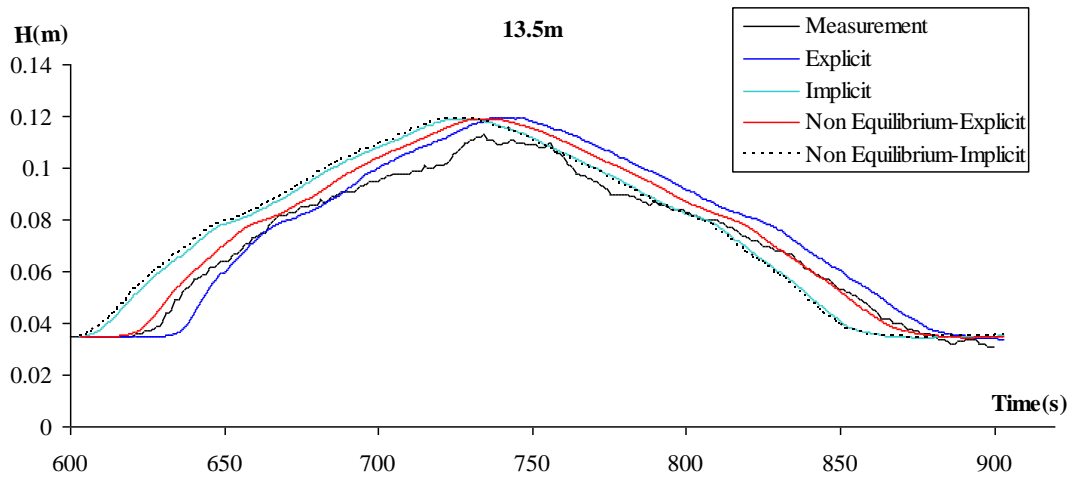
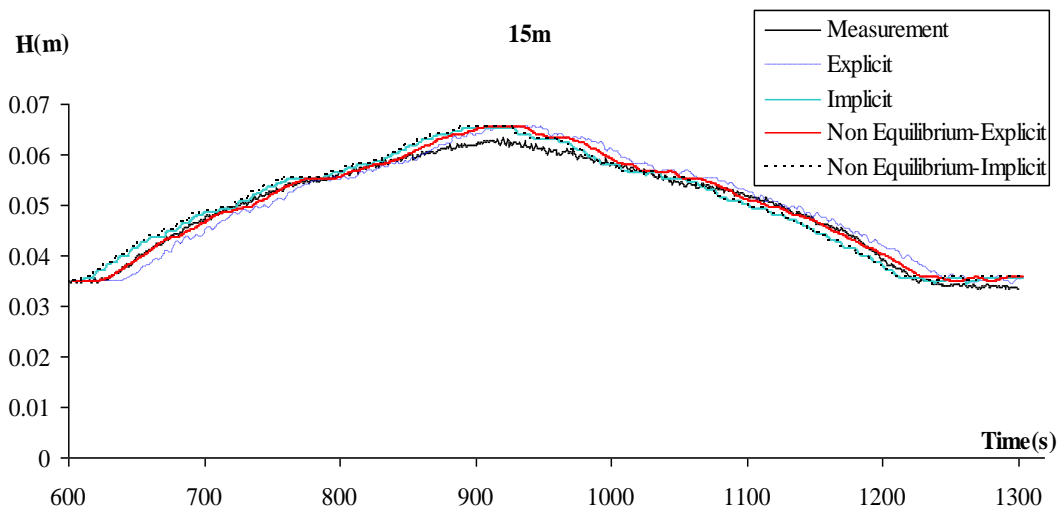Figure 7.34 View of comparison between measurement and predict flow depth in 13.5.m –Hyd. 1
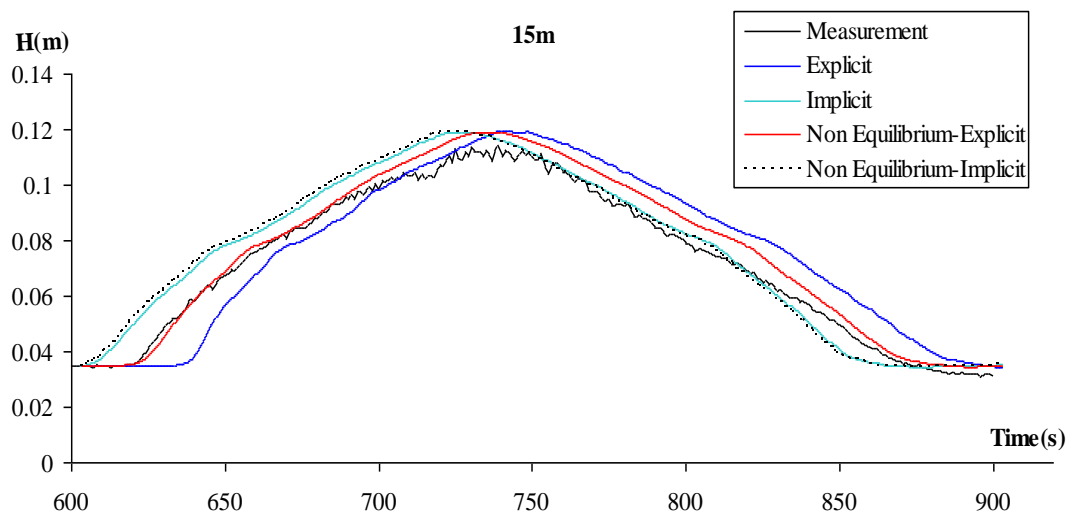
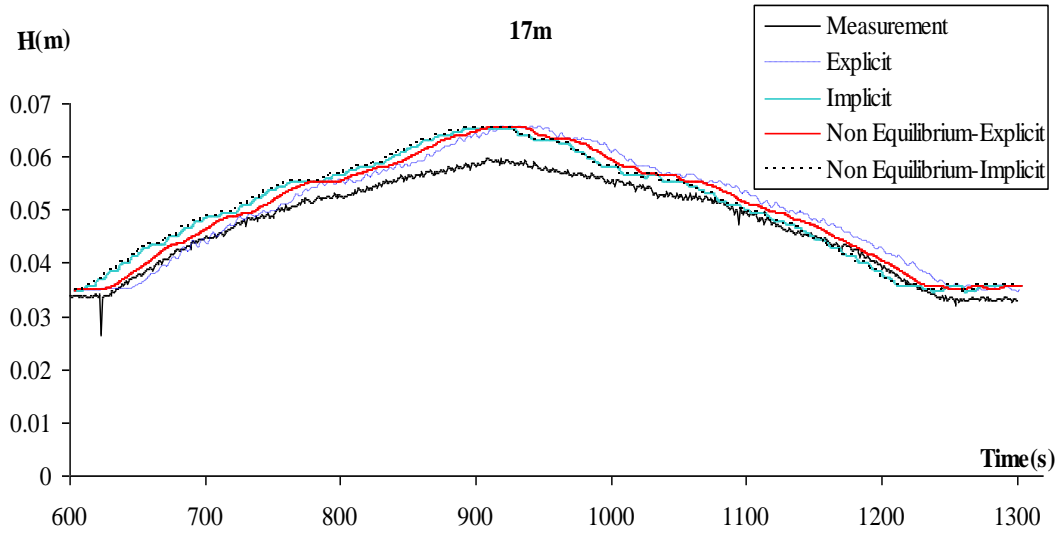Figure 7.35 View of comparison between measurement and predict flow depth in 15.m –Hyd 1
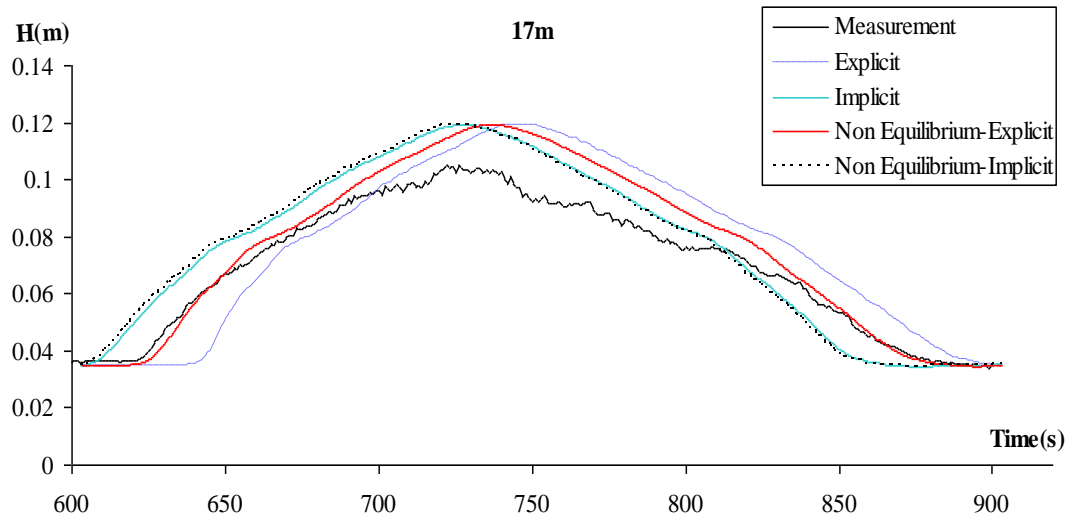
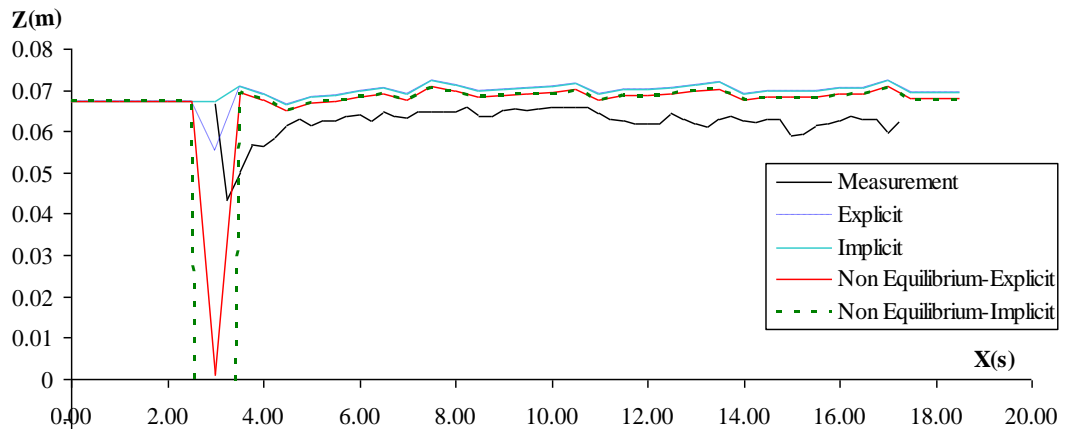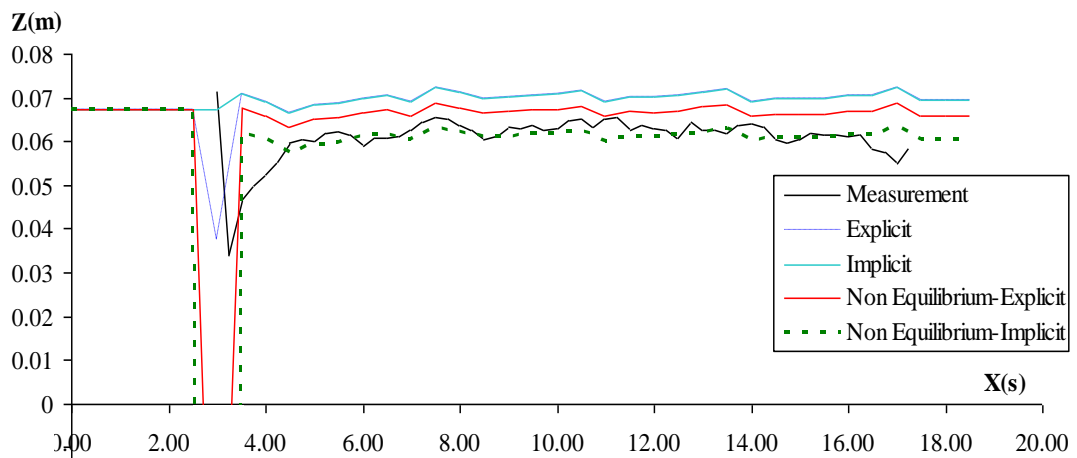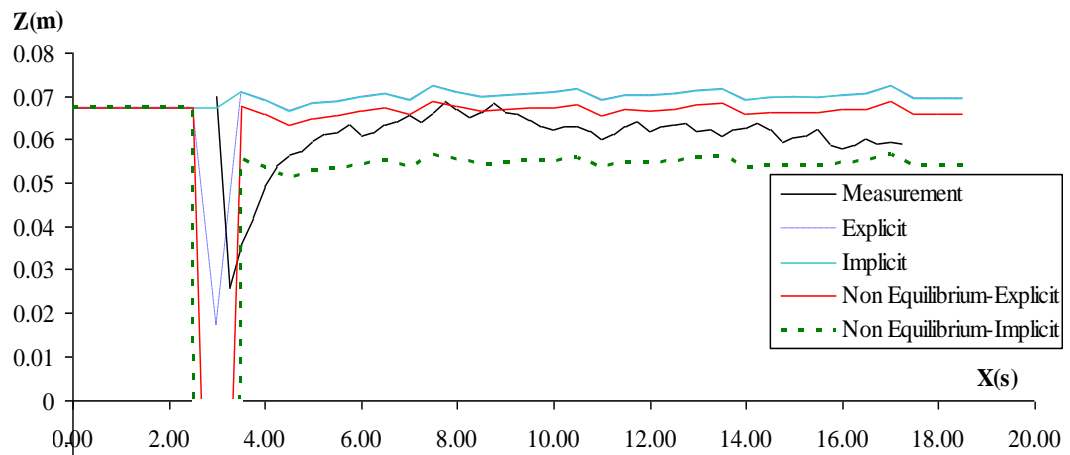Figure 7.36 View of comparison between measurement and predict flow depth in17.m –Hyd 1
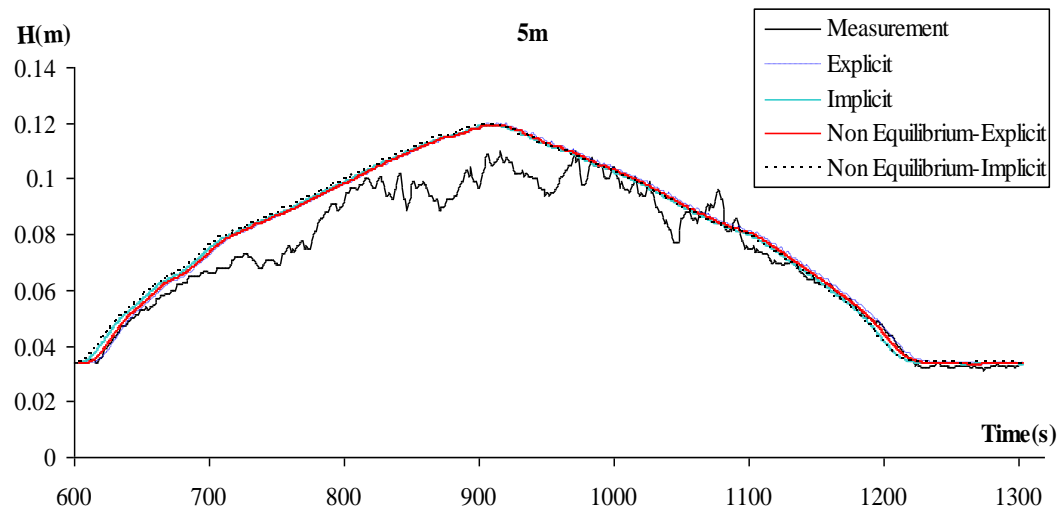
Figure 7.37 View of comparison between measurement and predict flow depth in 5.m –Hyd.2
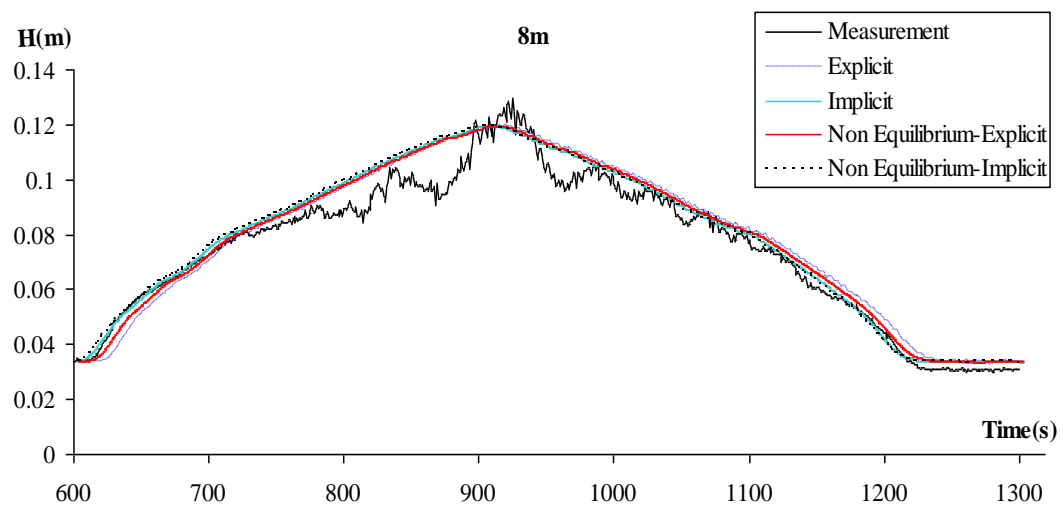
Figure 7.38 View of comparison between measurement and predict flow depth in 8.m –Hyd. 2
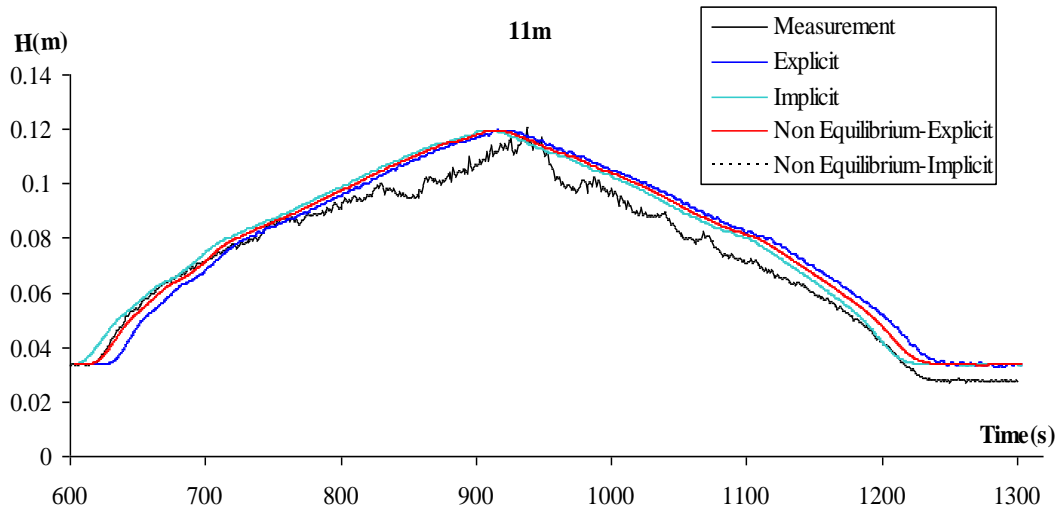
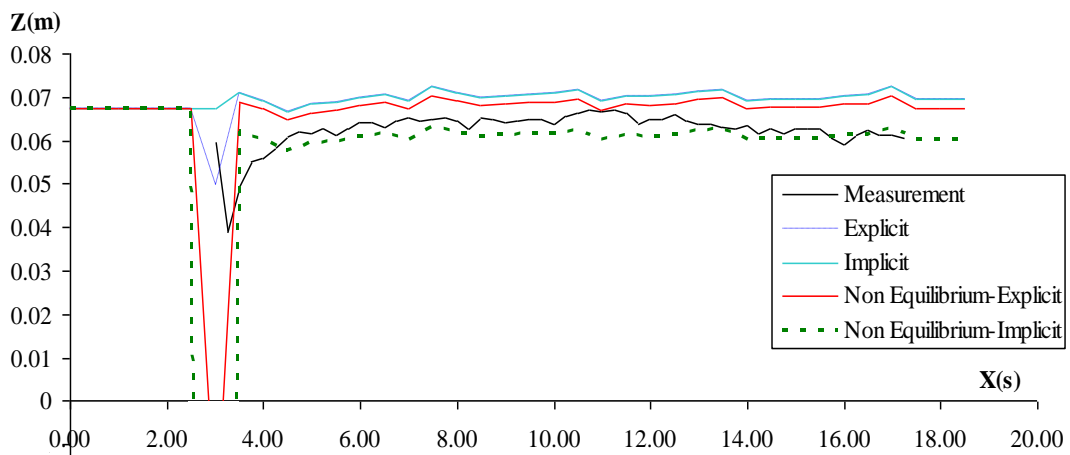Figure 7.39 View of comparison between measurement and predict flow depth in 11.m –Hyd. 2
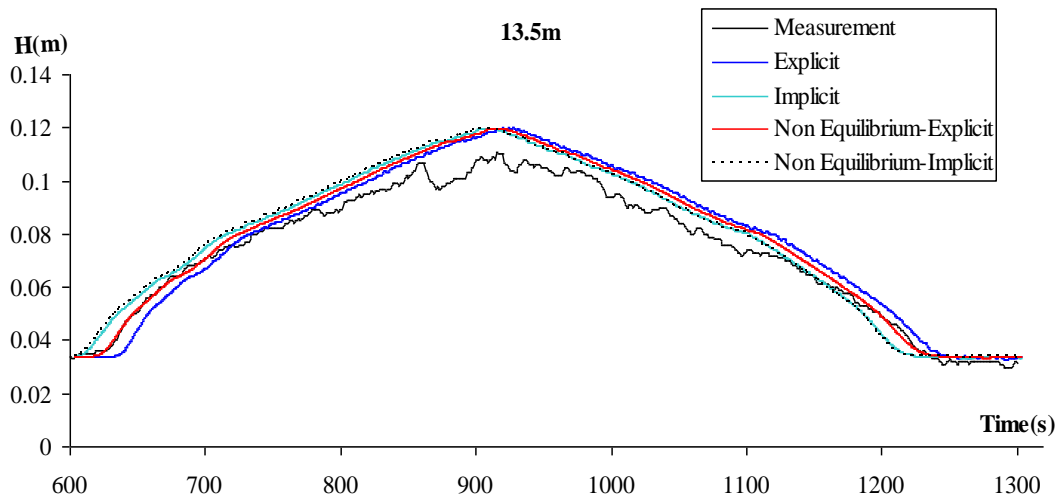
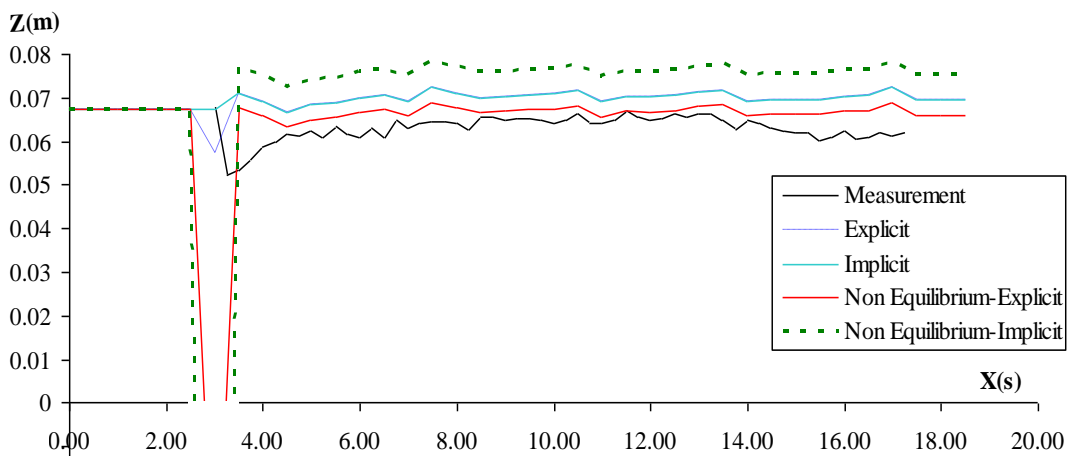Figure 7.40 View of comparison between measurement and predict flow depth in 13.5.m –Hyd. 2
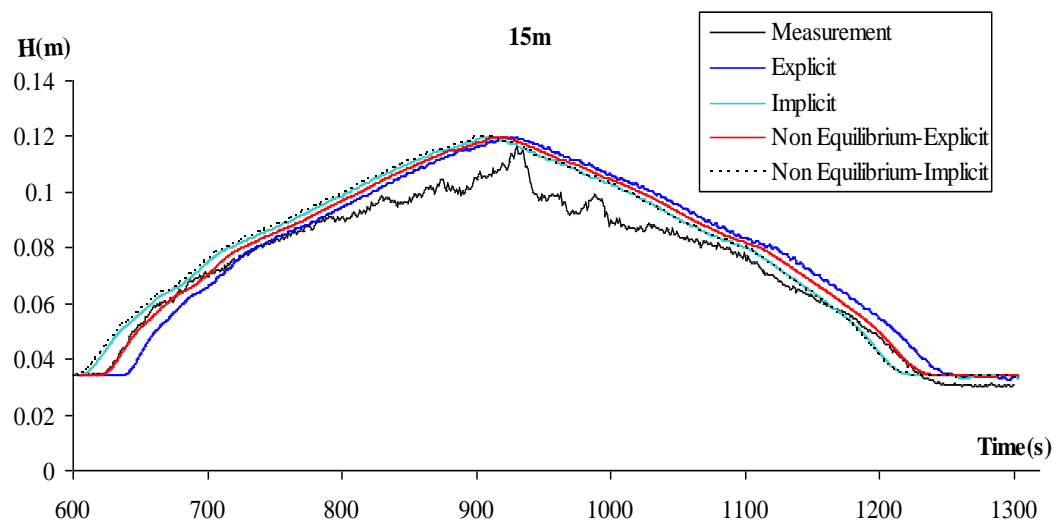
Figure 7.41 View of comparison between measurement and predict flow depth in 15.m –Hyd.2
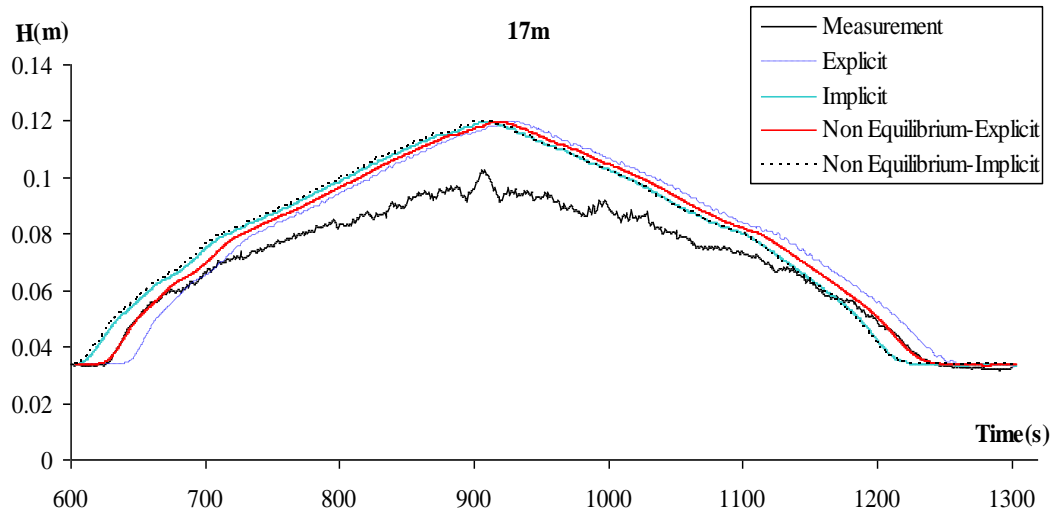
Figure 7.42 View of comparison between measurement and predict flow depth in 17.m –Hyd. 2
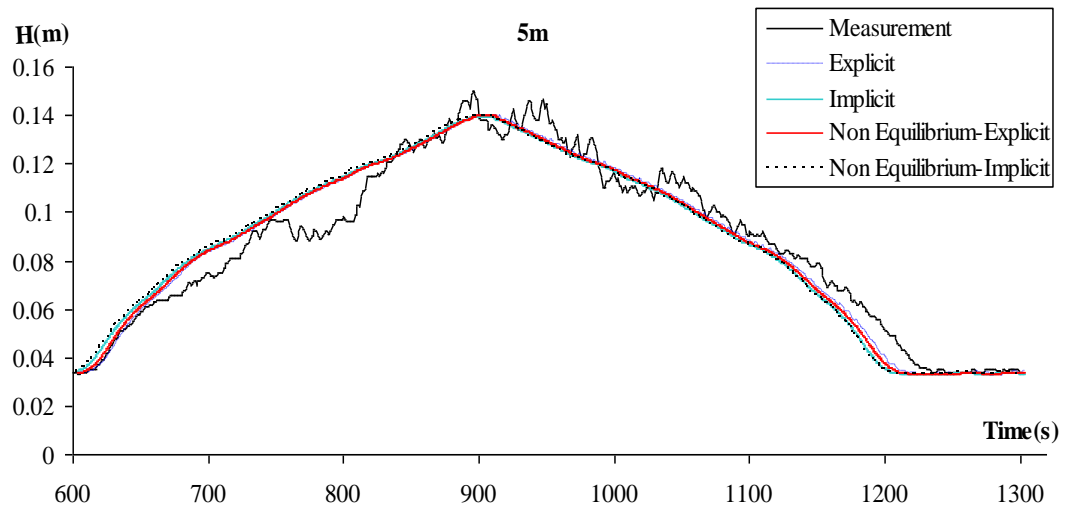
Figure 7.43 View of comparison between measurement and predict flow depth in 5.m –Hyd.3
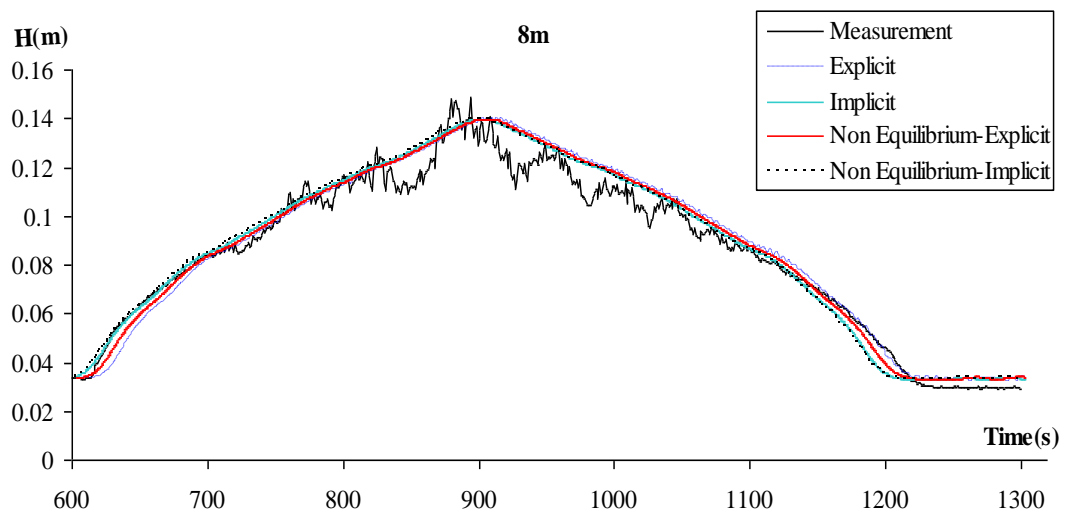
Figure 7.44 View of comparison between measurement and predict flow depth in 8.m –Hyd. 3
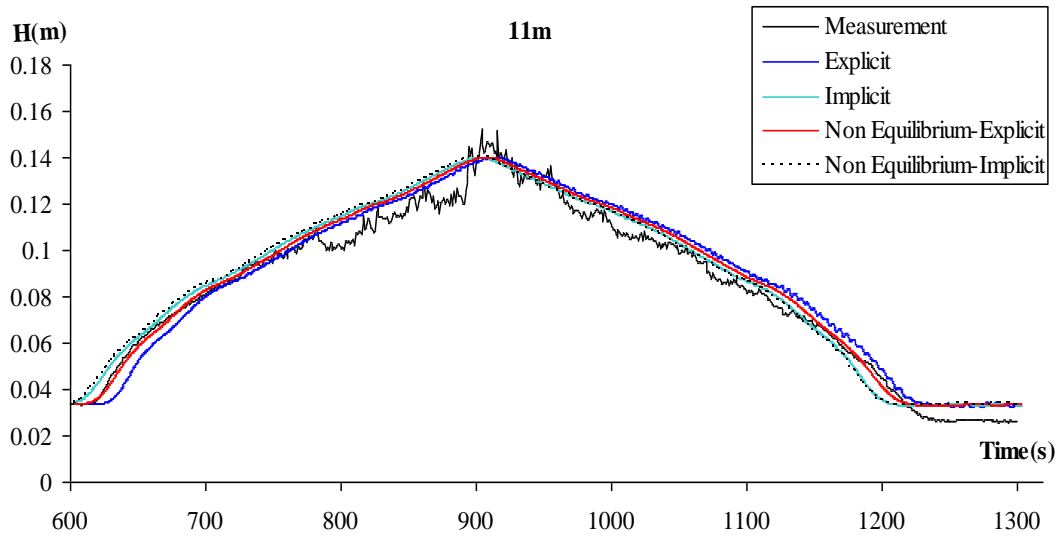
Figure 7.45 View of comparison between measurement and predict flow depth in 11.m –Hyd. 3
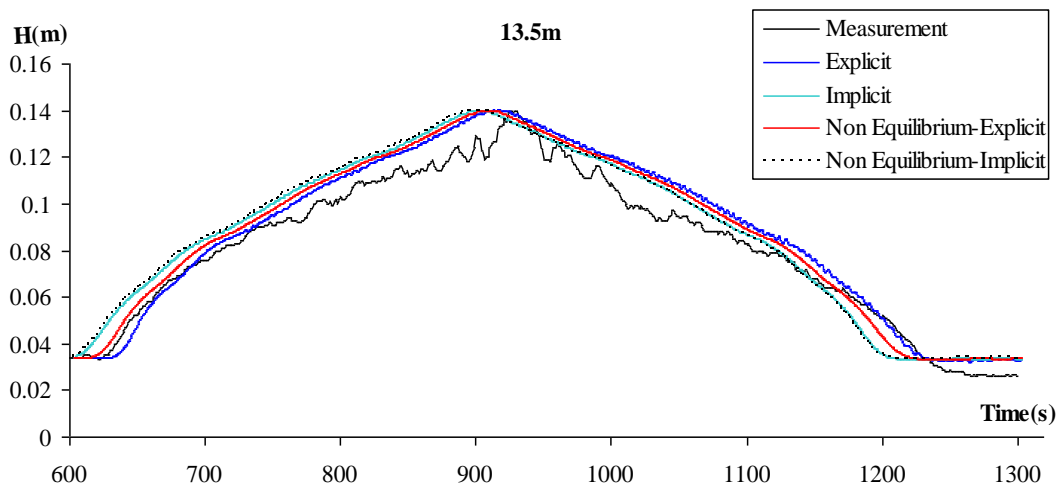
Figure 7.46 View of comparison between measurement and predict flow depth in 13.5.m –Hyd.3
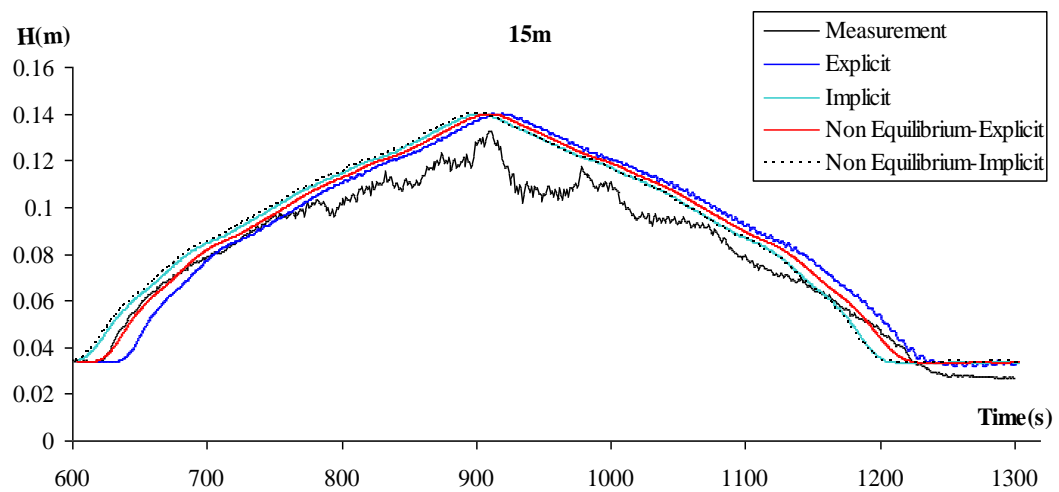
Figure 7.47 View of comparison between measurement and predict flow depth in 15.m –Hyd. 3
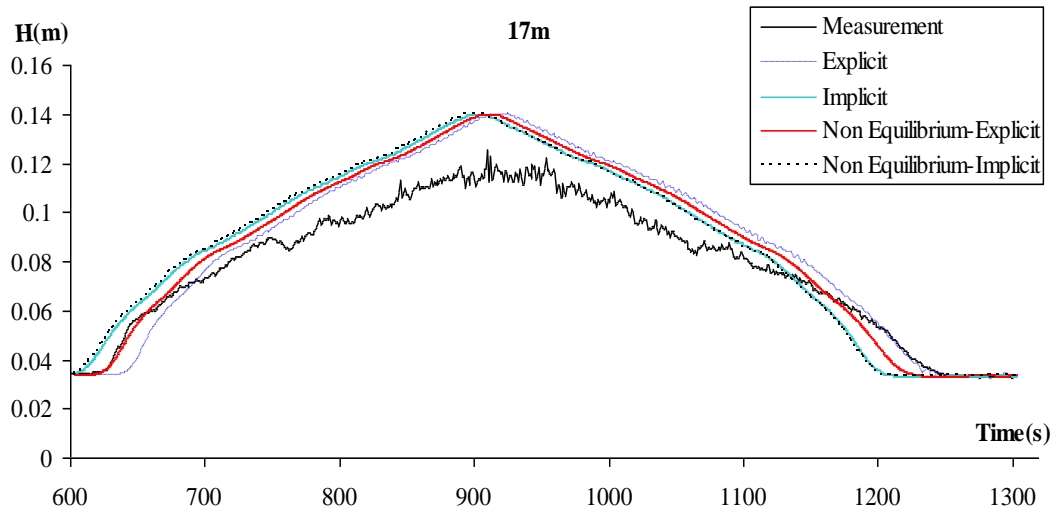
Figure 7.48 View of comparison between measurement and predict flow depth in 17.m –Hyd. 3
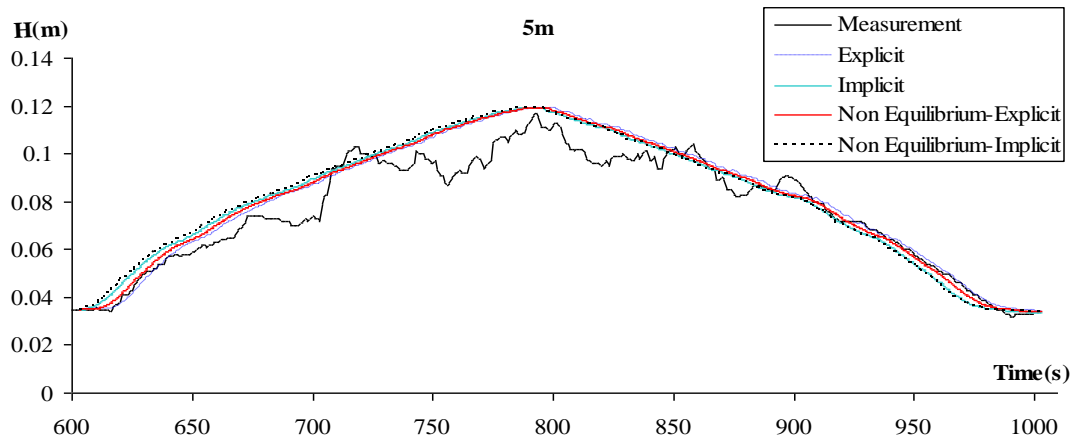
Figure 7.49 View of comparison between measurement and predict flow depth in 5.m –Hyd. 4
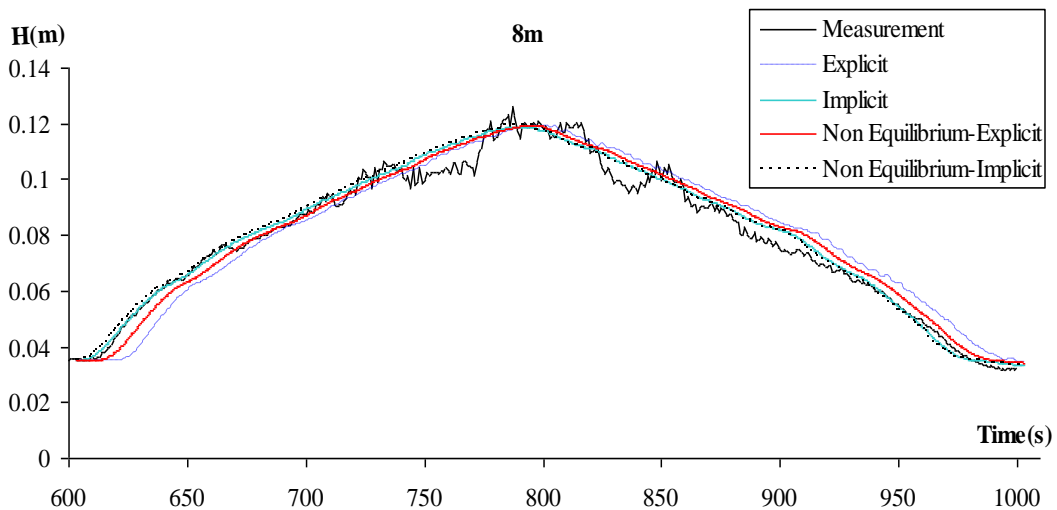
Figure 7.50 View of comparison between measurement and predict flow depth in 8.m –Hyd. 4
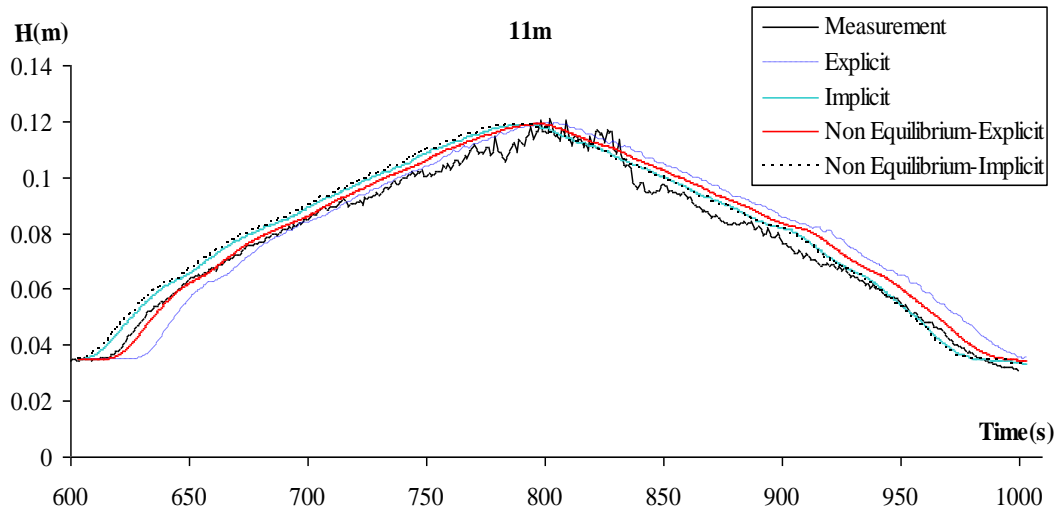
Figure 7.51 View of comparison between measurement and predict flow depth in 11.m –Hyd. 4
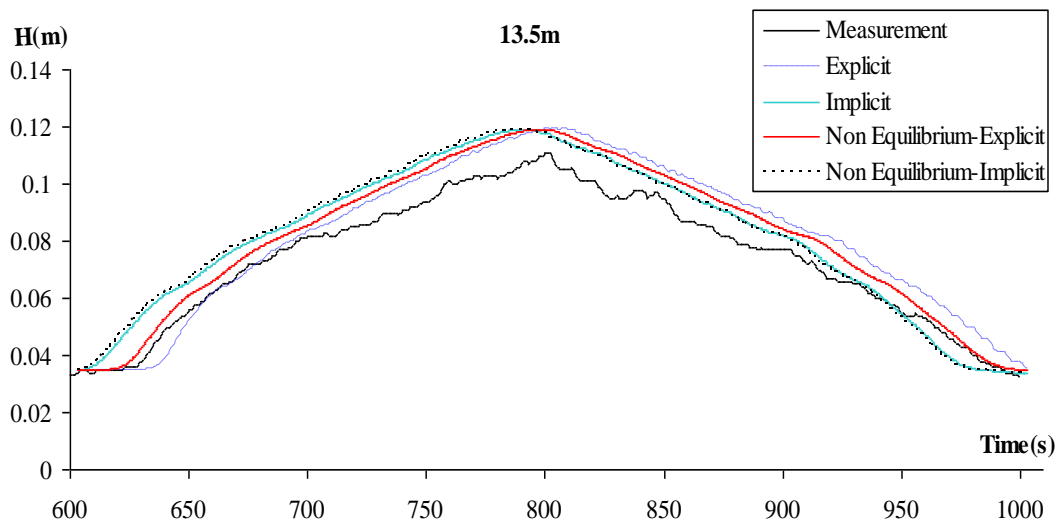
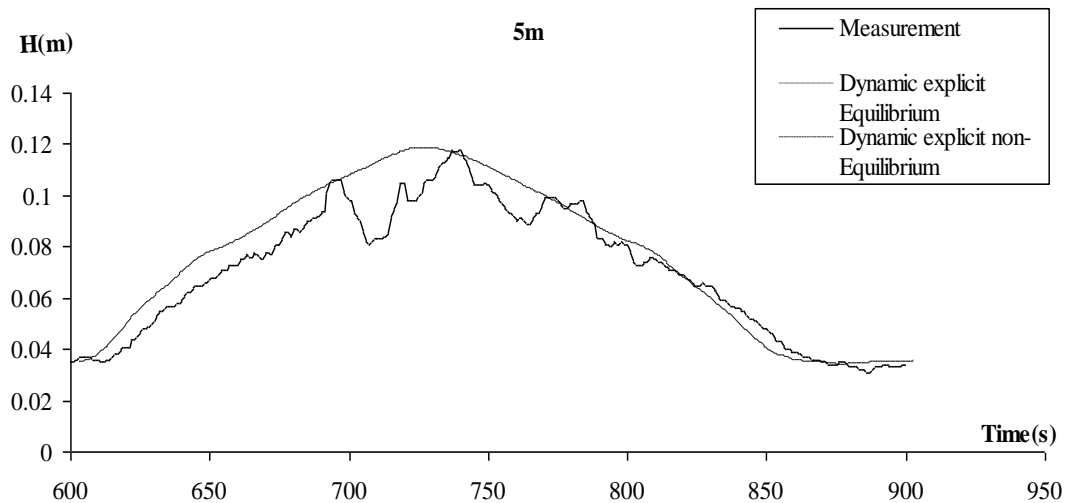Figure 7.52 View of comparison between measurement and predict flow depth in 13.5.m –Hyd. 4
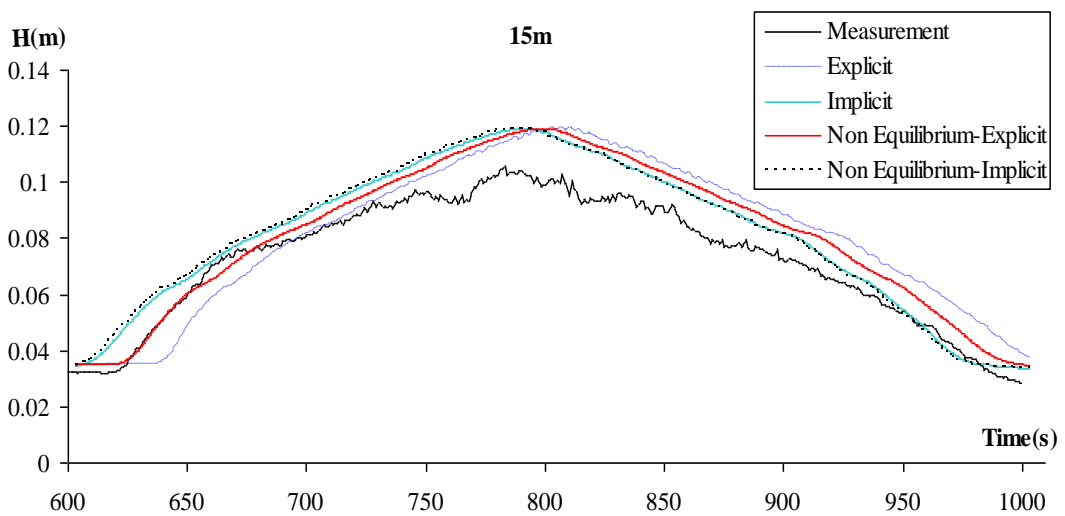
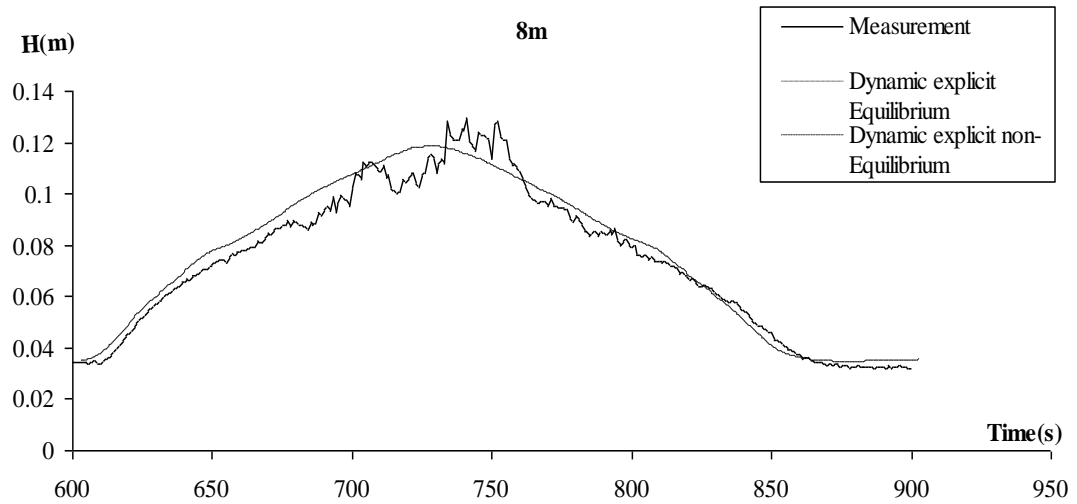Figure 7.53 View of comparison between measurement and predict flow depth in 15.m –Hyd. 4
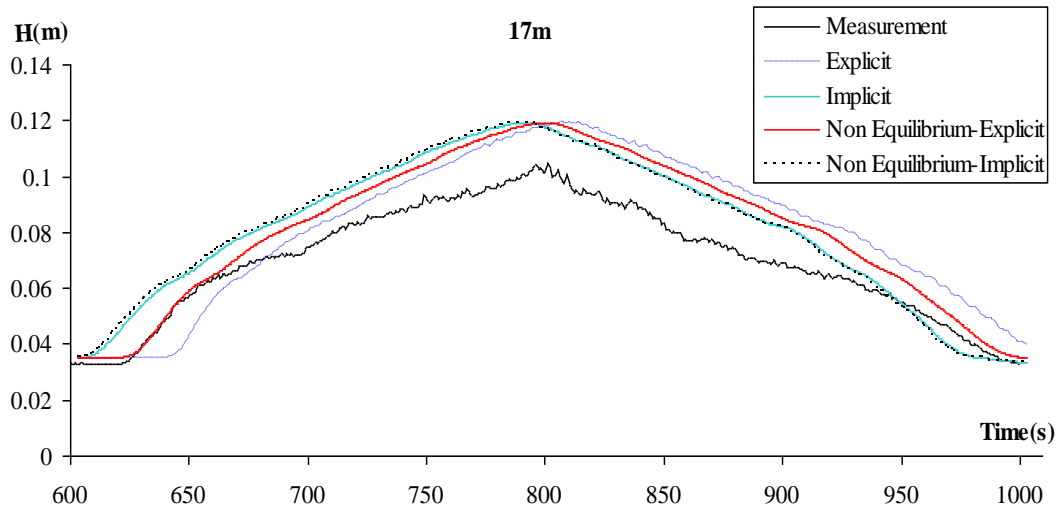
Figure 7.54 View of comparison between measurement and predict flow depth in 17.m –Hyd. 4
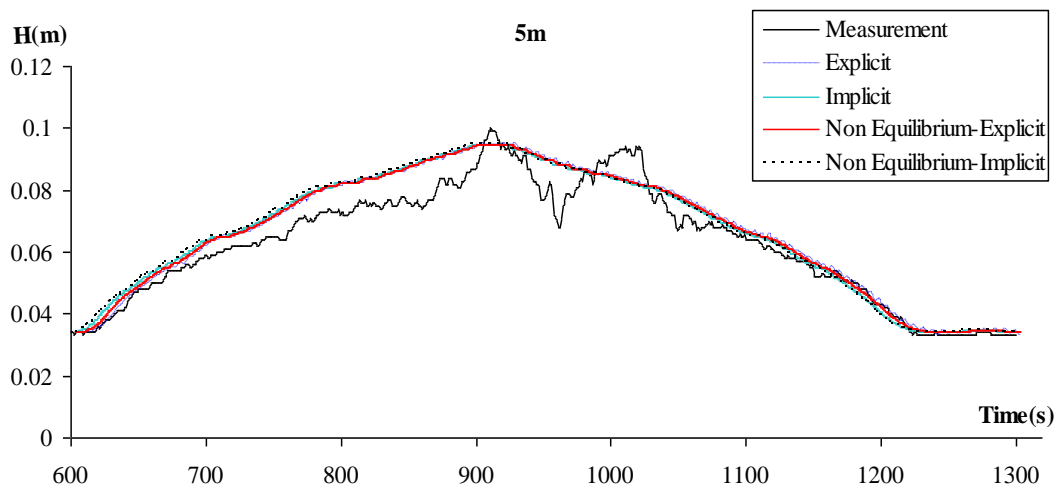
Figure 7.55 View of comparison between measurement and predict flow depth in 5.m –Hyd 5
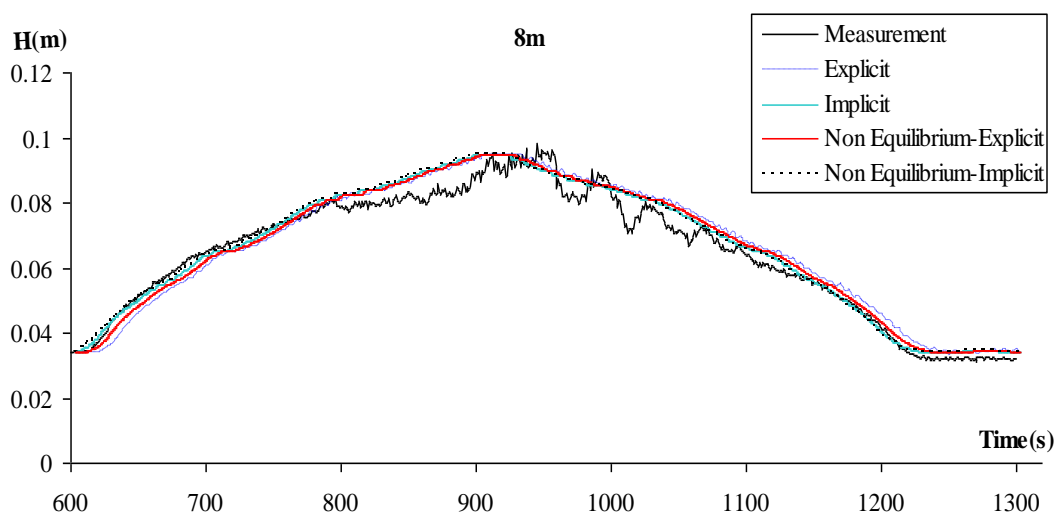
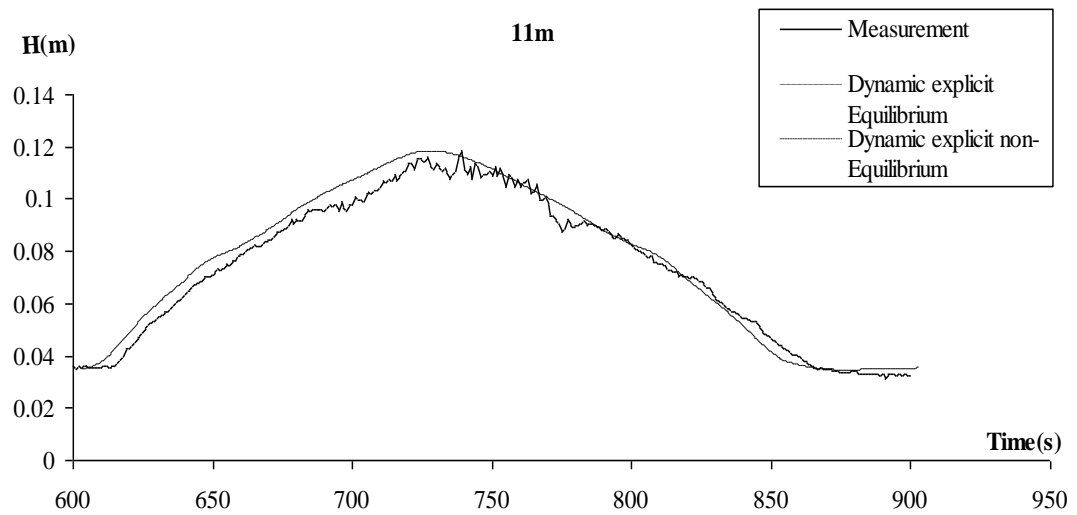Figure 7.56 View of comparison between measurement and predict flow depth in 8.m –Hyd 5
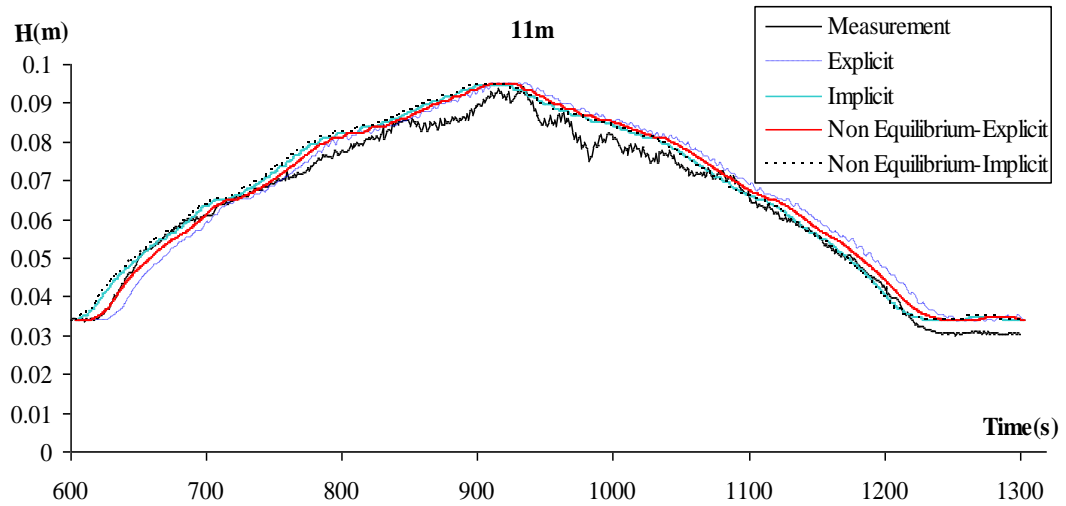
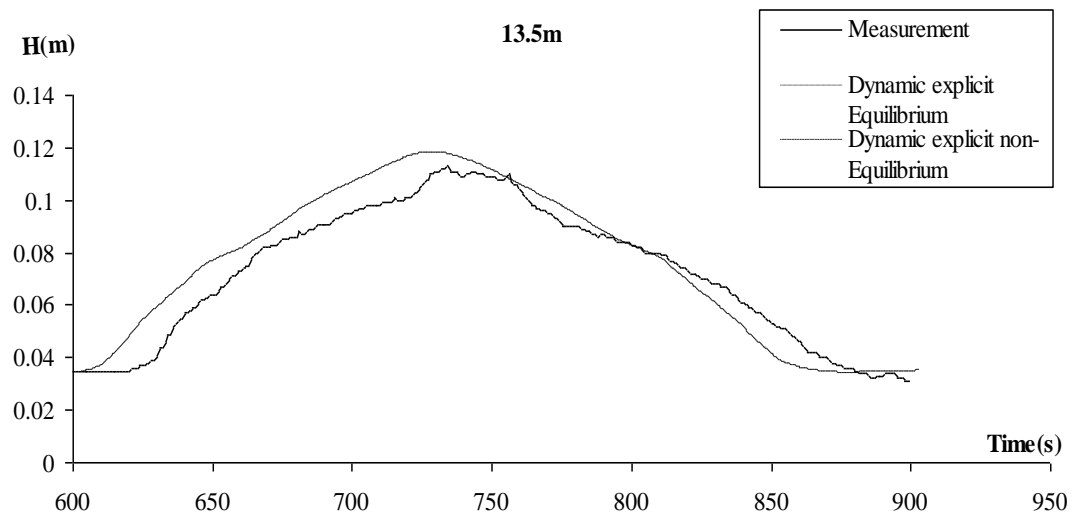Figure 7.57 View of comparison between measurement and predict flow depth in 11.m –Hyd 5
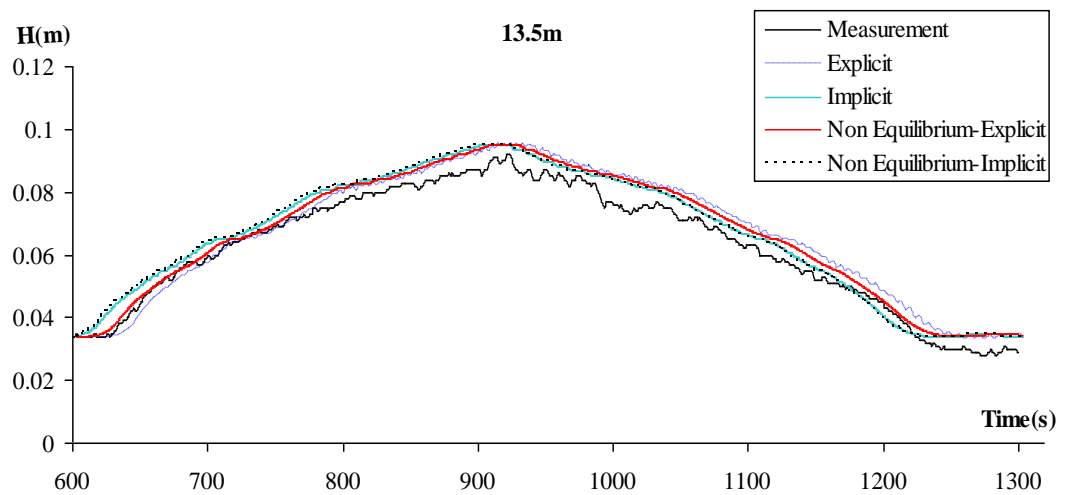
Figure 7.58 View of comparison between measurement and predict flow depth in 13.5.m –Hyd 5
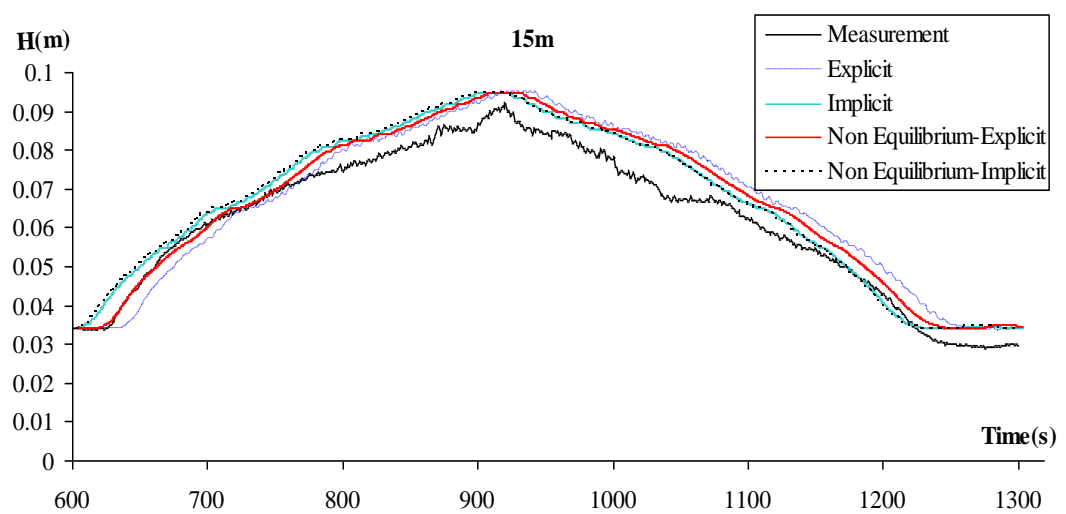
Figure 7.59 View of comparison between measurement and predict flow depth in 15.m –Hyd 5
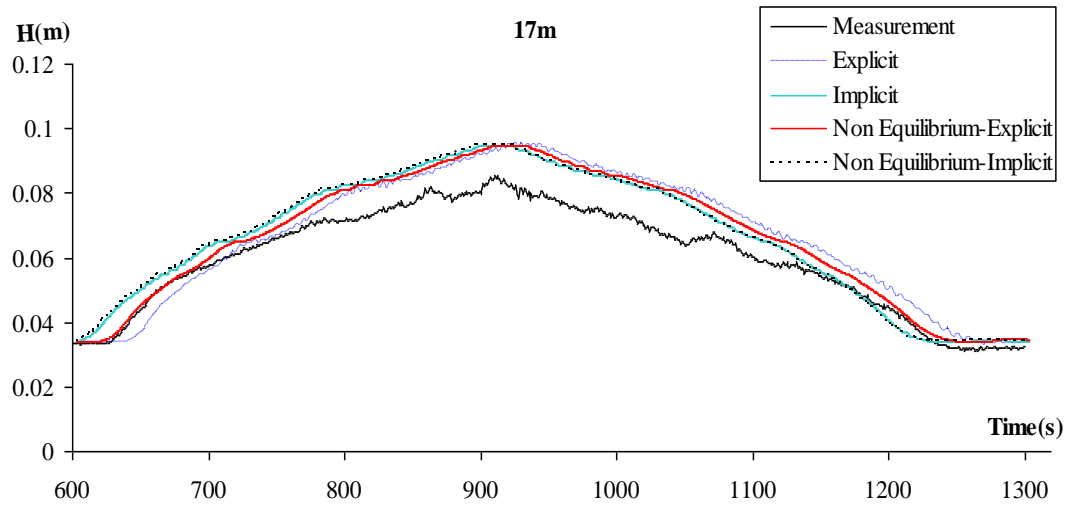
Figure 7.60 View of comparison between measurement and predict flow depth in 17.m –Hyd. 5
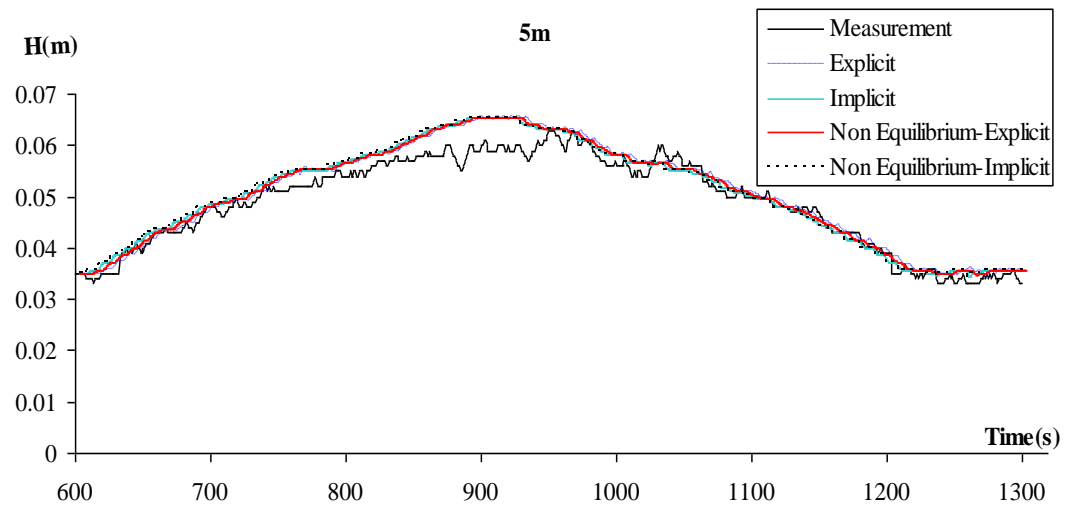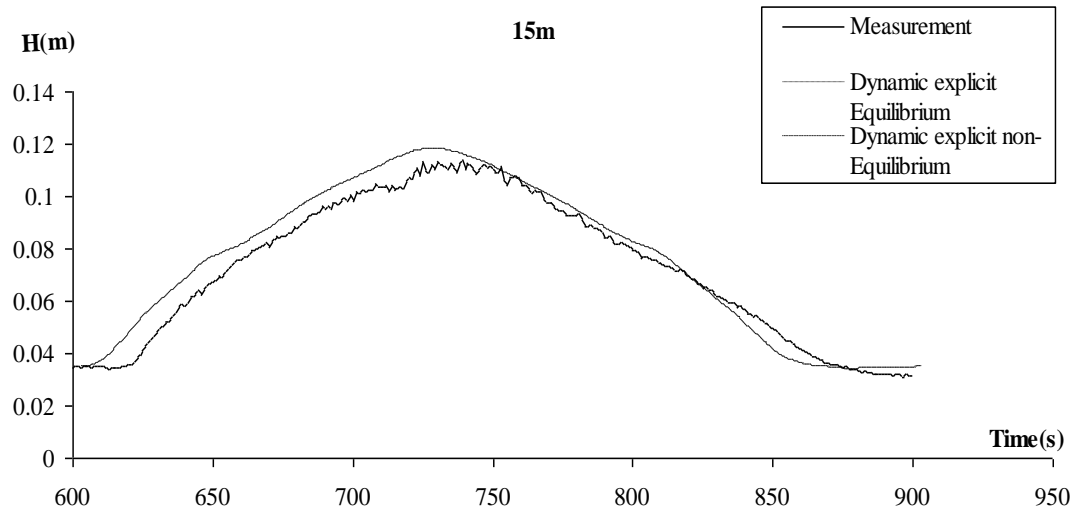

Figure 7.61 View of comparison between measurement and predict flow depth in 5.m –Hyd. 6
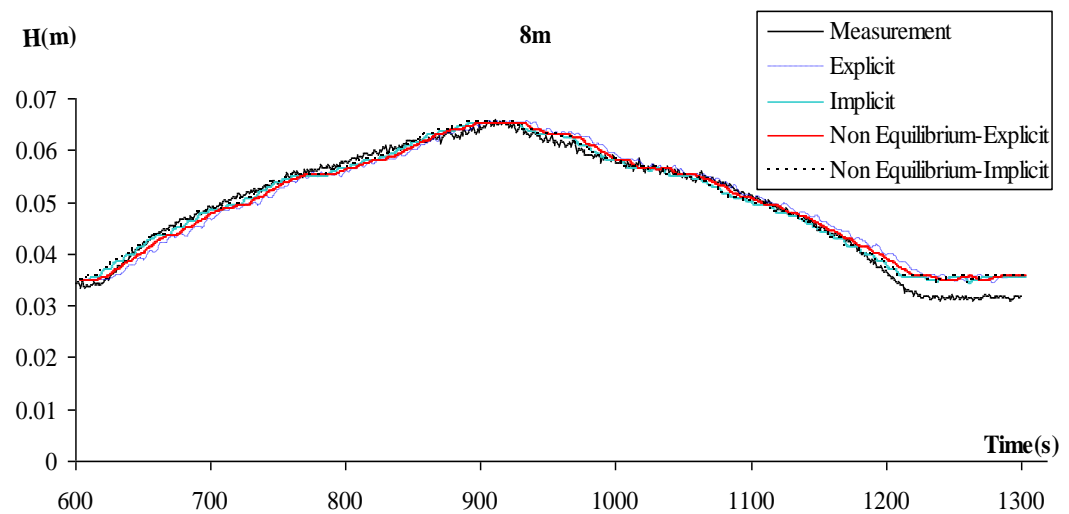
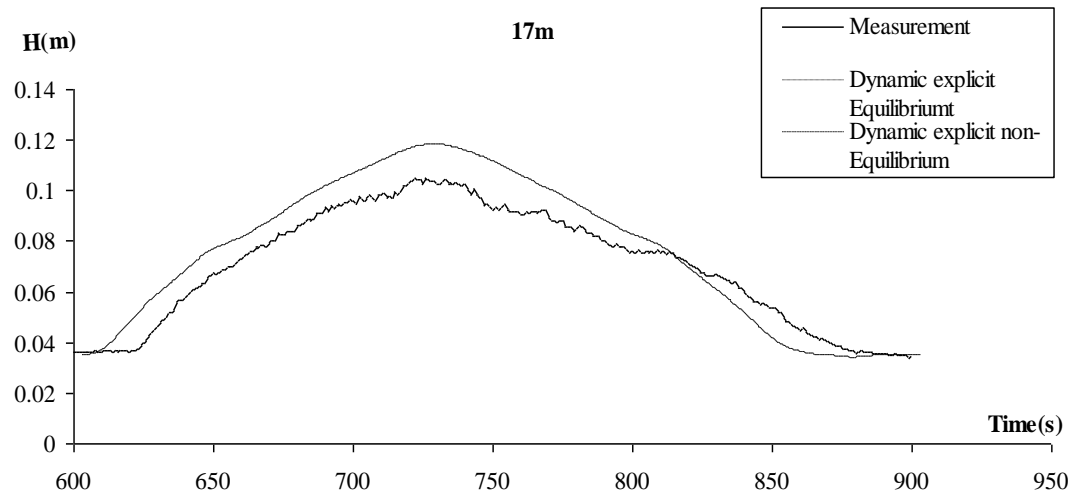Figure 7.62 View of comparison between measurement and predict flow depth in 8.m –Hyd. 6
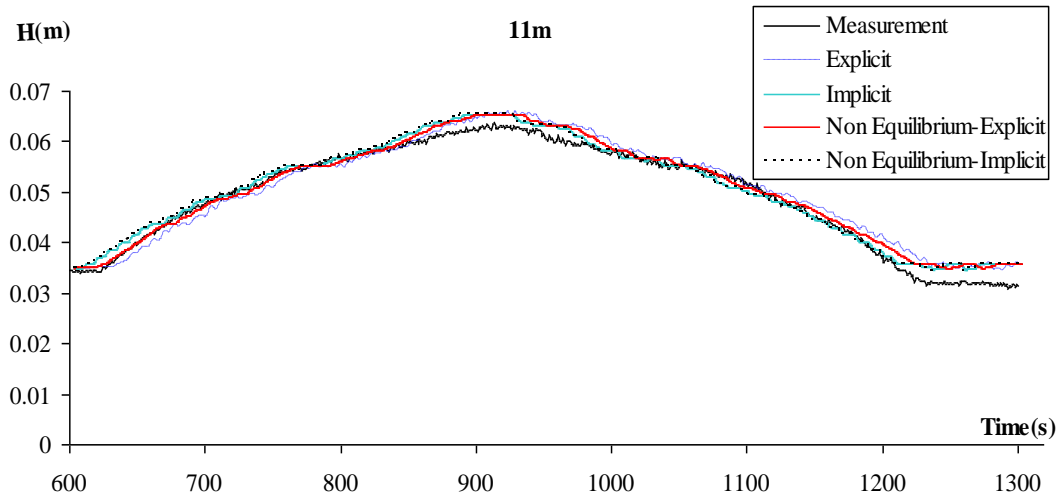
Figure 7.63 View of comparison between measurement and predict flow depth in 11.m –Hyd. 6

Figure 7.64 View of comparison between measurement and predict flow depth in 13.5.m –Hyd. 6

Figure 7.65 View of comparison between measurement and predict flow depth in 15.m –Hyd. 6
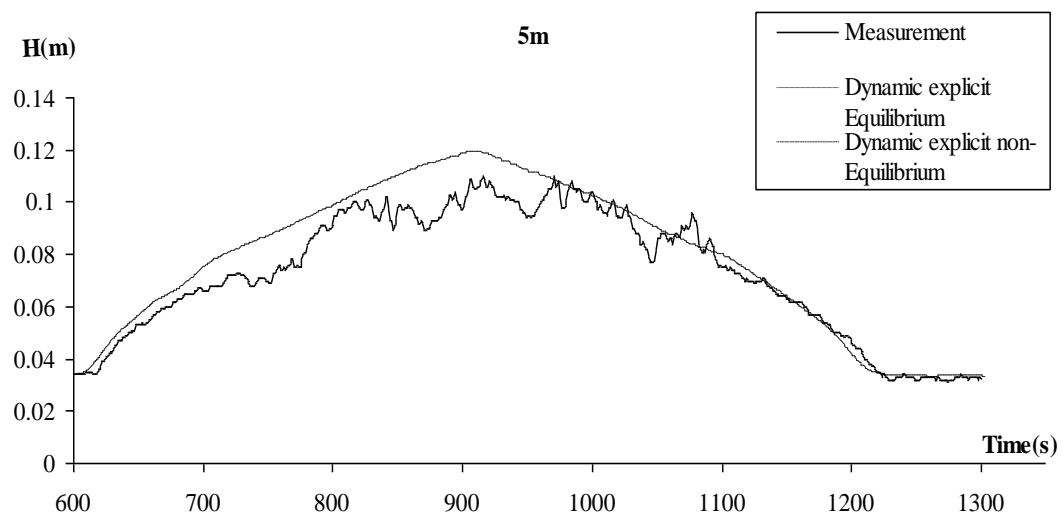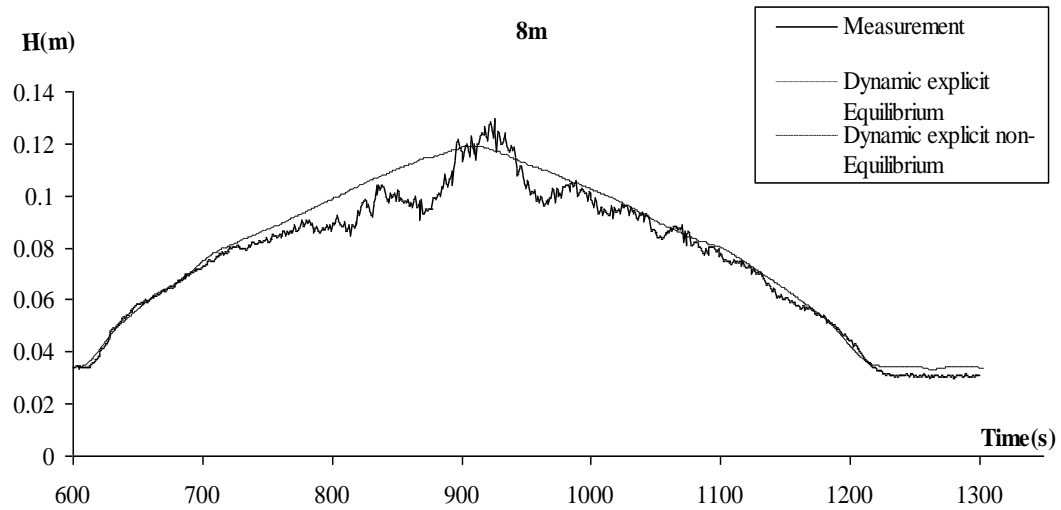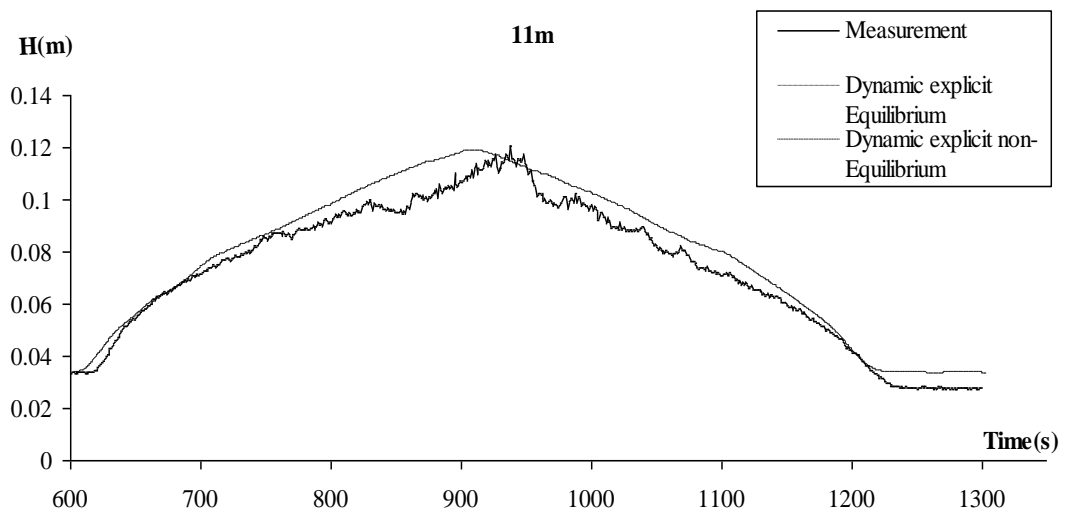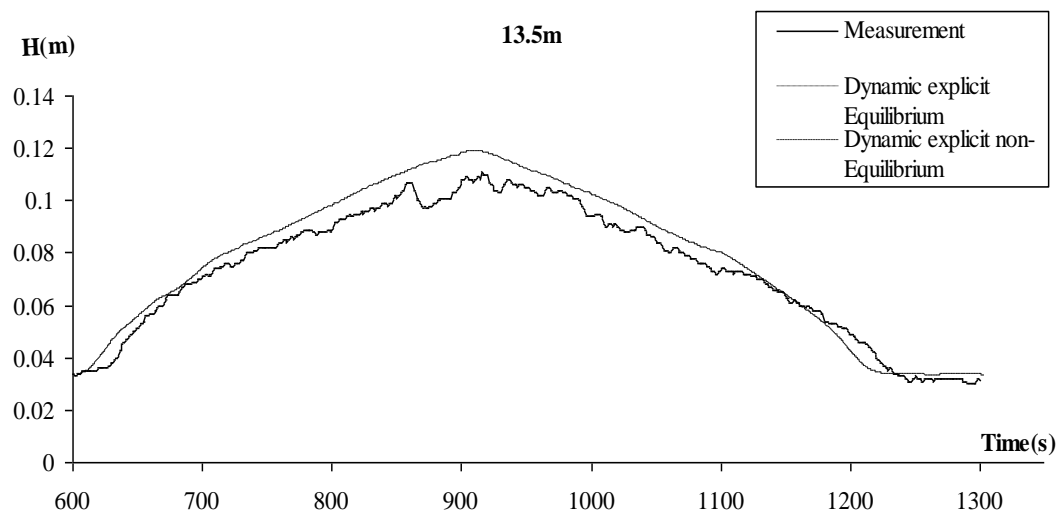
Figure 7.66 View of comparison between measurements and predict flow depth in 17.m –Hyd. 6

Figure 7.67 View of comparison between measurements and model predicts for bed profiles in hyd1.

Figure 7.68 View of comparison between measurements and model predicts for bed profiles in hyd. 2.

Figure 7.69 View of comparison between measurements and model predicts for bed profiles in hyd. 3.

Figure 7.70 View of comparison between measurements and model predicts for bed profiles in hyd. 4.

Figure7.71 View of comparison between measurements and model predicts for bed profiles in hyd. 5.
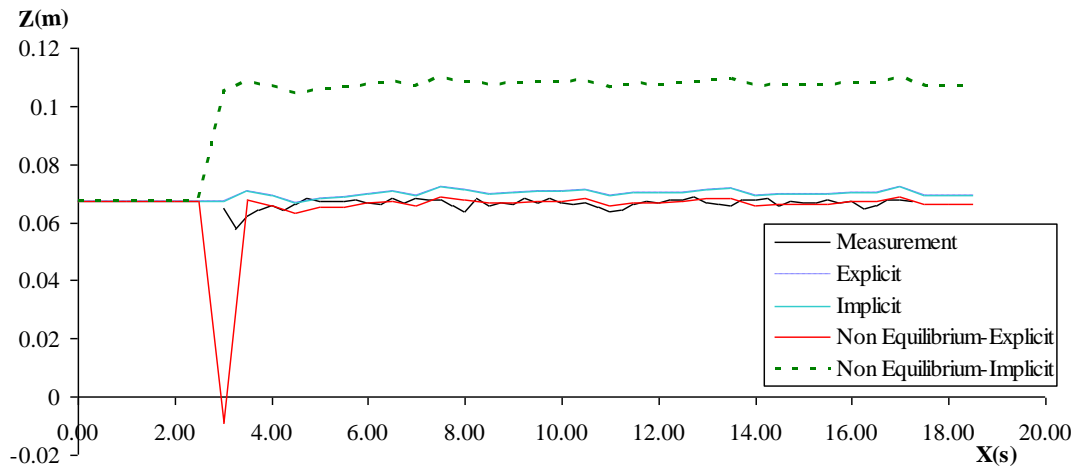
Figure7.72 View of comparison between measurements and model predicts for bed profiles in hyd. 6.

In the kinematic wave model, the experimental water depth results are in accord with those obtained from the numerical solution. The difference between experimental and theoretical bed elevation values are in order of a grain size. Therefore the compatibility is acceptable.

7.3 Comparison of Dynamic Wave Models

For the dynamic wave models, in different sections (5m, 8m, 11m, 13.5m, 15m and 17m.) for the six hygrographs h values depending on time are given in Figures 7.73 − 7.108. z values after carried out hydrographs at the last time are given in Figure 7.109 - 7.114.

Figure 7.73 View of comparison between measurement and flow depth prediction in 5.m –Hydr.1

Figure 7.74 View of comparison between measurement and flow depth prediction in 8.m –Hyd. 1

Figure 7.75 View of comparison between measurement and flow depth prediction in 11.m –Hyd. 1

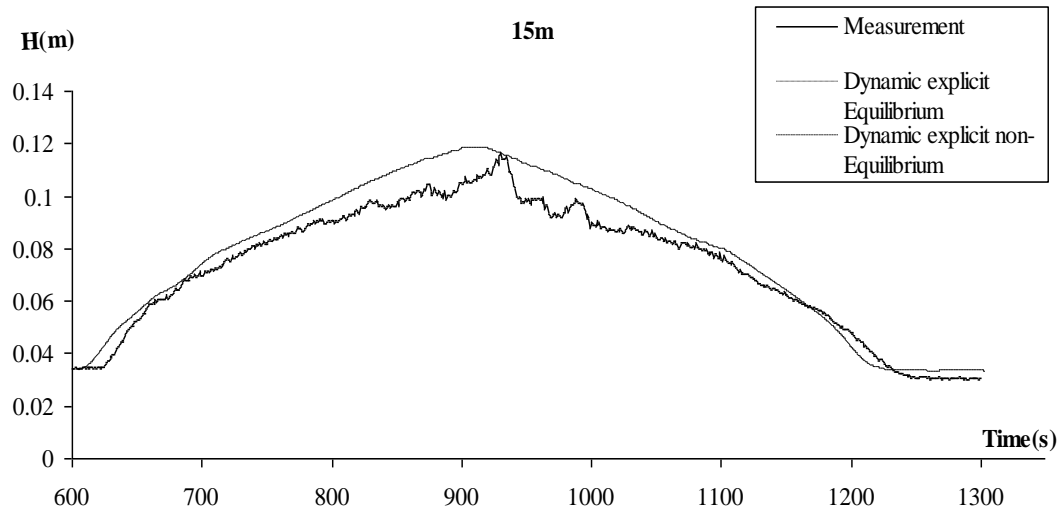Figure 7.76 View of comparison between measurement and flow depth prediction in 13.5.m –Hyd. 1

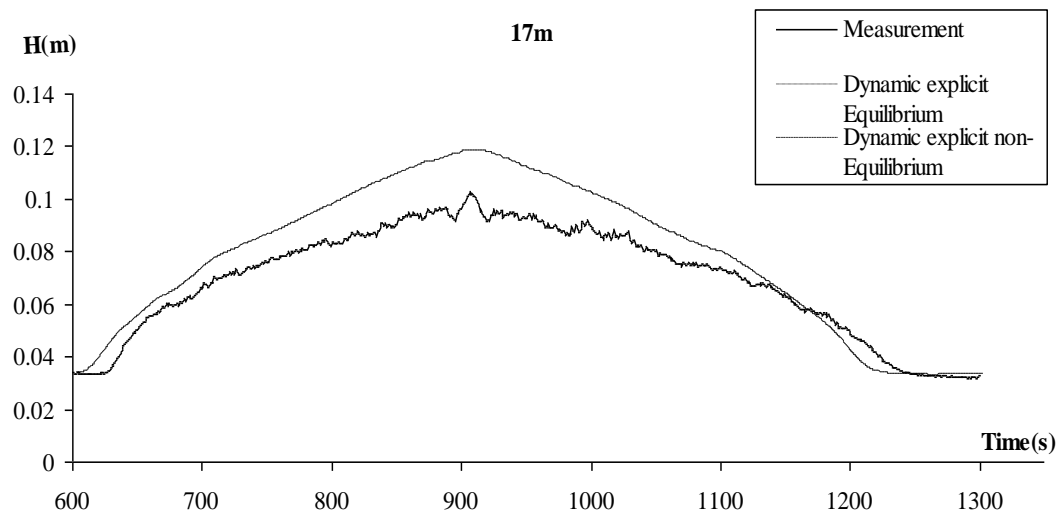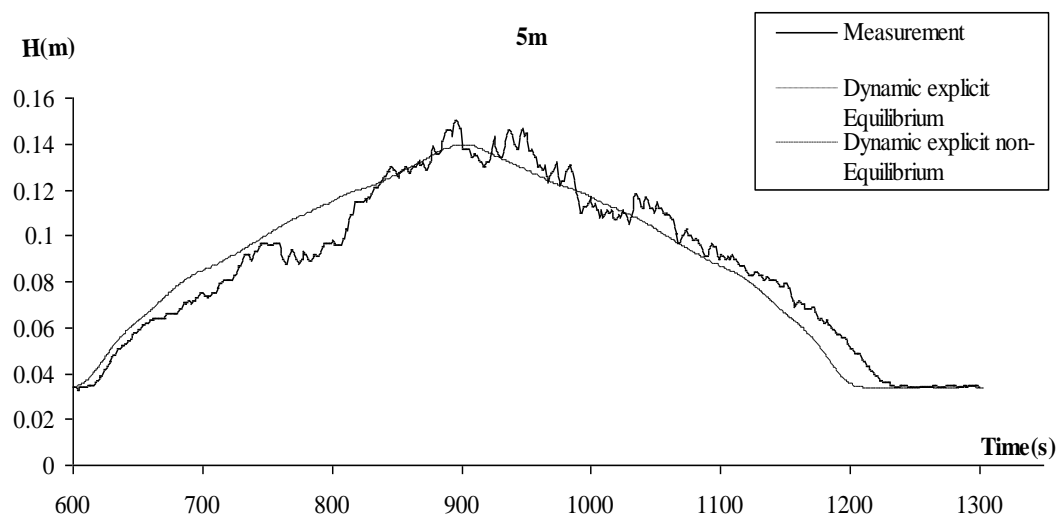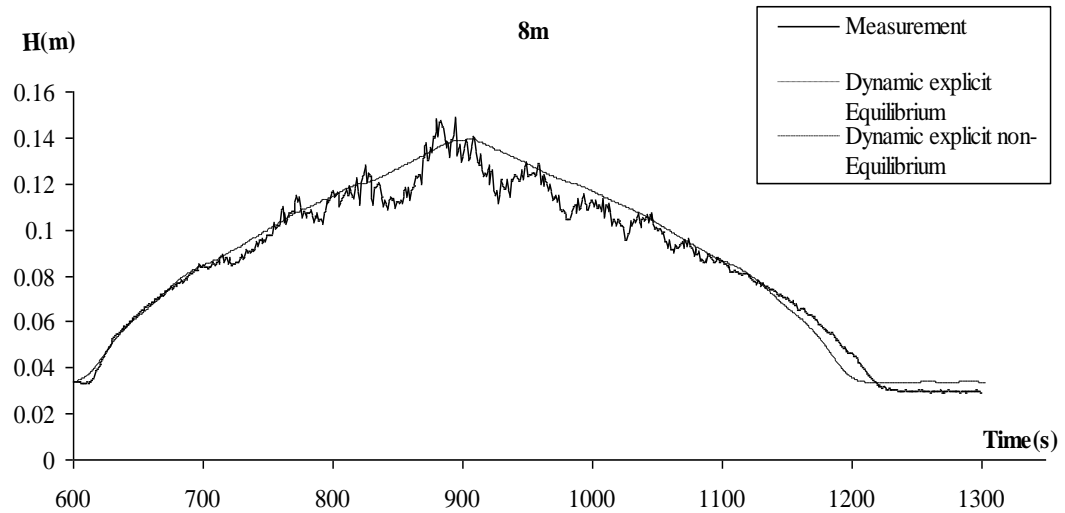Figure 7.77 View of comparison between measurement and flow depth prediction in 15.m –Hyd. 1

Figure 7.78 View of comparison between measurement and flow depth prediction in 17.m –Hyd.1

Figure 7.79 View of comparison between measurement and flow depth prediction in 5.m –Hyd.2

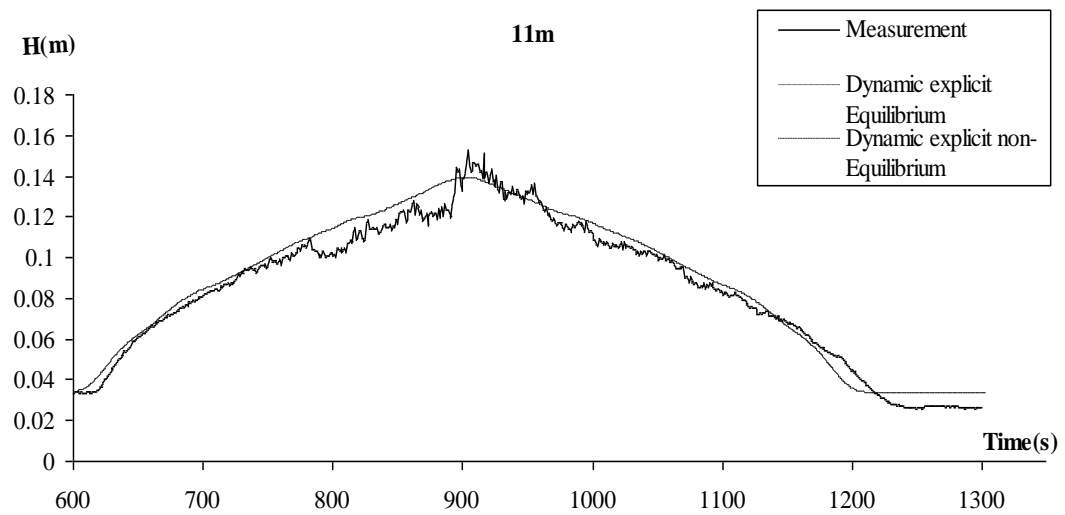Figure 7.80 View of comparison between measurement and flow depth prediction in 8.m –Hyd. 2

Figure 7.81 View of comparison between measurement and flow depth prediction in 11.m –Hyd.2
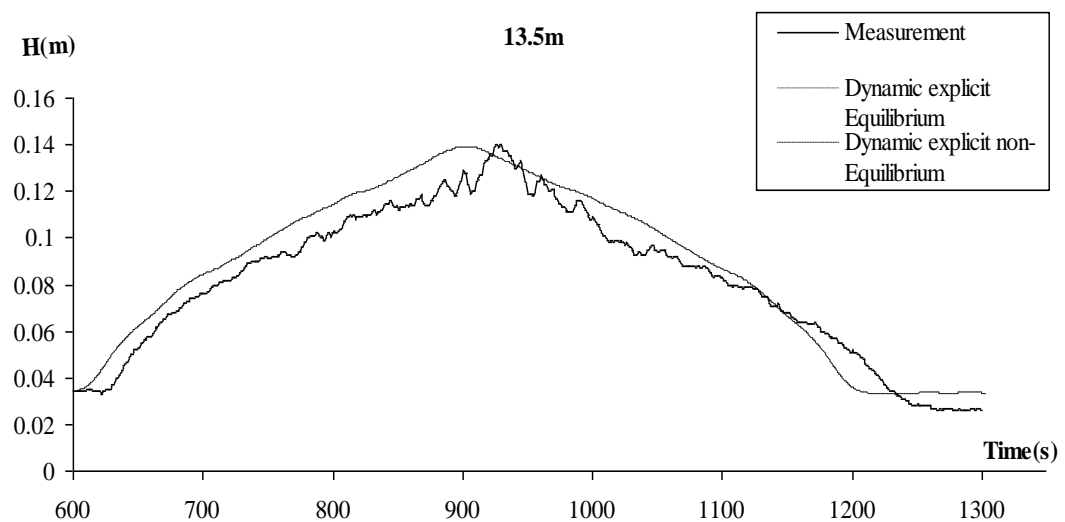

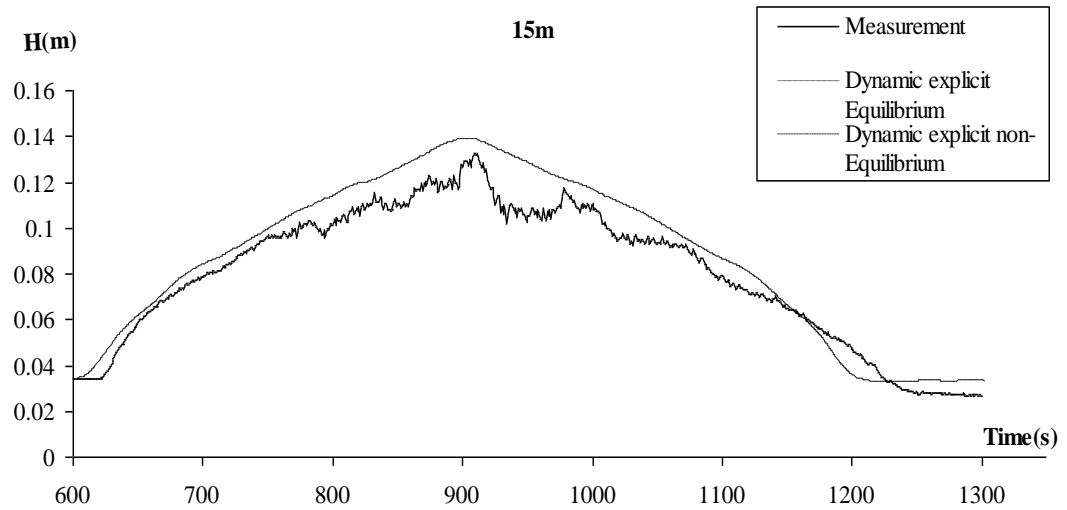Figure 7.82 View of comparison between measurement and flow depth prediction in 13.5.m –Hyd.2

Figure 7.83 View of comparison between measurement and flow depth prediction in 15.m –Hyd. 2

Figure 7.84 View of comparison between measurement and flow depth prediction in 17.m –Hyd. 2

Figure 7.85 View of comparison between measurement and flow depth prediction in 5.m –Hyd. 3

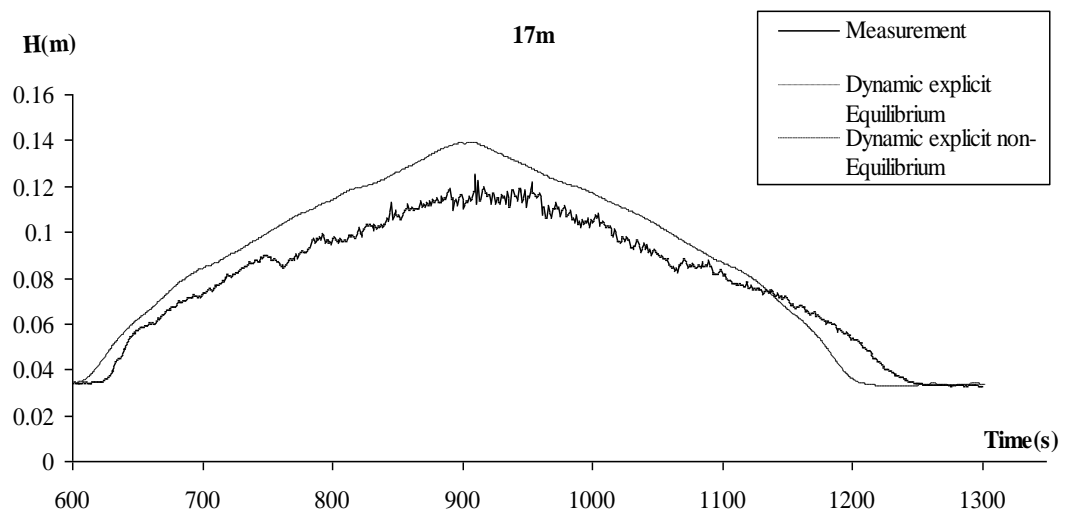Figure 7.86 View of comparison between measurement and flow depth prediction in 8.m –Hyd. 3
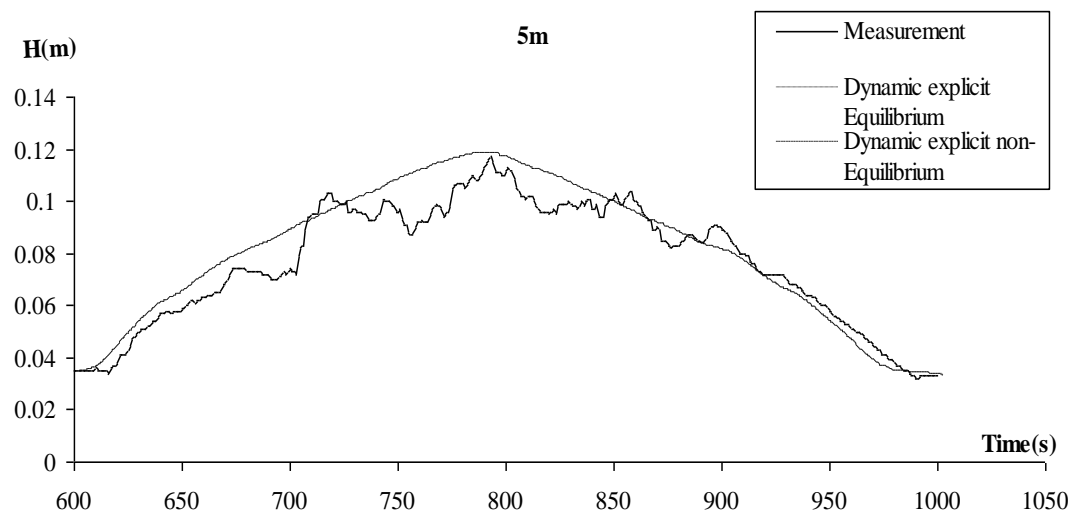

Figure 7.87 View of comparison between measurement and flow depth prediction in 11.m –Hyd. 3

Figure 7.88 View of comparison between measurement and flow depth prediction in 13.5.m –Hyd. 3

Figure 7.89 View of comparison between measurement and flow depth prediction in 15.m –Hyd.3

Figure 7.90 View of comparison between measurement and flow depth prediction in 17.m –Hyd. 3

Figure 7.91 View of comparison between measurement and flow depth prediction in 5.m –Hyd. 4
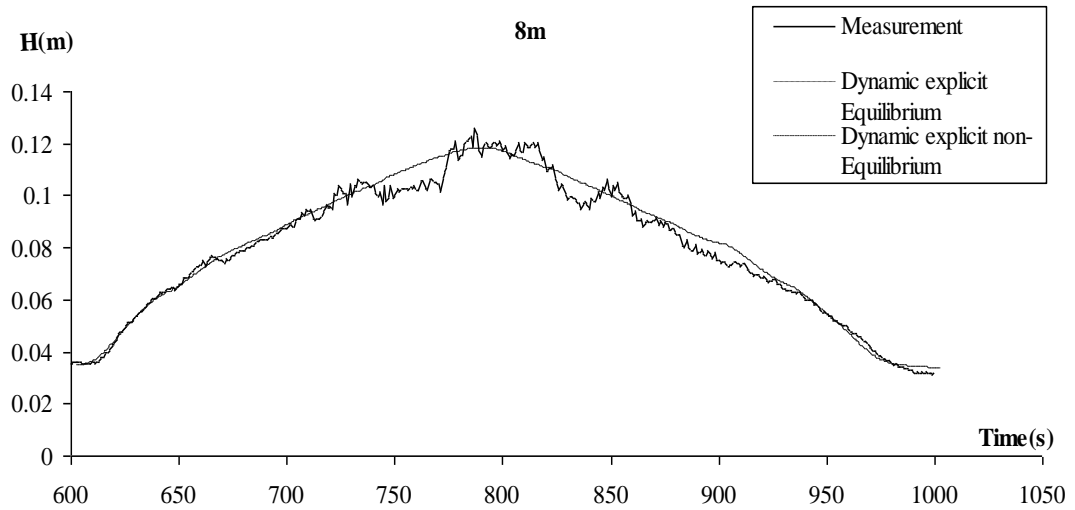
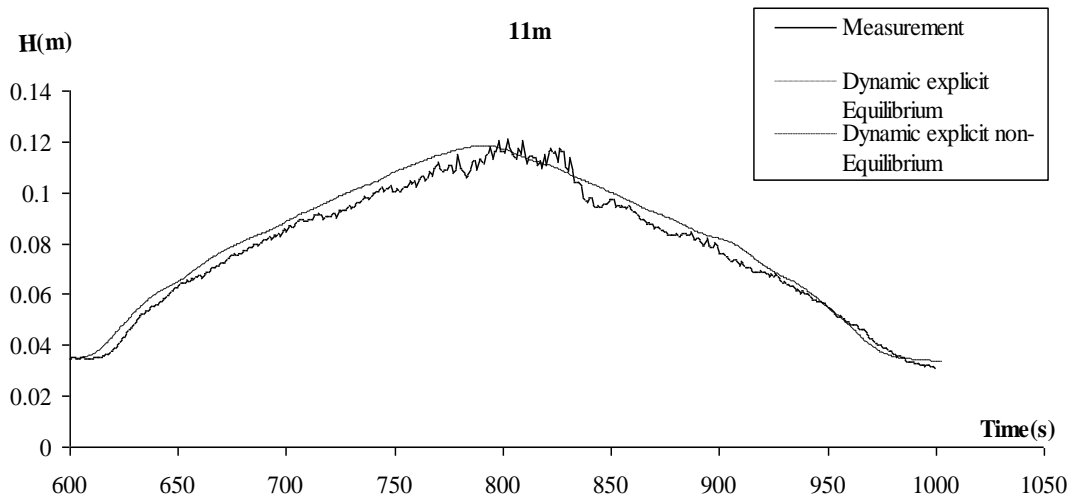Figure 7.92 View of comparison between measurement and flow depth prediction in 8.m –Hyd. 4

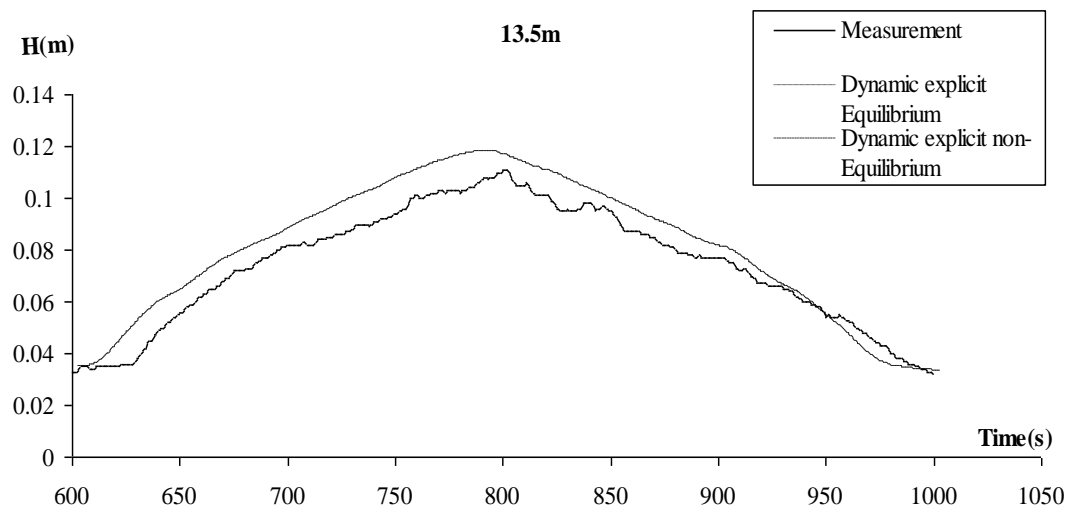Figure 7.93 View of comparison between measurement and flow depth prediction in 11.m –Hyd. 4

Figure 7.94 View of comparison between measurement and flow depth prediction in 13.5.m –Hyd. 4
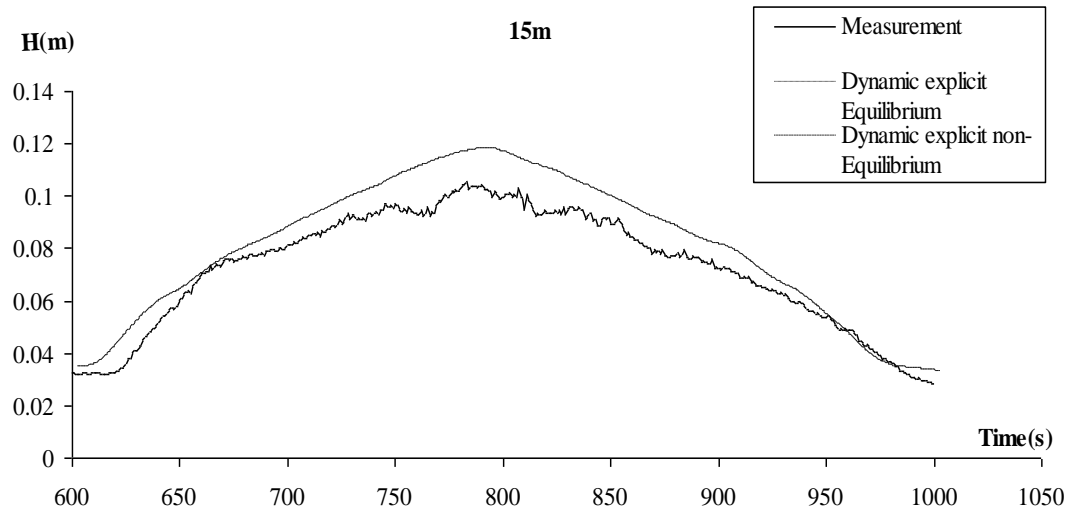
Figure 7.95 View of comparison between measurement and flow depth prediction in 15.m –Hyd. 4

Figure 7.96 View of comparison between measurement and flow depth prediction in 17.m –Hyd.4

Figure 7.97 View of comparison between measurement and flow depth prediction in 5.m –Hyd. 5

Figure 7.98 View of comparison between measurement and flow depth prediction in 8.m –Hyd. 5

Figure 7.99 View of comparison between measurement and flow depth prediction in 11.m –Hyd. 5

Figure 7.100 View of comparison between measurement and flow depth prediction in 13.5.m –Hyd. 5

Figure 7.101 View of comparison between measurement and flow depth prediction in 15.m –Hyd. 5
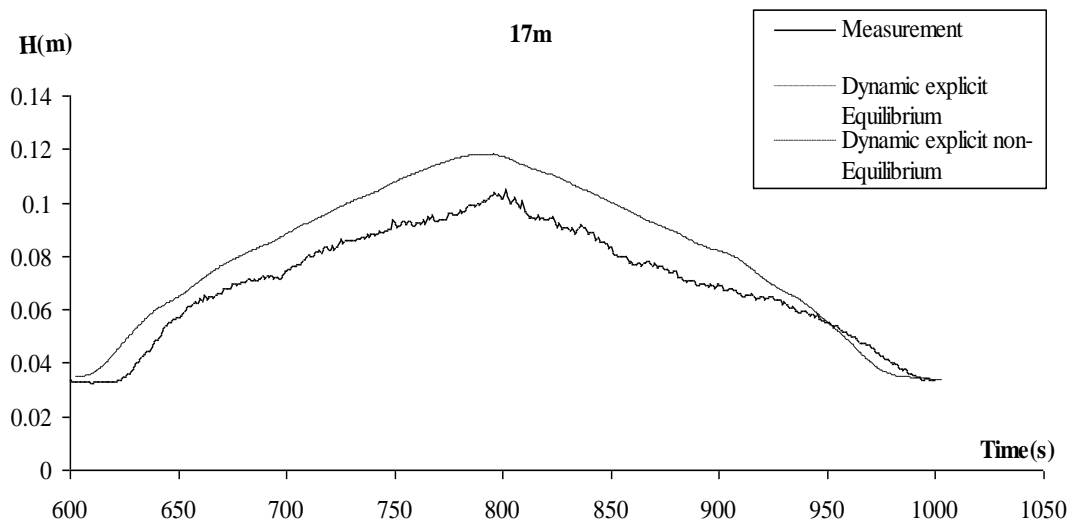

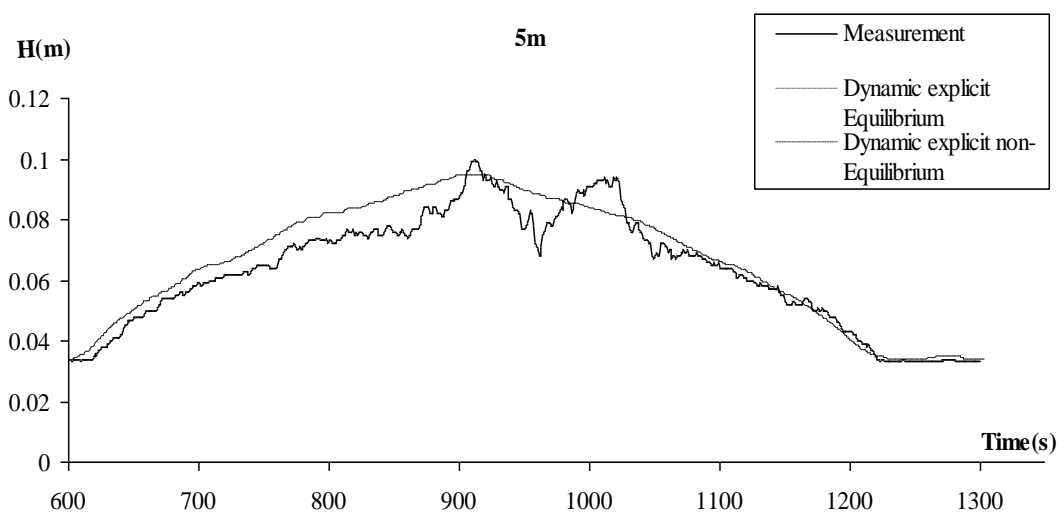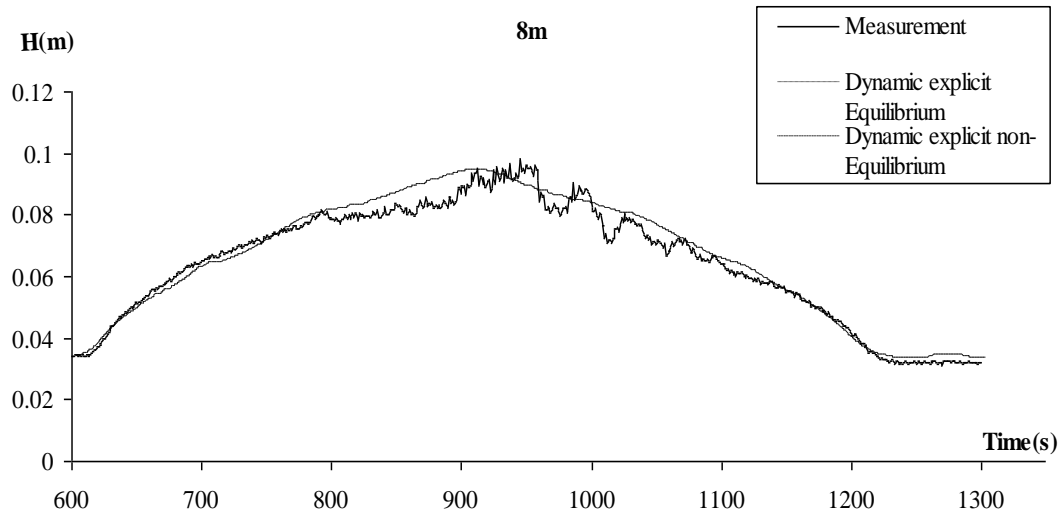Figure 7.102 View of comparison between measurement and flow depth prediction in 17.m –Hyd 5
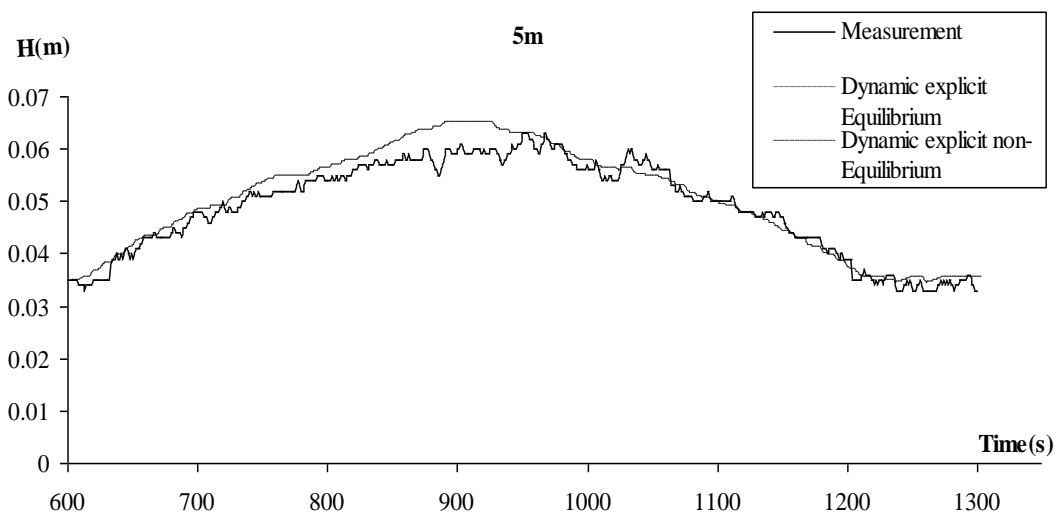
Figure 7.103 View of comparison between measurement and flow depth prediction in 5.m –Hyd. 6
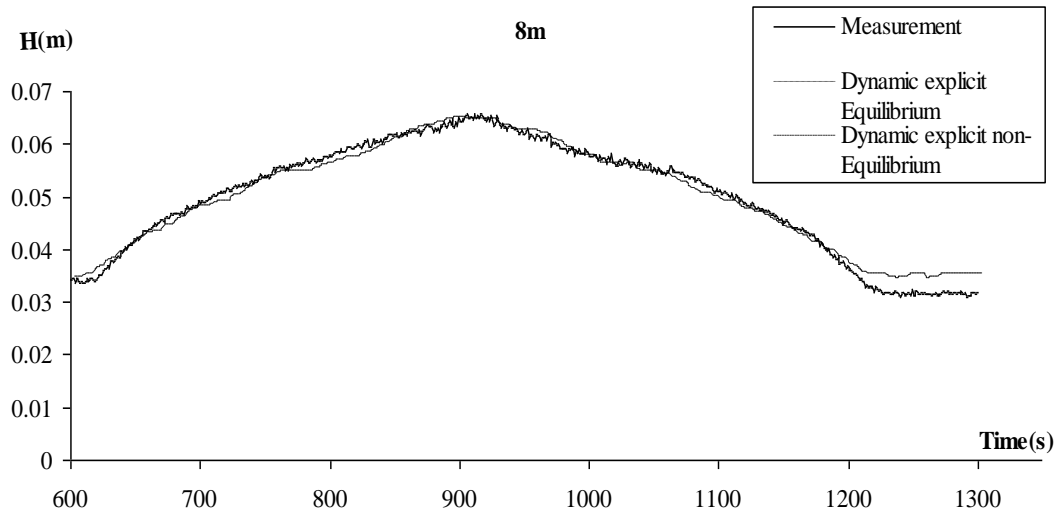
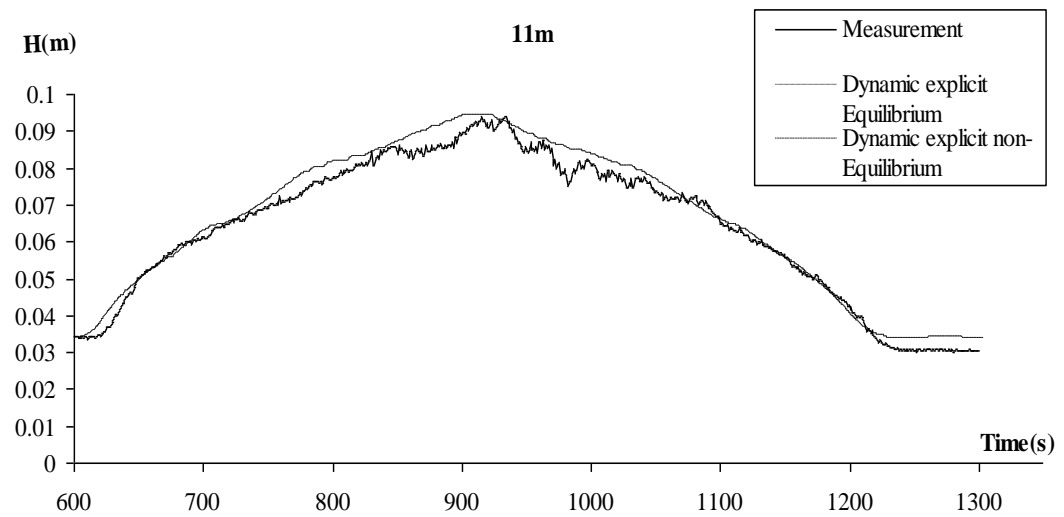Figure 7.104 View of comparison between measurement and flow depth prediction in 8.m –Hyd.6
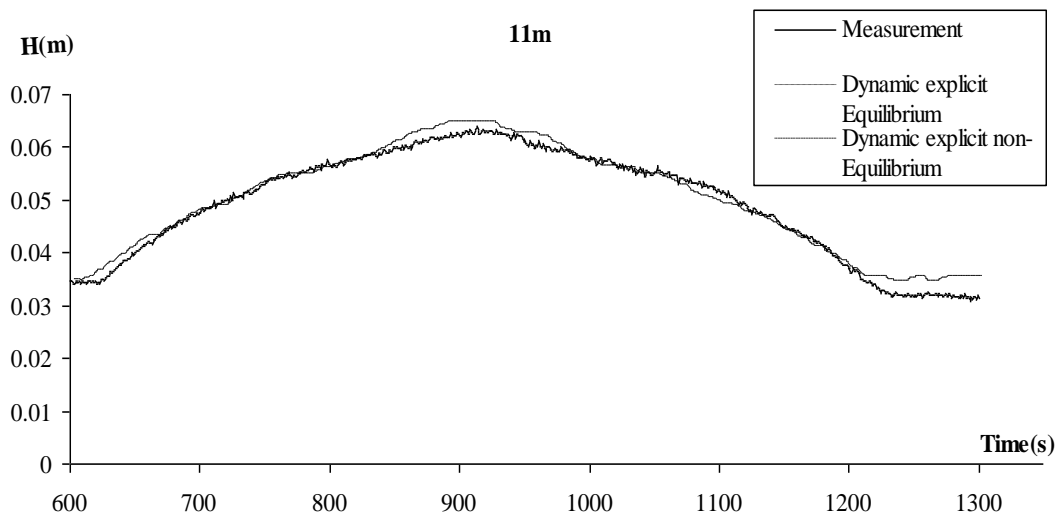
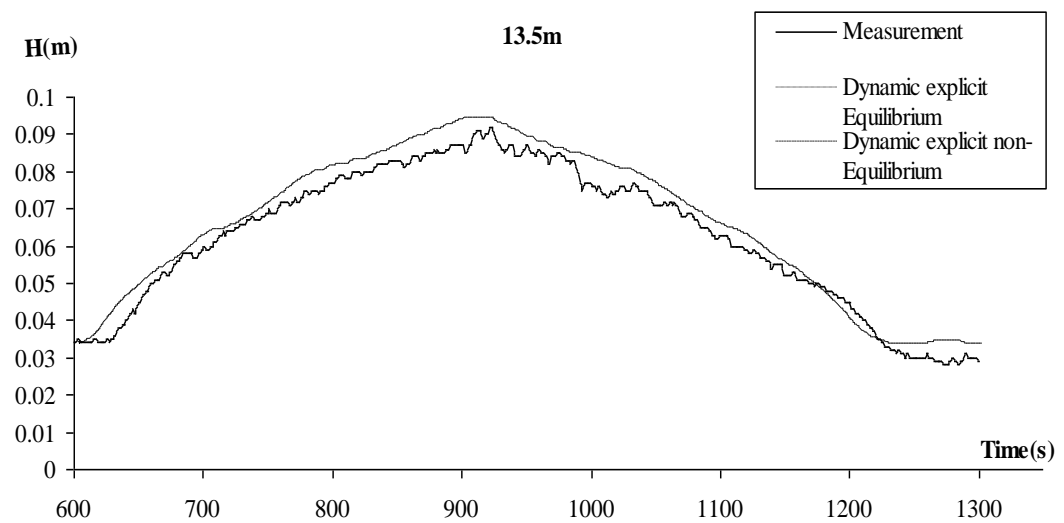Figure 7.105 View of comparison between measurement and flow depth prediction in 11.m –Hyd. 6
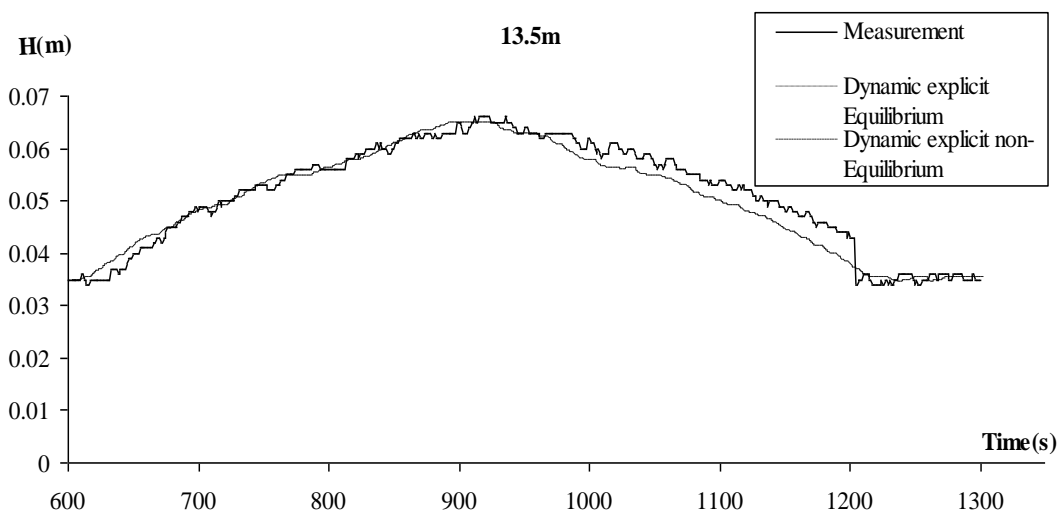
Figure 7.106 View of comparison between measurement and flow depth prediction in 13.5.m –Hyd. 6
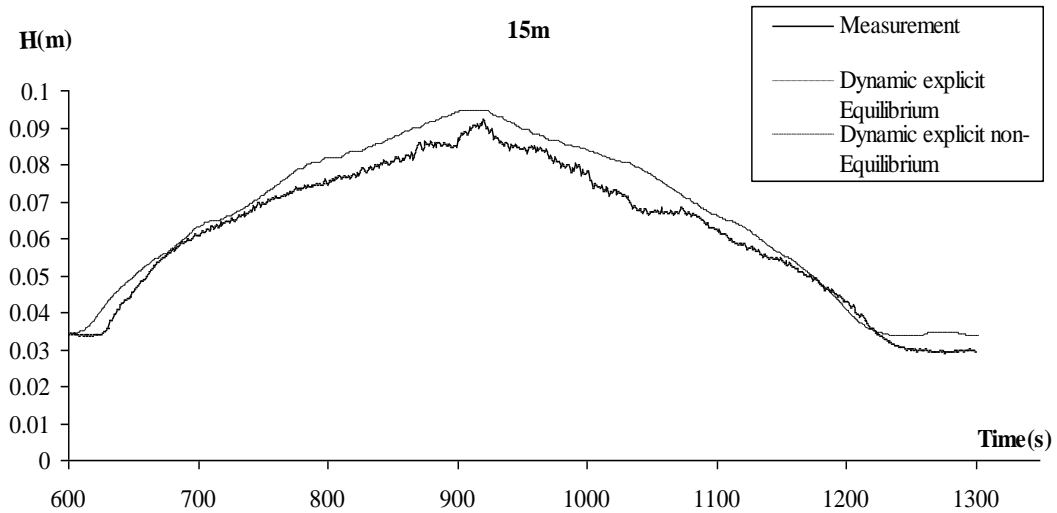
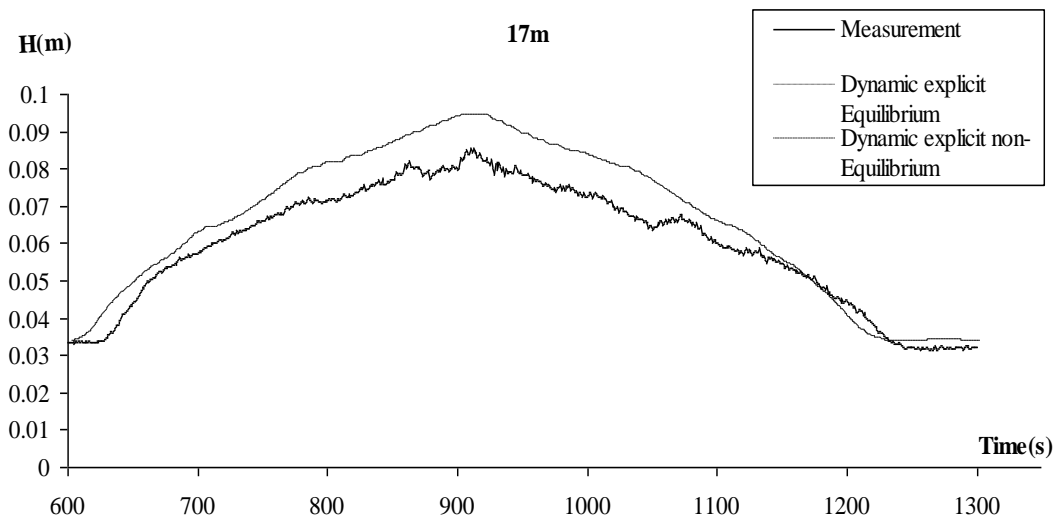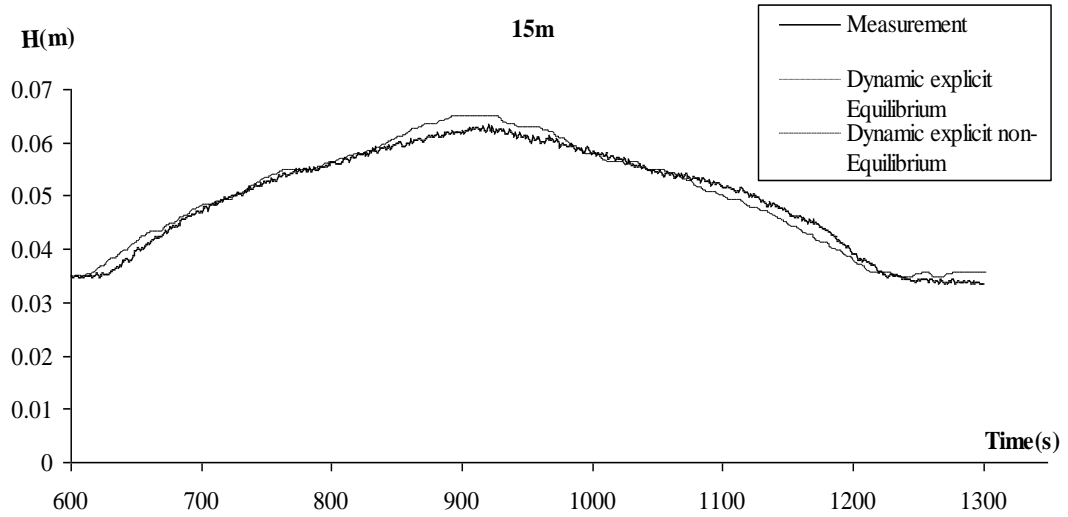Figure 7.107 View of comparison between measurement and flow depth prediction in 15.m –Hyd. 6
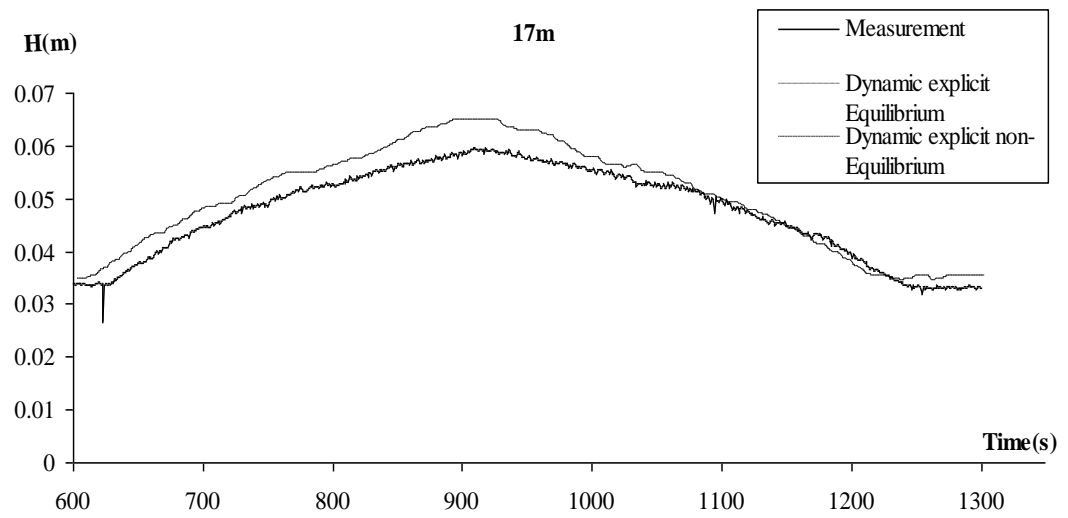
Figure 7.108 View of comparison between measurement and flow depth prediction in 17.m –Hyd.6
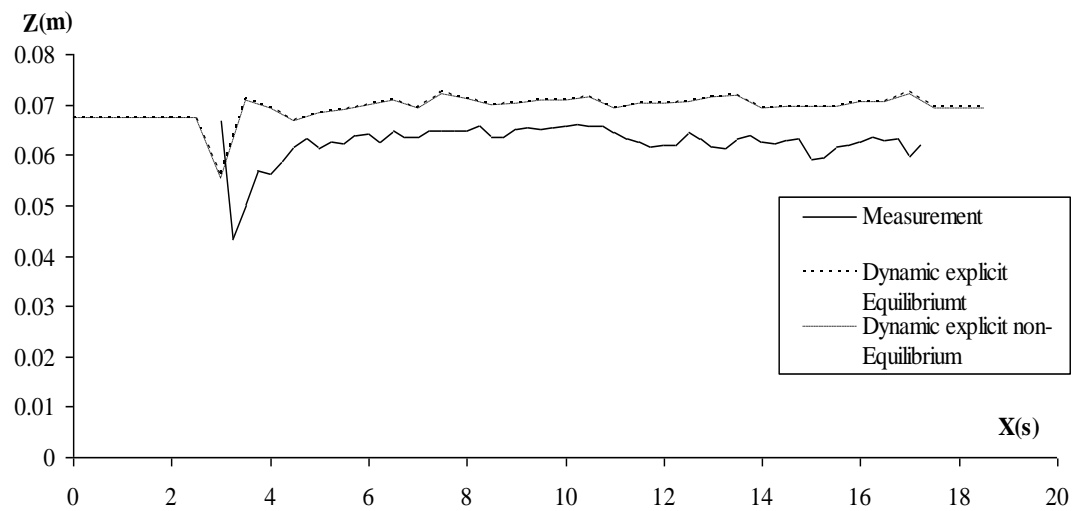
Figure 7.109 View of comparison between measurements and model predicts for bed profiles in hyd.1
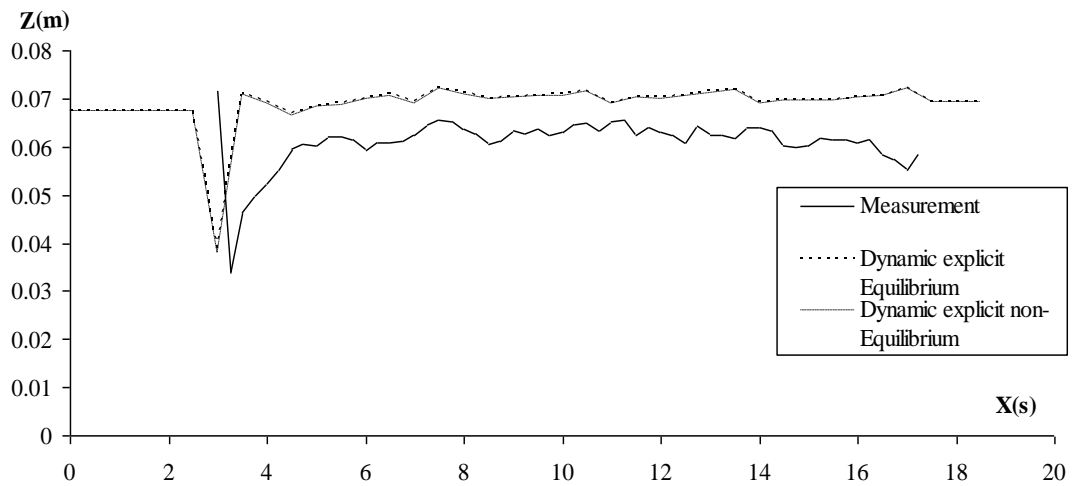
Figure 7.110 View of comparison between measurements and model predicts for bed profiles in hyd.2.
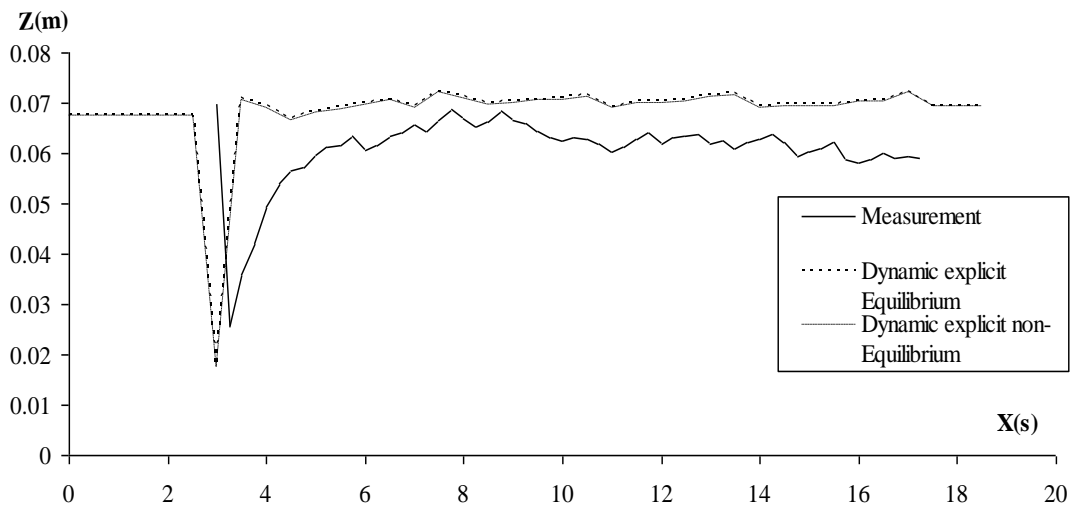
Figure 7.111 View of comparison between measurements and model predicts for bed profiles in hyd.3
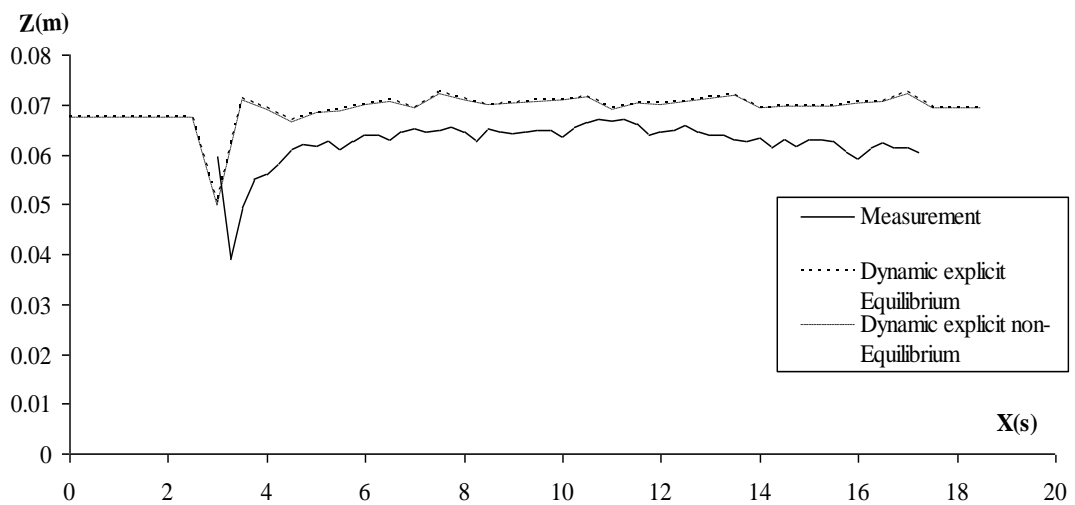
Figure 7.112 View of comparison between measurements and model predicts for bed profiles in hyd.4.

Z(m)
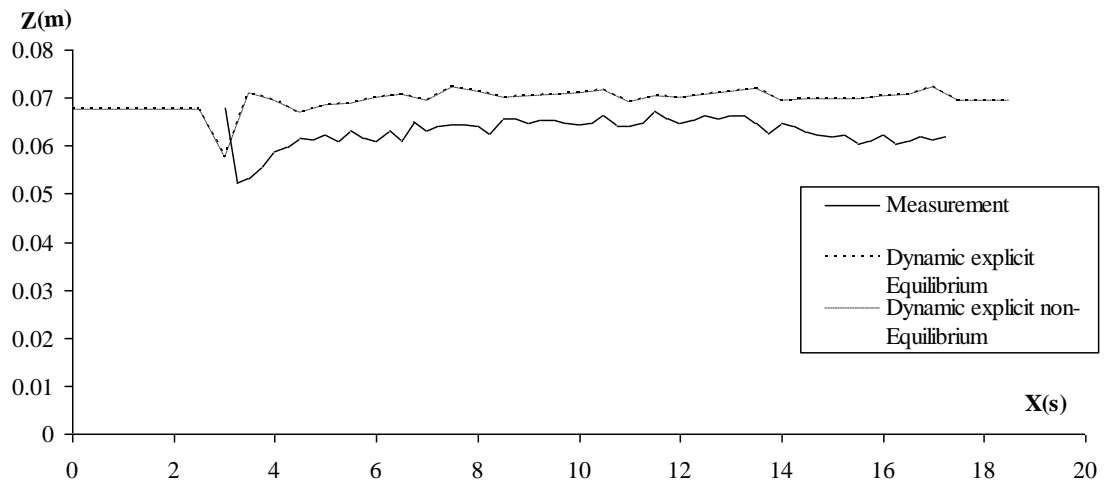
Figure 7.113 View of comparison between measurements and model predicts for bed profiles in hyd.5

Z(m)
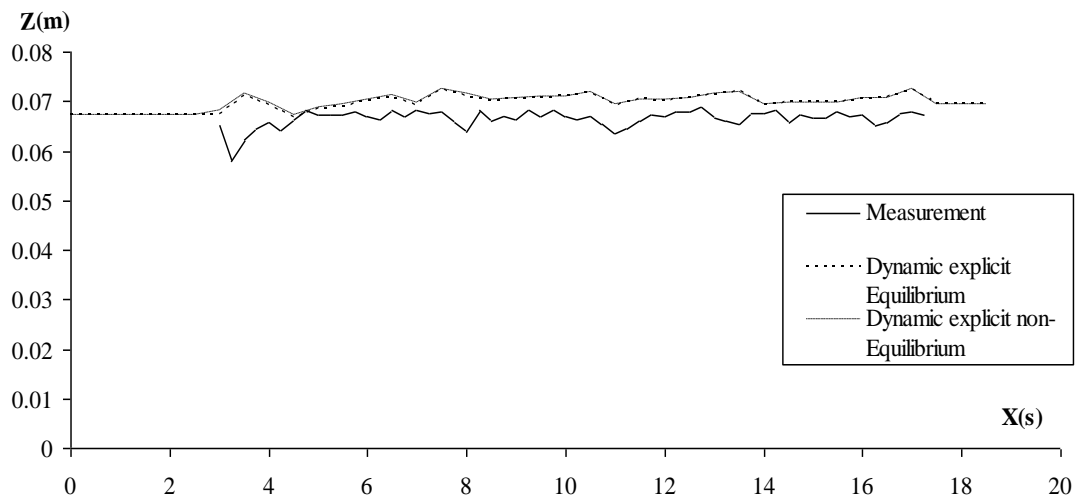
Figure 7.114 View of comparison between measurements and model predicts for bed profiles in hyd.6.

In dynamic wave model, as in the case of kinematic wave model, the computed water depth values are in accord with the measured ones. The difference between experimental and theoretical bed elevation values are in order of a grain size. Therefore the compatibility is acceptable in dynamic wave model too.

CHAPTER EIGHT
CONCLUSIONS

In this study kinematic and dynamic wave models are used in the one dimensional unsteady sediment transport by using the finite volume method. Equilibrium and nonequilibrium cases are taken into consideration. Explicit and implicit approaches are introduced. The numerical results are compared with the experimental findings. The compatibility between experimental and numerical results is acceptable.

The relation of Engelund and Fredsoe seems to be the most compatible to calculate the sediment flux, except for small discharges for which the relation proposed by Luque and Van beek is more suitable. The empirical relations need to be used with some attention since they are obtained from the experiments realized in particular conditions.

In this study, the numerical results are compared with those obtained from the experiments performed in the laboratory. It will be also very beneficial to compare them with field measurements. The use of two or three dimensional equations should be attempted in order to get a better compatibility between experimental and theoretical results.

REFERENCES

Aydöner, E. (2010). *Theoretical and experimental study of changes in channels bottoms due to sediment transport*. Thesis of Master of Science., DEU, Izmir.

Ashida, K., & Michiue M. (1972). Study on hydraulic resistence and bedload transport rate in alluvial streams. *Transactions, Japon Society of civil Engineerin ,206*,59-69

Balayn P., Paquier A., & Lapuszek M. (2003). 1-D Sediment transport model : representation of mixtures and calibration *XXX IAHR Congress, Greece ,557-564*

Bombar, G. (2009). *Experimental and Theoretical Study of Sediment Transport in Unsteady Flows,* Thesis of PhD., DEU, Izmir.

Bombar, G., Elçi, Ş., Tayfur, G., Güney, M.Ş., Bor, A.,(2011). Experimental and Numerical Investigation of Bedloas Transport Under Unsteady Flows. *Jurnal of Hydraulic Engineering.* doi:10.1061/(ASCE).

Bor, A. (2008). *Numerical modeling of unsteady and non-equilibrium sediment transport in rivers*, Thesis of Master of Science., IYTE, Izmir.

Cao R. X. (1979). Study on sediment transport capacity for sediment-laden flow with high silt concentration. *Water Resource and Hydropower Engineering, No. 5,* 55–61

Cao, Z., & Egiashira, S. (1999). Coupled Mathematical Modelling of Alluvial Rivers. *Journal of Hydraulic Engineering 17(2),* 71-85.

Cao, Z., Day, R., & Egiashira, S. (2001). Coupled and Decoupled Numerical Modelling of Flow and Morphological Evolution in Alluvial Rivers. *Journal of Hydraulic Engineering, ASCE 128(3)*, 306-321.

Capart, H. (2000). *Dam break induced geomorphic flows and the transition from solid to fluid like behavior across evolving interfaces*. Thesis of PhD. Catholic University.

Capart, H., & Young, D. L. (2002). Two Layer Shallow Water Computation of Torrential Geomorphic Flows. *River Flow International Conference on Fluvial Hydraulics,* Louvain-la-Neuve, Belgium, River flow 2002, 2- 1003.

Chang, H. H. (1982). Mathematical Model for Erodible Channels. J. *Hydraul. Div. Am.Soc. Civ. Eng. 108*(5),678-689.

Chaudhry, M. H. (1993). *Open – Channel Flow*. New Jersey: Prentice Hall, Englewood Cliffs, 07632.

Chaudhry, M. H. (1996). *Principles of flow of water*. Chapter 2 in Handbook of Water Resources.(2.1-2.43) L.Mays (ed.). McGraw-Hill.

Cunge, J. A., Holly, F. M., & Verwey, A. (1980). *Practical Aspects of computational River Hydraulics*. Pitman, USA.

Daneshfaraz, R. & Kaya, B. (2008). Solution of the propagation of the waves in open channels by transfer matrix method, *Ocean Engineering*, 35(2008) 1075-1079.

de Vries, M. (1965). Consideration About Non – Steady Bed Load Transport in Open Channels. *XI Congress, Int Assoc. of Hydraul. Eng. and Res.* St. Petersburg, Russia.

di Cristo, C. , Leopardi, A., & Greco, M. (2002). A Bed-Load Transport Model for Non- Uniform Flows. *River Flow International Conference on Fluvial Hydraulics,* Louvain-laNeuve, Belgium. River flow 2002, 2- 859.

Egiazaroff, I. V. (1965). Calculation of nonuniform sediment concentration, *J. Hydr. Div.,ASCE, 91(HY4)*, 225–247.

Einstein, H. A. (1942). Formulas for the transportation of bed load, *Trans.*, *ASCE, 107*, 561–573.

Einstein, H. A. (1950). The bed-load function for sediment transportation in open channel flows,*Technical Bulletin No. 1026*, U.S. Department of Agriculture, Soil Conservation Service, Washington D.C., USA.

Einstein, H. A., & Barbarossa, N. L. (1952). River channel roughness, *Trans*., ASCE, *117*, 1121–1132.

Einstein, H. A., & Chien, N. (1954). Second approximation to the solution of the suspendedload theory, *MRD Series Report No. 3*, Univ. of California and Missouri River Division, U.S. Corps of Engineers, Omaha, Nebr., USA.

Einstein, H. A., & Chien, N. (1955). Effects of heavy sediment concentration near the bed on velocity and sediment distribution, *MRD Series Report No. 8*, Univ. of California and Missouri River Division, U.S. Corps of Engineers, Omaha, Nebr., USA.

Engelund, F., & J. Fredsoe. (1976). A sediment transport model for straight alluvial channels, *Nordic Hydrology*, 7, pp 293-306.

Fang, H., Chen, M., & Chen, Q. (2008). One-dimensional numerical simulation of non-uniform sediment transport under unsteady flows, *International Journal of Sediment Research ,23 (4),* 316-328

Fuladipanah, M., Musavi-Jahromi, S. H., Shafai-Bajestan, M., & Khosrojerdi, A. (2010).One dimensional flow and sediment transport fully coupled model applicable to sandy river streams. *World applied science journal, 9(4),*427-433.

Güney, M.Ş., Bombar, G., Aksoy, A.Ö. (2011). Effect of coarse surface development on the bed load transport of bimodal sediment under under unsteady flow conditions. *Jurnal of Hydraulic Enginnering* (under review).

Güney, M.Ş., Bombar, G., Aksoy, A.Ö. (2011). Investigation of the effect of unsteadiness on the transport of bimodal sediments. *Jurnal of Hydrology.* (under review).

Han Q. W. (1980). A study on the non-equilibrium transportation of suspended load. *Proc., Tthe First International Symposium on River Sedimentation,* Beijing, China.

Karim, F. (1995). Bed configuration and hydraulic resistance in alluvial-channel flows, *J. Hydraulic Eng.*, *ASCE, 121(1)*, 15–25.

Kassem, A. & Chaudhry, M. H. (1998). Comparison of Coupled and Semicoupled Numerical Models for Alluvial Channels. *Journal of Hydraulic Engineering, ASCE 124(8)*, 794-802.

Kaya, B. & Arısoy, Y. (2010). Differential Quadrature Method for Linear Long Wave Propagation in Open Channels, *Wave Propagation in Materials for Modern Applications*, Andrey Petrin, ISBN 978-953-7619-65-7,Published by Intech, Vukovar, Crotia,(2010), p.253-266.

Kaya, B., Arısoy, Y. & Ülke, A.(2010). Differential Quadrature Method (DQM) For Numerical Solution of The Diffusion Wave Model. *Journal of Flood Engineering*. Vol.1 No.2.

Kaya, B., & Tayfur, G. (2011). Differential Quadrature Method For Solving Bed Load Sediment Transport. *International Balkans Conference on Challenges of Civil Engineering,* 19-21 May 2011, EPOKA University, Tirana, Albania.

Kaya, B., Ülke, A. & Kazezyilmaz-Alhan, C. M. (2011). Differential Quadrature Method in Open Channel Flows: Aksu River, Turkey, *Journal of Hydrologic Engineering.* (minor revision).

Kebapcıoğlu, E. (2009). Experimental and theoretical study of unsteady flows in open channels with different bed slopes. Thesis of Master of Science., DEU, Izmir.

Kuhnle, R. A. (1993). Fluvial transport of sand and gravel mixtures with bimodal size distributions, *Sedimentary Geology*, *85*, 17–24.

Laser Distance Measurer, Bosch DLE 70.(2011) Laser Distance Measurer Users Guide.

Leupi, C., & Altinakar., M. S. (2005). 3D Finite Element Modeling of Free-Surface Flows with Efficient $k - \varepsilon$ Turbulence Model and Non-hydrostatic Pressure, *Springer, LNCS 3516*,33-40

Met-flow. (2002).UVP Monitor Model UVP-DUO with software Version 3,User's Guide,Lausanne, Switzerland

Meyer-Peter, E., & Müller, R. (1948). Formulas for bed load transport, *International Association of Hydraulic Research. IAHR.* Stockholm, Sweden, 39-64.

Misri, R. L., Ranga Raju, K. G., & Garde, R. J. (1984). Bed load transport of coarse nonuniform sediments, *J. Hydraulic Eng.*, *ASCE, 110(3)*, 312–328.

Patel, P. L., & Ranga Raju, K. G. (1996). Fractionwise calculation of bed load transport,*J. Hydr. Res.*, *IAHR, 34(3)*, 363–379.

Papanicolaou. A. N., Bdour, A., & Wicklein, E. (2004). One-dimensional hydrodynamic / sediment transport model applicable to steep mountain streams, *Journal of Hydraulic Research* Vol. 00, No. 0 , 1–19.

Pe $\tilde{n}$ a, E., Fe, J., Puertas,J., & Sanchez-Tembleque, F. (2002). A 2D numerical model using finite volume method for sediment transport in rivers, *River Flow 2002, Proceedings of the International Conference on Fluvial Hydraulics*.6 pages.

Qin, Y. Y. (1980). Incipient motion of nonuniform sediment. *J. Sediment Res.*, No. 1 (in Chinese).

Rahuel, J. L., & Holly, F. M. (1989). Modeling of River Bed Evolution for Bed Load Sediment Mixtures. *Journal of Hydraulic Engineering, ASCE 115(11)*, 1521-1542.

Rahuel J. L. , Holly Chollet J. P. Belleudy P. J., & Yang G. (1989). Modeling of riverbed evolution for bedload sediment mixtures. *Journal of Hydraulic Engineering, ASCE, Vol. 115, No. 11*, 1521–1542.

Rubey, W. (1933). Settling velocities of gravel, sand and silt particles, *Amer. J. Sci.*, 225, 325–338.

Seo, I. W. ,Jun, I., & Choi, H.S. (2009). One-dimensional finite element model for suspended sediment transport analysis. *World City Water Forum.ss-p24,*3107-3112.

Sleigh. P. A., & Goodwill. M. (2000). The St Venant Equations, School of Civil Engineering, University of Leeds, 18 page.

Tayfur, G., & Singh,P. (2006). Kinematic wave model of bed profiles in alluvial channels. *Water Resources Research, W06414*,1-13.

Tayfur,G., & Singh, P. (2007). Kinematic wave model for transient bed profiles in alluvial channels under nonequilibrium conditions. *Water Resources Research, W12412*,1-11.

Van Rijn, C. (1993).*Principles of sediment transport in rivers,esturies and coastal seas*.(1th ed.) Netherland:Aqua publications.

Van Niekerk, A., Vogel, K. R., Slingerland, R. L. and Bridge, J. S. (1992). 'Routing of heterogeneous sediments over movable bed: Model development', *J. Hydraulic Eng.*, *ASCE, 118(2)*, 246–262.

Versteeg, H. K., & Malalasekera, W. (1995). *An introduction to computational fluid dynamics the finite volue method* (1th ed.).New york:Longman scientific & technical.

Wang, D., Yang, G., & Wang, M. (2008). Improved method for non-equilibrium sediment transport equations with confluence, *Proceedings of 16th IAHR-APD Congress and 3rd Symposium of IAHR-ISHS*, 883-888

Wilcock, P. R., & Southard, J. B. (1988). Experimental study of incipient motion in mixed-size sediment, *Water Resources Res.*, 24(7), 1137–1151.

Wu,W. (2007). .*Computational River Dynamics* (1th ed.). Netherland: Taylor & Francis e-Library.

Wu, W., & S. Y. WANG, S. (2008). One-dimensional explicit finite-volume model for sediment transport with transient flows over movable beds. *Journal of Hydraulic Research, 46(1),*87- 98.

Wu, W., & Yang, G. (2001). One-dimensional sediment numerical model and its application, *us-china workship on advanced computational modeling in hydroscience & engineering ,1-11*

Wu W. (2004). Depth-averaged 2-D numerical modeling of unsteady flow and non-uniform sediment transport in open channels. J*ournal of Hydraulic Engineering, ASCE, Vol. 130, No. 10,* 1013–1024.

Wu W., Vieira D. A., & Wang S. S. Y. (2004). One-dimensional numerical model for non-uniform sediment transport under unsteady flows in channel networks. *Journal of Hydraulic Engineering, ASCE, Vol. 130, No. 9*, 914–923.

Wu, W., & Wang, S.S.Y. (1999). Movable bed roughness in alluvial rivers, *J. Hydraulic Eng.*, *ASCE, 125(12)*, 1309–1312.

Zhang, R. J. (1961) *River Dynamics*, Industry Press, Beijing, China (in Chinese).

Zhang, R. J., Xie, J. H., Wang, M. F., & Huang, J. T. (1989). Dynamics of River Sedimentation,*Water and Power Press*, Beijing, China (in Chinese).

Zhang, R. J. (1961). *River Dynamics*, Industry Press, Beijing, China (in Chinese).

Yongjun L. (2001). 2D Numerical simulation of water flow and sediment transport for sandy and gravel shoal reaches in the downstream of tag,*Us-China workshop on advanced computaitional modelling in hydroscience and engineering* ,Oxford, Mississippi, USA.